PCT

INTERNATIONAL APPLICATION PUBLISHED UNDER THE PATENT COOPERATION TREATY (PCT)

(51) International Patent Classification 6 : C08F 6/26	**A1**	**(11) International Publication Number:** WO 99/47570 **(43) International Publication Date:** 23 September 1999 (23.09.99)

(72) Inventors: JENEKHE, Samson, A.; 50 South Village Trail, Fairport, NY 14450 (US). CHEN, X., Linda; Apartment #4H, 100 Vail Road, Parsippany, NJ 07054 (US).

(54) Title: MACROMOLECULAR SELF-ASSEMBLY OF MICROSTRUCTURES, NANOSTRUCTURES, OBJECTS AND MESO-POROUS SOLIDS

(57) Abstract

The present invention relates to a method for producing microstructures, nanostructures, or objects. This method involves providing a rod–coil block copolymer including a rigid–rod block and a flexible–coil block, mixing the rod–coil block copolymer and a selective solvent for one of the blocks which solubilizes that block, and permitting the rod–coil block copolymer to self–assemble into organized mesostructures with a region of the unsolubilized block and a region of the solubilized block. Also disclosed are organized mesostructures produced by such a method. Another aspect of the present invention is to produce the organized mesostructure in the form of a mesoporous solid. Yet another aspect of the present invention is a method of producing an adsorption layer of the rod–coil block copolymer and an optical article formed with such an adsorption layer. The present invention also relates to encapsulating and solubilizing large molecules, macromolecules, or nanoparticles by adding large molecules, macromolecules, or nanoparticles to the solution of rod–coil block copolymer and solvent.

5   **MACROMOLECULAR SELF-ASSEMBLY OF MICROSTRUCTURES,
         NANOSTRUCTURES, OBJECTS, AND MESOPOROUS SOLIDS**

         This application claims the benefit of U.S. Provisional Patent Application

No. 60/078,473, filed March 18, 1998, which is hereby incorporated by reference.

10   **FIELD OF THE INVENTION**

         The present invention relates to microstructures, nanostructures, objects, or

mesoporous solids formed from rod-coil block copolymers. The present invention also

relates to methods of making microstructures, nanostructures, objects, or mesoporous

solids.

15   **BACKGROUND OF THE INVENTION**

         Development of methods for the preparation and characterization of

robust, functional, structurally well-defined, three-dimensional self-assembled

nanostructures (1-100 nm) and microstructures (10^2- 10^5 nm) is considered to be one of

the "grand challenges now facing chemistry" through the early decades of the twenty-first

20   century (Whitesides et al., Science, 254:1312-1319 (1991); Whitesides, Angew. Chem.

Int. Ed. Engl., 29:1209-1218 (1990)). Such mesostructures ($1-10^5$ nm) are of broad

fundamental and applied interests not only in chemistry but also biology, physics,

materials science, colloid science, and surface science, while also addressing societal

concerns in health care, the environment, energy needs, and national security (Whitesides,

25   Angew. Chem. Int. Ed. Engl., 29:1209-1218 (1990)). The successful development of the

science and technology of molecular self-assembly for producing functional

mesostructures could have a revolutionary impact on the products, product design, and

manufacturing processes in many industries including those concerned with food,

pharmaceuticals, cosmetics, biomaterials, lubricants, separation membranes, adhesives,

30   thin films, coatings, paints, photographic films, storage and imaging media, catalysts and

catalyst supports, microfabrication, microelectronics, and nanoscale electronics and

photonics.

         The design and synthesis of self-assembling molecules and

macromolecules, construction of diverse, functional, mesostructures ($1-10^5$ nm) by self-

35   assembly, and investigation of their functions and properties are among the central goals

of supramolecular chemistry (Lehn, Supramolecular Chemistry, VCH, Weinheim and

New York (1995); Lehn et al., Comprehensive Supramolecular Chemistry, Pergamon,

5   New York, 11 vols., (1996)). The many advances in the field of supramolecular

chemistry in the last 20 years have recently been reviewed extensively (Lehn,

Supramolecular Chemistry, VCH, Weinheim and New York (1995); Lehn et al.,

Comprehensive Supramolecular Chemistry, Pergamon, New York, 11 vols., (1996); Conn

et al., Chem. Rev., 97:1647-1668 (1997); Chapman et al., Tetrahedron, 53:15911-15945

10   (1997); Fyfe et al., Acc. Chem. Res., 30:393-401 (1997); Ciferri, Prog. Polym Sci.,

20:1081-1120 (1995)). Although numerous one- and two-dimensional self-assembled

systems are known, reports of three-dimensional (3-D) self-assembled nanostructures

such as capsules, spheres, and nanotubes are fewer, and the size scale of the largest self-

assembled 3-D objects reported to date is only in the few tens of nanometers (ca. 10-30

15   nm) (Whitesides et al., Science, 254:1312-1319 (1991); Whitesides, Angew. Chem. Int.

Ed. Engl., 29:1209-1218 (1990); Lehn, Supramolecular Chemistry, VCH, Weinheim and

New York (1995); Lehn et al., Comprehensive Supramolecular Chemistry, Pergamon,

New York, 11 vols., (1996); Connet al., Chem. Rev., 97:1647-1668 (1997); Chapman et

al., Tetrahedron, 53:15911-15945 (1997); Fyfe et al., Acc. Chem. Res., 30:393-401

20   (1997); Ciferri, Prog. Polym Sci., 20:1081-1120 (1995); Lehn et al., Chem. Macromol.

Symp., 69:1-17 (1993)). One-, two-, and three-dimensional supramolecular structures

have been designed and constructed by using weak non-covalent interactions such as

hydrogen bonding (Zimmerman et al., Science, 271:1095-1098 (1996)), metal-ligand

complexes (Goodgame et al., Angew. Chem., Int. Ed. Engl., 34:574-575 (1995); Beissel

25   et al., Angew. Chem., Int. Ed. Engl., 35:1084-1086 (1996)), and π-π stacking interactions

(Ashton et al., J. Am. Chem. Soc., 118:4931-4951 (1996)). However, up to now, discrete

synthetic supramolecular structures with desired functionality remain a rarity and

represent a great challenge (Lehn, Angew. Chem., Int. Ed. Engl., 27:89-112 (1988); Lehn,

Supramolecular Chemistry Concepts and Perspectives, VCH, Weinheim, Germany

30   (1995); Whitesides et al., Science, 254:1312-1319 (1991); Terfort et al., Nature, 386 et

seq. (1997); Bowden et al., Science, 276:233 et seq.(1997); Whitesides et al., Acc. Chem.

Res., 28:37 et seq. (1995); Lindsey, New J. Chem., 15:153-180 (1991); Gomez-Lopez et

al., Nanotechnology, 7:183-192 (1996); Lawrence et al., Chem. Rev., 95:2229-2260

(1995); Conn et al., Chem. Rev., 97:1647 et seq. (1997); Zimmerman et al., Science,

35   271:1095-1098 (1996); (Goodgame et al., Angew. Chem., Int. Ed. Engl., 34:574-575

(1995); Beissel et al., Angew. Chem., Int. Ed. Engl., 35:1084-1086 (1996); and Ashton et

al., J. Am. Chem. Soc., 118:4931-4951 (1996)). One of the most important reasons is

5   that the number of building subunits for construction of such multicomponent systems is quite small, leading to limited sizes of the resulting supramolecular structures and their poor functionality. In order to achieve 3-D well-defined nanostructures and microstructures with desired functionality, more extended controls of chemical interactions in two or more dimensions are needed. Much larger objects are needed for

10   many near term technological applications, including drug delivery systems, microreactors, biomimetic structures, biosensors, and imaging materials. In principle, the best prospects for achieving robust, functional, and technologically important self-assembled mesostructures larger than 50 nm would seem to be through supramolecular polymer chemistry. This is because the characteristic length scales of polymer chains are

15   already on the order of 5-100 nm. In fact, nanostructured assemblies of segregated block copolymers (e.g., micelles, layered thin films, microphase separated materials, adsorbed layers, and liquid crystals) and phase separated polymer blends with length scales on the order of 5-100 nm are already well known (Halperin et al., Adv. Polym. Sci., 100:31-71 (1992); Tuzar et al., Surface and Colloid Science, 15:1-83 (1993); Weber et al., Ed.

20   Solvents and Self-Organization of Polymers, Kluwer Academic, Dordrecht (1996); Zhang et al., Science, 272:1777-1779 (1996); Chen et al., Science, 273:343-346 (1996)). However, the nanostructured assemblies of current block copolymers lack functionality and control of size, interfaces, order, and 3-D shape due to the inability to control the underlying non-covalent intermolecular interactions between the macromolecular

25   building blocks (Whitesides et al., Science, 254:1312-1319 (1991)). Further, self-assembly or aggregation experiments, such as micellization and adsorption in selective solvents, on flexible coil-coil block copolymers have been widely reported in the past 30 years (Halperin et al., Adv. Polym. Sci., 100:31-71 (1992); Tuzar et al., Surface and Colloid Science, 15:1-83 (1993); Weber et al., Ed. Solvents and Self-Organization of

30   Polymers, Kluwer Academic, Dordrecht (1996); Zhang et al., Science, 272:1777-1779 (1996); Chen et al., Science, 273:343-346 (1996); MacDonald et al., Chem. Rev., 94:2383-2420 (1994)); however, few such reports can be found for rod-coil block copolymers. Two main aspects of supramolecular polymer chemistry have been reported: (i) the successful synthesis of diverse main-chain and side-chain polymers by

35   molecular recognition driven self-assembly of complementary monomers or oligomers (Lehn et al., Chem. Macromol. Symp., 69:1-17 (1993), Stewart et al., Macromolecules, 30:877-884 (1997); Kato et al., Macromolecules, 29:8734-8739 (1996)); and (ii) the synthesis of flexible-chain polymers with tapered, rigid, side groups which self-organize

into tubular architectures akin to the tobacco mosaic virus (TMV) (Percec et al., Nature, 391:161-164, (1998)). However, the use of synthetic polymers as subunits for molecular recognition driven self-assembly of large discrete aggregates and mesostructures remains largely unexplored.

Block copolymers can produce numerous phase-separated microstructures and nanostructures that are of wide scientific and technological interest (Muthukumar et al., Science, 277:1225-1232 (1997); Chen et al., Science, 277:1248-1253 (1997); Park et al., Science, 276:1401-1404 (1997); Bates, Science, 251:898-905 (1991); Milner, Science, 251:905-914 (1991); Fredrickson et al., Annu. Rev. Mater. Sci., 26:501-550 (1996); Halperin et al., Adv. Polym. Sci., 100:31-71 (1992); Tirrell, Acc. Chem. Res., 30:281-308 (1997); Noshay et al., Block Copolymers: Overview and Critical Survey, Academic Press, New York (1977); Chen et al., Science, 273:343-346 (1996); Chen et al., Macromolecules, 28:1688-1697 (1995); Radzilowski et al., Macromolecules, 26:879-882 (1993); Radzilowski et al., Macromolecules, 27:7747-7753 (1994); Widawski et al., Nature, 369:387-389 (1994); Vernino et al., Polym. Mater. Sci. Eng., 71:496-497 (1994); Tuzar et al., Surface and Colloid Science, 15:1-83 (1993); Weber et al., Solvents and Self-Organization of Polymers, Kluwer Academic, Dordrecht (1996); Gast, Acc. Chem. Res., 30:259-280 (1997); Vagberg et al., Macromolecules, 24:1670-1677 (1991); Nagarajan et al., Langmuir, 2:210-215 (1986); Nagarajan, Acc. Chem. Res., 30:121-165 (1997); Chen et al., Macromolecules, 29:6189-6192 (1996); Chen et al., Appl. Phys. Lett., 70:487-489 (1997); Semenov et al., Sov. Phys. JETP, 63:70-79 (1986); Semenov, Mol. Cryst. Liq. Cryst., 209:191-199 (1991); Halperin, Macromolecules, 23:2724-2731 (1990); Halperin, Europhys. Lett., 10:549-553 (1989); Williams et al., Macromolecules, 25:3561-3568 (1992); Raphael et al., Makromol. Chem., Macromol. Symp., 62:1-17 (1992); Zhang et al., Science, 272:1777-1779 (1996); Zhang et al., Science, 268:1728-1731 (1995); Zhang et al., J. Am. Chem. Soc., 118:3168-3181 (1996)). Conventional applications of such block copolymer assemblies include thermoplastic elastomers, pressure-sensitive adhesives, colloidal dispersants, compatibilizers of polymer blends, foams, and surface modification (Bates, Science, 251:898-905 (1991); Milner, Science, 251:905-914 (1991); Fredrickson et al., Annu. Rev. Mater. Sci., 26:501-550 (1996); Halperin et al., Adv. Polym. Sci., 100:31-71 (1992); Tirrell, Acc. Chem. Res., 30:281-308 (1997); Noshay et al., Block Copolymers: Overview and Critical Survey, Academic Press, New York (1977); Tuzar et al., Surface and Colloid Science, 15:1-83 (1993); Weber et al., Solvents and Self-Organization of Polymers, Kluwer Academic, Dordrecht

5   (1996); Gast, Acc. Chem. Res., 30:259-280 (1997); Vagberg et al., Macromolecules,
    24:1670-1677 (1991)). Of the factors that determine the microstructure of block
    copolymers, conformational asymmetry between the blocks is perhaps the least
    understood (Chen et al., Science, 273:343-346 (1996); Chen et al., Macromolecules,
    28:1688-1697 (1995); Radzilowski et al., Macromolecules, 26:879-882 (1993);

10 Radzilowski et al., Macromolecules, 27:7747-7753 (1994); Widawski et al., Nature,
    369:387-389 (1994); Vernino et al., Polym. Mater. Sci. Eng., 71:496-497 (1994);
    Semenov et al., Sov. Phys. JETP, 63:70-79 (1986); Semenov, Mol. Cryst. Liq. Cryst.,
    209:191-199 (1991); Halperin, Macromolecules, 23:2724-2731 (1990); Halperin,
    Europhys. Lett., 10:549-553 (1989); Williams et al., Macromolecules, 25:3561-3568

15 (1992); Raphael et al., Makromol. Chem.. Macromol. Symp., 62:1-17 (1992)).
    Theoretical studies of rigid-rod-flexible-coil block copolymers, in which the ultimate
    conformational asymmetry is achieved, have predicted major differences in phase
    behavior, self-assembly, and microstructures compared to flexible coil-coil block
    copolymers (Semenov et al., Sov. Phys. JETP, 63:70-79 (1986); Semenov, Mol. Cryst.

20 Liq. Cryst., 209:191-199 (1991); Halperin, Macromolecules, 23:2724-2731 (1990);
    Halperin, Europhys. Lett., 10:549-553 (1989); Williams et al., Macromolecules, 25:3561-
    3568 (1992); Raphael et al., Makromol. Chem.. Macromol. Symp., 62:1-17 (1992)).
    However, only a few experimental studies of synthetic rod-coil block copolymers have
    been reported (Chen et al., Science, 273:343-346 (1996); Chen et al., Macromolecules,

25 28:1688-1697 (1995); Radzilowski et al., Macromolecules, 26:879-882 (1993);
    Radzilowski et al., Macromolecules, 27:7747-7753 (1994); Widawski et al., Nature,
    369:387-389 (1994); Vernino et al., Polym. Mater. Sci. Eng., 71:496-497 (1994)). The
    most detailed of these by Chen et al. involved an alpha-helical rod-like poly(hexyl
    isocyanate) as the rigid-rod block. However, such alpha-helical polymers are known to

30 be capable of existing in both rod-like and flexible-coil conformations (Halperin,
    Macromolecules 23:2724-2731 (1990)) which can compromise their ability to self-
    organize.

            In addition, ordered mesoporous solids with nanoscale pore sizes are of
    interest in areas such as catalysis, sensors, size- and shape-selective separation media,

35 adsorbents, and scaffolds for composite materials synthesis (Kresge et al., Nature,
    359:710-712 (1992); Sayari, Chem. Mater., 8:1840-1852 (1996); Huo et al., Chem.
    Mater., 8:1147-1160 (1996); Zhao et al., Science, 279:548-552 (1998); Krämer et al.,
    Langmuir, 14:2027-2031 (1998); Wijnhoven et al., Science, 281:802-804 (1998)). Those

5   with pore sizes on the order of 50 nm to 30 μm are also of interest for applications in photonics, optoelectronics, light-weight structural materials, and thermal insulation (Wijnhoven et al., Science, 281:802-804 (1998); Imhor et al., Nature, 389:948 et seq. (1997); Yablonovitch, J. Opt. Soc. Am. B., 10:283-295 (1993); Joannopoulos et al., Nature, 386:143-145 (1997); Martorell et al., Phys. Rev. Lett., 65:1877-1880 (1990);

10   Miguez et al., Appl. Phys. Lett., 71:1148-1150 (1997); Bitzer, Honeycomb Technology, Chapman & Hall, London (1997)). In particular, photonic crystals or photonic band gap materials, i.e., structures that can create and manipulate light signals precisely, transmitting certain wavelengths while blocking others, are of interest. Photonic crystals were first envisioned by Eli Yablonovitch more than a decade ago (Yablonovitch, J. Opt.

15   Soc. Am. B., 10:283-295 (1993)). In these crystals, composite materials are ordered so that light traveling through them is modulated in a highly controlled fashion. Groups at Sandia National Laboratory, at Allied Signal, and in the Netherlands have built photonic crystals, but most current efforts involve a great deal of technological hand-holding: either laborious and expensive fabrication like drilling tiny holes into a material, or

20   providing a template to begin the assembly process, then somehow removing the starting material. Most current general methods for preparing diverse porous materials use self-organized surfactants, block copolymers, or colloidal particles as templates in conjunction with sol-gel techniques (Kresge et al., Nature, 359:710-712 (1992); Sayari, Chem. Mater., 8:1840-1852 (1996); Huo et al., Chem. Mater., 8:1147-1160 (1996); Zhao et al., Science,

25   279:548-552 (1998); Krämer et al., Langmuir, 14:2027-2031 (1998); Wijnhoven et al., Science, 281:802-804 (1998); Imhor et al., Nature, 389:948 et seq. (1997)). In these methods, the organic templates are eventually removed by thermal decomposition or solvent extraction to achieve the porous solid. Those involving inorganic colloid templates use solvent extractions at the final stages of making the mesoporous solid.

30   Polymer latex and silica spheres are known to form colloidal crystals (Kose et al., Colloid Interface Sci., 46:460-469 (1974); Hachisu et al., Nature, 283:188-189 (1980); Clark et al., Nature, 281:57-60 (1979); Pieranski et al., Contemp. Phys., 24:25-73 (1983); Pusey et al., Nature, 320:340-342 (1986); Bartlett et al., Phys. Rev. Lett., 68:3801-3804 (1992); van Blaaderen et al., Nature, 385:321-324 (1997); Weissman

35   et al., Science, 274:959-960 (1996)), but long-range ordering of suspensions of block copolymer micelles into body-centered cubic (bcc) and face-centered cubic (fcc) lattices was observed and elucidated more recently (McConnell et al., Phys Rev. Lett., 71:2102-

5   2105 (1993); McConnell et al., Macromolecules, 28:6754-6764 (1995); McConnell et al.,
Macromolecules, 30:435-444 (1997); McConnell et al., Phys. Rev. E., 54:5447-5455
(1996)). Micelles of coil-coil block copolymers in a selective solvent for one of the
blocks are spheres consisting of a dense core of the insoluble block and a diffuse corona
of the solvated block (McConnell et al., Phys Rev. Lett., 71:2102-2105 (1993);

10   McConnell et al., Macromolecules, 28:6754-6764 (1995); McConnell et al.,
Macromolecules, 30:435-444 (1997); McConnell et al., Phys. Rev. E., 54:5447-5455
(1996); Webber et al., Solvents and Self-Organization of Polymers, Kluwer Academic,
Dordrecht (1996); Webber, J. Phys. Chem. B, 102:2618-2626 (1998); Tuzar et al., In
Surface and Colloid Science, 15:1-83, Plenum, New York (1993); Halperin et al., Adv.

15   Polym. Sci., 100:31-71 (1992); Förster et al., Adv. Mater., 10:195-217 (1998); Zhang et
al., J. Am. Chem. Soc., 118:3168-3181 (1996); Zhang et al., Science, 268:1728-1731
(1995)). Copolymer architecture and solution chemistry have been used to vary their
diameter between about 10 to 80 nm and the corona thickness relative to the core radius
(McConnell et al., Phys Rev. Lett., 71:2102-2105 (1993); McConnell et al.,

20   Macromolecules, 28:6754-6764 (1995); McConnell et al., Macromolecules, 30:435-444
(1997); McConnell et al., Phys. Rev. E., 54:5447-5455 (1996); Webber et al., Solvents
and Self-Organization of Polymers, Kluwer Academic, Dordrecht (1996); Webber, J.
Phys. Chem. B, 102:2618-2626 (1998); Tuzar et al., In Surface and Colloid Science,
15:1-83, Plenum, New York (1993); Halperin et al., Adv. Polym. Sci., 100:31-71 (1992);

25   Förster et al., Adv. Mater., 10:195-217 (1998); Zhang et al., J. Am. Chem. Soc.,
118:3168-3181 (1996); Zhang et al., Science, 268:1728-1731 (1995)). Micellar
crystallization into either an fcc or a bcc lattice is determined by the length scale and
steepness of repulsive interactions that can be controlled by the ratio of the coronal layer
thickness to the core radius (McConnell et al., Phys Rev. Lett., 71:2102-2105 (1993);

30   McConnell et al., Macromolecules, 28:6754-6764 (1995); McConnell et al.,
Macromolecules, 30:435-444 (1997); McConnell et al., Phys. Rev. E., 54:5447-5455
(1996)). Theoretical studies of the possible equilibrium structures of micelles of rod-coil
block copolymers in a selective solvent for the coil-like block have been reported
(Semenov et al., Sov. Phys., 63:70-79 (1986); Semenov, Mol. Cryst. Liq. Cryst., 209:191-

35   199 (1991); Halperin, Macromolecules, 23:2724-2731 (1990); Holyst et al., J. Chem.
Phys., 96:721-729 (1992); Müller et al., Macromolecules, 29:8900-8903 (1996); Williams
et al., Macromolecules, 25:3561-3568 (1992); Williams et al., Phys. Rev. Lett., 71:1557-
1560 (1993); Raphael et al., Physica A, 177:294-300 (1991); Raphael et al., Makromol.

5   Chem.. Macromol. Symp., 62:1-17 (1992)). Because of the perceived difficulty of
efficient space-filling packing of rod-like blocks into a spherical or a cylindrical core,
various alternative space-filling core-corona models. such as disk-like cylindrical micelles
and monolayer and bilayer "hockey puck" micelles, have been proposed (Semenov et al.,
Sov. Phys., 63:70-79 (1986); Semenov, Mol. Cryst. Liq. Cryst., 209:191-199 (1991);

10   Halperin. Macromolecules, 23:2724-2731 (1990); Holyst et al., J. Chem. Phys., 96:721-
729 (1992); Müller et al., Macromolecules, 29:8900-8903 (1996); Williams et al.,
Macromolecules, 25:3561-3568 (1992); Williams et al., Phys. Rev. Lett., 71:1557-1560
(1993); Raphael et al., Physica A, 177:294-300 (1991); Raphael et al., Makromol. Chem..
Macromol. Symp., 62:1-17 (1992)). However, experimental data have heretofore been

15   unavailable to test these models (Widawski et al.. Nature, 369:387-389 (1994); Francois
et al., Adv. Mater., 7:1041-1044 (1995)). Thus, the implications of the unusual micellar
structures of rod-coil block copolymers (Jenekhe et al., Science, 279:1903-1907 (1998))
for regulating these repulsive interactions. micellar crystallization, and crystal lattice
selection are currently unknown.

20   The present invention is directed toward overcoming the above-noted
deficiencies in the prior art.

SUMMARY OF THE INVENTION

         The present invention relates to a method for producing microstructures,

25   nanostructures. or objects. This method involves providing a rod-coil block copolymer
including a rigid-rod block and a flexible-coil block, mixing the rod-coil block copolymer
and a selective solvent for one of the blocks which solubilizes that block, and permitting
the rod-coil block copolymer to self-assemble into organized mesostructures with a
region of the unsolubilized block and a region of the solubilized block.

30   The present invention also relates to a microstructure, nanostructure. or
object including a rod-coil block copolymer which includes a rigid-rod block and a
flexible-coil block, wherein the rod-coil block copolymer forms an organized
mesostructure with a region of one block and a region of the other block.

         Another aspect of the present invention is a method for producing a

35   mesoporous solid. This method involves providing a rod-coil block copolymer including
a rigid-rod block and a flexible-coil block, mixing the rod-coil block copolymer and a
selective solvent for the flexible-coil block which solubilizes that block, permitting the

5 rod-coil block copolymer to self-assemble into organized mesostructures with a region of
the unsolubilized block and a region of the solubilized block, evaporating the solvent, and
permitting the organized mesostructures to self-organize into a mesoporous solid.

The present invention also relates to a method for producing a polymer
adsorption layer on a substrate. This method involves providing a rod-coil block

10 copolymer including a rigid-rod block and a flexible-coil block, mixing the rod-coil block
copolymer and a selective solvent for one of the blocks to form a solution of rod-coil
block copolymer and solvent, inserting a substrate into the solution, permitting the rod-
coil block copolymer to adsorb to the substrate, and removing the substrate from the
solution under conditions effective to form an adsorption layer of a polymer on the

15 substrate.

Another aspect of the present invention is a substrate with a polymeric
adsorption layer, wherein the adsorption layer is a rod-coil block copolymer including a
rigid-rod block and a flexible-coil block, wherein one of the blocks of the rod-coil block
copolymer is adsorbed to the substrate.

20 The present invention also relates to an optical article including a
substrate, a transparent conductor formed as a coating on the substrate, a polymeric
adsorption layer including a rod-coil block copolymer including a rigid-rod block and a
flexible-coil block, wherein one of the blocks of the rod-coil block copolymer is adsorbed
to the transparent conductor, and a coating formed on the surface of the adsorption layer,

25 wherein the adsorption layer allows the emission of polarized light.

Another aspect of the present invention is a method for encapsulating
guest molecules, macromolecules, or nanoparticles. This method involves providing a
rod-coil block copolymer including a rigid-rod block and a flexible-coil block, mixing the
rod-coil block copolymer with a selective solvent for one of the blocks which solubilizes

30 that block to form a solution of rod-coil block copolymer and solvent, adding guest
molecules, macromolecules, or nanoparticles to the solution, and permitting the rod-coil
block copolymer to self-assemble into organized mesostructures with a region of the
unsolubilized block and a region of the solubilized block under conditions effective to
encapsulate the guest molecules, macromolecules, or nanoparticles within the

35 mesostructure.

Yet another aspect of the present invention is an organized mesostructure
with an encapsulated guest molecule, macromolecule, or nanoparticle which includes a
rod-coil block copolymer including a rigid-rod block and a flexible-coil block, wherein

5   the rod-coil block copolymer forms an organized mesostructure with a region of one block and a region of the other block and a guest molecule, macromolecule, or nanoparticle, wherein the guest molecule, macromolecule, or nanoparticle is encapsulated within the mesostructure.

    The present invention also relates to a method for solubilizing guest

10   molecules, macromolecules, or nanoparticles. This method involves providing a rod-coil block copolymer including a rigid-rod block and a flexible-coil block, mixing the rod-coil block copolymer with a selective solvent for one of the blocks which solubilizes that block to form a solution of rod-coil block copolymer and solvent, adding guest molecules, macromolecules, or nanoparticles to the solution, and permitting the rod-coil block

15   copolymer to self-assemble into organized mesostructures with a region of the unsolubilized block and a region of the solubilized block under conditions effective to solubilize the guest molecules, macromolecules, or nanoparticles.

    The rod-coil block copolymers of the present invention form robust, functional, structurally well-defined, three-dimensional nanostructures, microstructures,

20   and objects. The nanostructures, microstructures, and objects may be used for encapsulating guest molecules, macromolecules, or nanoparticles. In addition, the nanostructures, microstructures, and objects may be used to form mesoporous solids, without a template, for use in various optical applications, tissue engineering and biomaterials, molecular electronic devices, optically tunable and responsive coatings, and

25   the processing of "soft" colloidal materials. Further, the rod-coil block copolymers of the present invention may be used to form an adsorption layer of a polymer.

BRIEF DESCRIPTION OF THE DRAWINGS

    Figure 1 shows preferred rod-coil block copolymer architectures of the

30   present invention.

    Figure 2 shows preferred rigid-rod blocks for the rod-coil block copolymers of the present invention.

    Figure 3 shows additional preferred rigid-rod blocks for the rod-coil block copolymers of the present invention.

35   Figure 4 shows preferred flexible-coil blocks for the rod-coil block copolymers of the present invention.

5   Figure 5 shows the synthetic scheme for the diblock copolymers PPQ_{50}-b-PS_{2000}, PPQ_{50}-b-PS_{1000}, PPQ_{50}-b-PS_{300}, PPQ_{10}-b-PS_{130}, PPQ_{10}-b-PS_{1000}, PPQ_{10}-b-PS_{300}, and PPQ_{10}-b-PS_{130} (54a-g).

Figure 6 shows the synthetic scheme for the triblock copolymers PPQ_{50}-b-PS_{500}-b-PPQ_{50}, PPQ_{50}-b-PS_{250}-b-PPQ_{50}, and PPQ_{50}-b-PS_{120}-b-PPQ_{50} (55a-c).

10   Figure 7 shows the chemical structure and schematic illustration of the self-assembly of poly (phenylquinoline)-*block*-polystyrene ("PPQ-b-PS") rod-coil block copolymers into hollow aggregates.

Figure 8 shows some relevant hydrogen-bonded structural motifs for influencing molecular packing and 3-D structure.

15   Figure 9 shows hydrogen-bonded layers and bilayers of AB rod-coil block copolymers which are structural motifs for self-assembly of 3-D structures.

Figure 10 shows hydrogen-bonded tapes for self-assembly of 3-D structures by ABA and BAB rod-coil block copolymers.

Figure 11 shows examples of rod-coil block copolymers.

20   Figure 12 shows the molecular structure of the rod-coil block copolymer PPQ_mPS_n and schematic illustration of its hierarchical self-assembly into ordered mesoporous materials.

Figure 13 shows examples of self-assembly of rod-coil block copolymers at surfaces of substrates to form adsorption layers.

25   Figure 14 shows schematic illustrations of the self-assembly of rod-coil PPQ-b-PS diblock and PPQ-b-PS-b-PPQ copolymers into hollow aggregates.

Figures 15A-D show the optical (Figures 15A to C) and scanning electron (Figure 15D) micrographs of the typical morphologies of PPQ_{50}-b-PS_{300}. Drops of dilute solutions (0.5 to 1.0 mg/ml) of the rod-coil block copolymers were spread and dried on

30   glass slides and aluminum substrates, respectively. (Figure 15A) spherical aggregates (1: 1 TFA:DCM, v/v, 95 °C); (Figure 15B) lamellae (1:1 TFA:DCM, 25 °C); (Figure 15C) cylinders (9:1 TFA:DCM, 25 °C); (Figure 15D) vesicles (1:1 - 1:4 TFA:DCM, 25 °C).

Figures 16A-F show optical (Figure 16A and Figure 16C) and fluorescence (Figure 16B, Figure 16D-F) micrographs of the typical morphologies of

35   PPQ_{50}-b-PS_{300} (54c). Drops of dilute solutions (0.5 to 1.0 mg/ml) of the diblock copolymers were spread and dried on glass slides. Spherical aggregates (Figure 16A) under cross-polarizers, (Figure 16B) fluorescence lamp (7:1 TFA:DCM, v/v, 25°C); lamellae (Figure 16C) under cross-polarizers, (Figure 16D) under fluorescence lamp (1:1

5   TFA:DCM, 25°C); (Figure 16E) cylinders (9:1 TFA:DCM, 25°C); (Figure 16F) rings (1:4
     TFA:DCM, 25°C).

              Figures 17A-F show optical (Figure 17A and Figure 17C-F) and
     fluorescence (Figure 17B) micrographs of the typical morphologies of diblock copolymer
     54b, 54e, 54f, and 54g. (Figure 17A) spherical aggregates from PPQ$_{50}$-b-PS$_{1000}$ (**54b**) (7:1
10   TFA:DCM, v/v, 25°C); (Figure 17B) cylinders from PPQ$_{50}$-b-PS$_{1000}$ (**54b**) (9:1
     TFA:DCM, 25°C); (Figure 17C) lamellea from PPQ$_{10}$-b-PS$_{1000}$ (**54e**) (1:1 TFA:DCM,
     25°C); (Figure 17D) lamellea from PPQ$_{10}$-b-PS$_{300}$ (**54f**) (1:1 TFA:DCM, 25°C); (Figure
     17E) lamellae from PPQ$_{10}$-b-PS$_{130}$ (**54f**) (1:1 TFA:DCM, 25°C); (Figure 17F) lamellae
     from PPQ$_{10}$-b-PS$_{130}$ (**54f**) (1:1 TFA:DCM, 25°C).

15   Figure 18 shows schematic illustrations of the self-assembly of rod-coil
     PPQ-b-PS diblock copolymers.

              Figures 19A-B show photoluminescence ("PL") emission and excitation
     ("PLE") (Figure 19A)spectra and PL decay dynamics of spherical, lamellar, and
     cylindrical aggregates of PPQ$_{50}$-b-PS$_{300}$ (Figure 19B). PL emission spectra are for 380-
20   nm excitation, and PLE spectra were obtained by monitoring the emission peaks. PL
     decay data are for 380-nm laser excitation in time-correlated single-photon counting
     experiments.

              Figures 20A-F show optical and fluorescence micrographs of hollow
     spherical vesicles from triblock copolymers PPQ$_{50}$-b-PS$_{500}$-b-PPQ$_{50}$ (**55a**) (Figure 20A,
25   Figure 20B); PPQ$_{50}$-b-PS$_{250}$-b-PPQ$_{50}$ (**55b**) (Figure 20C, Figure 20D); PPQ$_{50}$-b-PS$_{120}$-b-
     PPQ$_{50}$ (**55c**) (Figures 20E, Figure 20F). Figures 20A, 20C and 20E were taken under
     cross-polarizers. The samples were prepared by allowing drops of dilute solutions (0.5 to
     1.0 mg/ml) of the triblock copolymers to spread and be dried on hot glass slides (6:4
     TFA:DCM, v/v, 95 °C).

30   Figures 21A-F show optical and fluorescence micrographs of vesicles
     from diblock and triblock copolymers PPQ$_{50}$-b-PS$_{500}$-b-PPQ$_{50}$ (**55a**) (Figures 21A-D) and
     PPQ$_{50}$-b-PS$_{250}$-b-PPQ$_{50}$ (**55b**) (Figures 21E-F). The images were taken in-situ from
     sample solutions (6:4 TFA:DCM, 25°C, 1.0 mg/ml) sealed inside 6 mm x 50 mm tubes.
     Figures 21A, 21E, and 21F were take under bright field. Figure 21C was taken under
35   cross-polarizers. Figures 21B and 21D were taken when excited with 400-nm light.

              Figures 22A shows schematic illustrations of the H-aggregates (Figure
     22A) and J-aggregates (Figure 22B) formed by rod-coil block copolymers.

Figures 23A-B show Photoluminescence (PL) emission and excitation (PLE) spectra (Figure 23A) and PL decay dynamics of spherical aggregates from triblock copolymers 55a-c and spherical, lamellar, and cylindrical aggregates from diblock copolymers 54a-g (Figure 23B). PL emission spectra are for 380-nm excitation, and PLE spectra were obtained by monitoring the emission peaks. PL decay data are for 380-nm laser excitation in time-correlated single-photon counting experiments.

Figures 24A-F show scanning electron micrographs of the spherical aggregates self-assembled from PPQ_{50}-b-PS_{300} (Figure 24A, Figure 24B, Figure 24E, Figure 24F) and PPQ_{10}-b-PS_{300} (Figure 24C, Figure 24D). All these aggregates were prepared by spreading dilute solution (0.1 wt%) with a solvent ratio TFA:DCM of 7/1 onto aluminum substrates (25°C).

Figures 25A-D show fluorescence photomicrographs of PPQ_{50}-b-PS_{300} aggregates as described in Figure 10: (Figure 25A) Spherical, (Figure 25B) lamellar, (Figure 25C) cylindrical, and (Figure 25D) vesicular aggregates.

Figures 26A-C show a fluorescence photomicrograph of PPQ-b-PS showing spheres (Figure 26A), lamellae (Figure 26B), and cylinders (Figure 26C).

Figure 27 shows examples of 3-D shaped objects that could be prepared by molecular self-assembly.

Figures 28A-F show scanning electron micrographs of the typical morphologies of triblock copolymers PPQ_{50}-b-PS_{500}-b-PPQ_{50} (55a) (Figure 28A, Figure 28B, Figure 28E); PPQ_{50}-b-PS_{250}-b-PPQ_{50} (55b) (Figure 28C, Figure 28F); PPQ_{50}-b-PS_{120}-b-PPQ_{50} (55c) (Figure 28D). Drops of dilute solutions (0.5 to 1.0 mg/ml) of the triblock copolymers (6:4 TFA:DCM, 25°C) were spread and dried on aluminum substrates (Figures 28A-E) or a copper grid (Figure 28F), respectively.

Figures 29A-D show TEM images of aggregates prepared from 5:5 TFA:DCM solutions at 20 °C. (Figure 29A) PPQ_{10}-b-PS_{300} (54f); (Figure 29B) PPQ_{50}-b-PS_{300} (54c); (Figure 29C) PPQ_{50}-b-PS_{500}-b-PPQ_{50} (55a); (Figure 29D) PPQ_{50}-b-PS_{250}-b-PPQ_{50} (55b).

Figures 30A-C show optical micrographs of aggregates of PPQ_{50}-b-PS_{300} containing 5 wt.% solubilized C_{60}. Figure 30A shows a sample from 1:1 TFA:DCM under bright field. Figure 30B shows a sample from 1:1 TFA:toluene under cross-polarizers. Figure 30C shows a schematic illustration of the cross-section of a spherical block copolymer aggregate with encapsulated fullerene-C_{60}.

Figure 31 shows TGA thermograms of homopolymer PPQ and PS, diblock copolymers **54a-g**, and triblock copolymers **55a-c** obtained in flowing nitrogen with a heating rate of 10 °c/min.

Figure 32 shows ^{1}H NMR shifts in δ (ppm) of PPQ_{50}-b-PS_{500}-b-PPQ_{50} (**55a**) in deuterated nitrobenzene/GaCl$_3$.

Figure 33 shows the FTIR spectrum of PPQ_{10}-b-PS_{300} (**54f**) in NaCl disk.

Figure 34 shows the micellar solubilization of C_{60} and C_{70} in TFA/DCM or TFA/toluene when PPQ_{50}-b-PS_{300} (**54c**) or PPQ_{10}-b-PS_{300} (**54f**) was present.

Figures 35A-C show optical absorption spectra of solutions of (Figure 35A) pure PPQ_{50}-b-PS_{300} (1:1 TFA:DCM, 0.05 wt.%), (Figure 35B) 5 wt % C_{60}/ PPQ_{50}-b-PS_{300} (1:1 TFA:DCM, 0.05 wt.%), and (Figure 35C) C_{60} in CS$_2$ (0.05 wt.%). Inset is the magnified spectrum of the 5 wt.% C_{60}/ PPQ_{50}-b-PS_{300} in the region of 450-700 nm.

Figure 35 shows the optical absorption spectra of solutions of 5 wt.% C_{70}/ PPQ_{50}-b-PS_{300} and 5 wt.% C_{70}/PPQ_{10}-b-PS_{300} (1:1 TFA:DCM, 0.05 wt.%). Also shown for comparison are the spectra of C_{70} in CS$_2$ (0.05 wt.%) and pure PPQ_{50}-b-PS_{300} (1:1 TFA:DCM, 0.05 wt.%).

Figure 37 show the normalized absorbance of fullerene-PPQ-PS solutions as a function of fullerene loading: (Figure 37A) C_{60}-PPQ-PS system and (Figure 37B) C_{70}-PPQ-PS system. The solvent is TFA/DCM (1/1, v/v).

Figure 38 shows fluorescence (Figures 38A and B) and polarized optical (Figure 38C) micrographs of aggregates of PPQ_{50}-b-PS_{300} containing 0.1 wt.% solubilized C_{70} and (Figure 38D) fluorescence optical micrograph of 0.1 wt.% C_{60} in PPQ_{50}-b-PS_{300}.

Figure 39 shows Fluorescence (Figures 39A and B) and polarized optical (Figure 39C) micrographs of aggregates of PPQ_{50}-b-PS_{300} containing 1 wt.% solubilized C_{60} prepared from 4:1 TFA:toluene.

Figure 40 shows fluorescence (Figures 40A and C) bright field (Figure 40B) and polarized optical (Figure 40D) micrographs of aggregates of PPQ_{50}-b-PS_{300} containing 6 wt.% solubilized C_{60} prepared from 1:1 TFA:DCM.

Figure 41 shows bright field optical micrographs of films of PPQ_{50}-b-PS_{300} aggregates dried from solutions containing 8 wt.% (Figure 41A) and 10 wt.% (Figure 41B) C_{60}.

5   Figure 42 shows the average diameters of spherical fullerene/PPQ-PS aggregates as a function of fullerene loading and block copolymer composition. The line is only a guide to eyes.

          Figure 43A shows DSC scans of PS homopolymer (1), pure C_{60} (2), and 3 wt.% C_{60}/PPQ$_{50}$-b-PS$_{300}$ aggregates. Figure 43B shows DSC scans of 1 wt.% C_{60}
10   dispersed in PS homopolymer. The inset is the scan magnified in the region 250K to 290K.

          Figures 44A-C show PL and PLE spectra of spherical PPQ$_{50}$-b-PS$_{300}$ aggregates containing no C_{60} (a), 1 wt.% C_{60} (Figure 44B) and 5 wt.% C_{60} (Figure 44C). The excitation wavelength for the PL spectra were 380 nm (Figure 44A), 360 nm (curve
15   1) and 475 nm (curve 2) (Figure 44B), and 475 nm (Figure 44C). The emission wavelengths monitored for the PLE spectra were 480 nm (Figure 44A), 480 nm (curve 3) and 600 (curve 4) (Figure 44B), and 600 nm (Figure 44C).

          Figure 45 shows a fullerene solubilization and encapsulation induced transformation of PPQ-PS rod-coil diblock copolymer chains in H-aggregates to J-
20   aggregates.

          Figures 46A-B shows TGA thermograms of block copolymer samples PPQ$_{50}$-b-PS$_{300}$ (**54c**) and PPQ$_{10}$-b-PS$_{300}$ (**54f**) and the PPQ and PS homopolymers at 10 °C/minute in N$_2$.

          Figures 47A-C show fluorescence photomicrographs of solution cast
25   micellar films of PPQ$_{10}$-b-PS$_{300}$ obtained by ambient air drying of different rod-coil block solution concentrations in CS$_2$: (Figure 47A) 0.005 wt.%; (Figure 47B) 0.01 wt.%; and (Figure 47C) 0.05 wt.%. Arrows in B indicate regions of self-ordering.

          Figures 48A-D show (Figure 48A) Polarized optical and (Figures 48B and C) SEM micrographs of microporous micellar films obtained from a 0.5 wt.% PPQ$_{50}$-b-
30   PS$_{2000}$ rod-coil block copolymer solution by solution casting on a glass slide and an aluminum substrate, respectively. The SEM samples were coated with a 10 nm gold layer. The SEM image in 48B is the top view and that in 48C is of the same sample tilted 45° from the beam axis to reveal 3-D structure. Figure 48D shows a variation of hole diameter (*D*), periodicity (*p*) and minimum wall thickness (*h*) of ordered microporous
35   films with the number of PS repeat units in the rod-coil block copolymers.

          Figures 49A-B show (Figure 49A) a polarized optical micrograph of a microporous micellar film of PPQ$_{10}$-b-PS$_{300}$ obtained from a 0.5 wt % solution containing

5   5 mg C_{70} /g rod-coil block copolymer and (Figure 49B) the dependence of microstructural

        parameters of micellar films of the same rod-coil block copolymer on fullerene loading.

                Figures 50A-B show the (Figure 50A) PL emission (390-nm excitation)

        and PLE excitation (460-nm emission) spectra of a micellar film of PPQ_{10}-b-PS_{300} and of

        the same rod-coil block copolymer chains homogeneously dispersed (0.1 wt.%) in a

10   poly(ethylene oxide) (PEO) film and (Figure 50B) PL decay dynamics of the same

        samples in A when excited at 360 nm and monitored at 490 nm.

DETAILED DESCRIPTION OF THE INVENTION

                The present invention relates to a method for producing microstructures,

15   nanostructures, or objects. This method involves providing a rod-coil block copolymer

        including a rigid-rod block and a flexible-coil block, mixing the rod-coil block copolymer

        and a selective solvent for one of the blocks which solubilizes that block, and permitting

        the rod-coil block copolymer to self-assemble into organized mesostructures with a

        region of the unsolubilized block and a region of the solubilized block.

20   Preferred rod-coil block copolymer architectures for the present invention

        include AB rod-coil diblock and ABA rod-coil-rod triblock copolymers illustrated in

        Figure 1, where A denotes a rigid-rod block and B denotes a flexible-coil block.

                Preferred rigid-rod blocks include polyquinolines (1) (Jenekhe et al.,

        Science 279:1903-1907 (1998); Agrawal et al., Macromolecules 26:895-905 (1993),

25   which are hereby incorporated by reference), polyquinoxalines (2), poly(p-phenylenes)

        (3, 4), poly(p-phenylene vinylenes) (5, 6), polypridines (7), poly(pyridine vinylenes) (8),

        poly(naphthylene vinylenes) (9, 10), polythiophenes (11), poly(thiophene vinylenes) (12),

        polypyrroles (13), polyanilines (14), polybenzimidazoles (15), polybenzothiazoles (16),

        polybenzoxazoles (17), and polybenzobisazoles (18-20) (Figure 2). Additional preferred

30   rigid-rod blocks include aromatic polyamides (21-24), aromatic polyhydrazides (25-27),

        aromatic polyazomethines (28-30), aromatic polyesters (31-33), and aromatic polyimides

        (34) (Yang, Aromatic High Strength Fibers, Wiley-Interscience, New York, (1989),

        which is hereby incorporated by reference) (Figure 3).

                Preferred flexible-coil blocks include polystyrene (35, PS), poly(α-methyl

35   styrene) (36, PMS), poly(ethylene oxide (37, PEO), poly(propylene oxide) (38, PPO),

        poly(acrylic acid) (39, PAA), poly(methylacrylic acid) (40, PMAA), poly(2-

        vinylpyridine) (41, P2VP), poly(4-vinylpyridine) (42, P4VP), polyurethane (43, PU),

5   poly(vinyl pyrrolidone) (**44**), poly(methyl methacrylate) (**45**, PMMA), poly(n-butyl
methacrylate) (**46**, PBMA), polyisoprene (**47**, PI), poly(butadiene) (**48**, PB),
poly(dimethylsiloxane) (**49**, PDMS), poly(styrene sulfonic acid) (**50**, PSSA), and sodium
poly(styrene sulfonate) (**51**, PSSNa) (Webber et al., Solvents and Self-Organization of
Polymers, Kluwer Academic, Dordrecht, (1996); Hamley, The Physics of Block

10 Copolymers, Oxford University Press, Oxford, (1998), which is hereby incorporated by
reference) (Figure 4).

Preferred selective solvents include those solvents or mixtures of solvents
which are selective for only the parent rigid-rod polymer, only the parent flexible-coil
polymer, and solvents or mixtures of solvents which dissolve only one block in a block

15 copolymer. As known in the art, a selective solvent is chosen by selecting a solvent from
the list of solvents known in the art and commonly tabulated for the parent rigid-rod
polymer and for the parent flexible-coil polymer (Brandrup et al., Polymer Handbook, 3rd
ed., Wiley-Interscience, New York, (1989), which is hereby incorporated by reference) or
mixtures of such known solvents for respectively the rigid-rod and flexible-coil polymers.

20 Thus, for the rod-coil poly(phenylquinoline) (PPQ)-*block*-polystyrene (PS) (PPQ-PS)
diblock copolymers, PPQ-PS-PPQ triblock copolymers, polyquinoxaline (PQx)-*block*-
polystyrene (PQx-PS) diblock copolymers, or PQx-PS-PQx triblock copolymers,
preferred selective solvents for the rigid-rod block include trifluoroacetic acid ("TFA"),
mixtures of TFA and dichloromethane, and mixtures of TFA and toluene. Preferred

25 selective solvents for rod-coil block copolymers comprising PS or PMS blocks include
carbon disulfide (CS_2), 1-nitropropane, ethylbenzene, cyclohexanone, and mixtures
thereof. Preferred selective solvents for rod-coil block copolymers comprising PEO,
PAA, PMAA, PSSA, or PSSNa blocks include water, dioxane/water, formamide, N,N-
dimethyl-formamide ("DMF"), ethanol, methanol, and mixtures thereof.

30 Preferred temperatures of the solution or surface where self-organization
of the rod-coil block copolymer is to take place varies from 20 °C up to about 5-25 °C
above the boiling point of the solvent. Typically, the self-assembly temperature is
between room temperature (about 22-25 °C) and 100 °C.

Preferred concentrations of rod-coil block copolymer in solution at room
35 temperature for self-assembly of nanostructures, microstructures, or objects include
concentrations greater than the critical micelle concentration (cmc) or the critical
vesiculation concentration (cvc). The cmc (or cvc) of a block copolymer is the
concentration below which the copolymer exists as individual molecules or chains in

5   solution and above which it exists primarily as aggregated species, and typically has

values of about 10^{-8} to 10^{-4} Molar or less (Tuzar et al., Surface and Colloid Science, 15:1-

83 (1993); Weber et al., Solvents and Self-Organization of Polymers, Kluwer Academic,

Dordrecht (1996), which are hereby incorporated by reference). A preferred solution

concentration for self-assembly of the rod-coil block copolymers of the invention is

10   between 10^{-4} wt.% (0.0001 wt.%) to 10.0 wt.% at room temperature. Evaporation of

solvent from solutions initially at room temperature by ambient air drying or by the

application of heat necessarily changes the initial solution concentration.

In a preferred embodiment of the present invention, the rod-coil block

copolymer has the diblock architecture: rod block$_m$coil block$_n$. Preferably, m=1 to 500

15   and n=10 to 5,000.

In another preferred embodiment, the rod-coil block copolymer has the

triblock architecture: rod block$_m$coil block$_n$rod block$_m$. Preferably, m=1 to 500 and n=10

to 5,000.

Preferred rod-coil block copolymers for use in the present invention are

20   poly(phenylquinoline)-*block*-polystyrene ("PPQ-b-PS") (**54a-g**, Figure 5) and

poly(phenylquinoline)-*block*-polystyrene-*block*-poly(phenylquinoline) ("PPQ-b-PS-b-

PPQ") (**55a-c**, Figure 6). The poly (phenylquinoline) (**1**, PPQ) homopolymer is a

conjugated polymer with high modulus and thermal stability, and found to exhibit liquid

crystalline ordered phases in solution (Sybert et al., Macromolecules, 14:493-502 (1981),

25   which is hereby incorporated by reference). It is soluble in strong acid, such as sulfuric

acid, trifluoroacetic acid, and its optical, optoelectronic, and electrochemical properties

have been reported (Agrawal et al., Macromolecules 26:895-905 (1993); Agrawal et al.,

Chem. Mater., 8:579-589 (1996), which are hereby incorporated by reference). The

polystyrene (**35**, PS) is a well-known non-photoactive and non-electroactive polymer,

30   soluble in common organic solvents such as tetrahydrofuran (THF), dichloromethane,

carbon disulfide (CS_2), and chloroform. Thus, PPQ-b-PS (**54**) and PPQ-b-PS-b-PPQ (**55**)

represent amphiphilic rod-coil diblock (Figure 5) and rod-coil-rod triblock copolymers

(Figure 6). Amphiphilic PPQ-b-PS (Figure 7) rod-coil block copolymers self-organize

into robust, micrometer-scale, spherical, vesicular, cylindrical, and lamellar aggregates

35   from solution. The heterocyclic rigid-rod polyquinoline block of the rod-coil block

copolymers allows tuning of their amphiphilicity. For example, through protonation or

quarternization of the imine nitrogen (Sybert et al., Macromolecules, 14:493-502 (1981);

Agrawal et al., Macromolecules, 26:895-905 (1993); Agrawal et al., Chem. Mater.,

5   8:579-589 (1996), which are hereby incorporated by reference), the rod-like block can be

turned into a polyelectrolyte. The π-conjugated nature of the rigid-rod block confers

electroactive and photoactive properties (Sybert et al., Macromolecules, 14:493-502

(1981); Agrawal et al., Macromolecules, 26:895-905 (1993); Agrawal et al., Chem.

Mater., 8:579-589 (1996); Jenekhe et al., Photonic and Optoelectronic Polymers,

10   American Chemical Society, Washington, DC, (1997), which are hereby incorporated by

reference) on the block copolymers while providing novel ways of probing the self-

assembly, molecular packing, morphology, and dynamics of the polymeric amphiphiles

by optical and photoelectronic techniques. The PPQ-b-PS copolymers, in selective

solvents for PPQ, form large aggregates with various morphologies (spheres, vesicles,

15   cylinders, and lamellae) that can be observed by optical microscopy (OM).

The amide linkage at the rod-coil interface in each block copolymer chain

provides a means of strong intermolecular interactions, through hydrogen bonding, that

enhance the stability of self-organized structures. More specifically, secondary amide

linkages (-NH-CO-) and their associated hydrogen bonding, when strategically placed,

20   can limit the number of possible arrangement of molecules in space with respect to one

another as has been successfully done in the field of crystal engineering of hydrogen-

bonded solid state structures (Figure 8) (MacDonald et al., Chem. Rev., 94:2383-2420

(1994), which is hereby incorporated by reference). Amide linkages may be incorporated

at the interfaces in AB and ABA block copolymers as shown in Figures 1, 9, and 10. In

25   addition to the strong and directional intermolecular interactions, such hydrogen bonding

also introduces the highly desired and novel feature of well-defined, sharp and precisely

controllable interfaces (Figures 9 and 10). In addition, a large conformational asymmetry

is introduced between the blocks by the presence of rigid-rod A blocks and flexible-coil B

blocks in the same macromolecule. The conformational asymmetry introduces

30   amphiphilicity and enhances the driving force for microphase separation and hence self-

assembly of rod-coil block copolymers; this further restricts the possible orientation of the

macromolecules in space (Figures 9 and 10). Moreover, although van der Waals

interactions are in general nondirectional and very weak in flexible chain polymers, and

heretofore difficult to use for molecular self-assembly (Whitesides et al., Science,

35   254:1312-1319 (1991), which is hereby incorporated by reference), they are relatively

more directional and can be very strong between rigid-rod polymers. Thus rigid rod-like

blocks also provide well-defined surfaces for directing and maximizing van der Waals

5   forces. Synthesis of rod-coil block copolymers imprinted with these structural features

produce macromolecular building blocks with encoded information for 3-D self-

assembly. Many specific structures are possible for implementing these ideas. Those

shown in Figures 1-11 are examples that can be readily synthesized and characterized.

These structures include blocks that are either soluble in organic solvents or in aqueous

10   media. The conjugated structure of some of the rod-like blocks is designed to introduce

electroactive and photoactive properties into self-assembled mesostructures. However,

non-conjugated rigid-rod blocks can also be readily utilized as shown in Figure 3.

Some specific areas of possible near-term technological impact due to the

rod-coil block copolymers of the present invention are novel types of ultralarge micelles,

15   colloids, microemulsions and macroemulsions that are thermodynamically stable,

polymer surface modification, photoregulation of surface properties, novel molecular

containers for encapsulation of large molecules or nanoparticles, novel self-assembled

nanoporous/microporous materials for photonic band gap applications, separation

membranes, scaffolds for tissue engineering, and photonic and optoelectronic materials.

20   In another embodiment, the present invention further includes evaporating

the solvent after permitting the rod-coil block copolymer to self-assemble into organized

mesostructures with a region of the unsolubilized block and a region of the solublized

block.

In another aspect of the present invention, the rod-coil block copolymers

25   of the present invention may be also be used as a compatibilizer in a method of making

molecular composites and nanocomposites of flexible-coil polymers and rigid-rod

polymers. This method involves providing a solution of flexible-coil polymer and rigid-

rod polymer and adding a rod-coil block copolymer of the present invention to the

solution under conditions effective to form a substantially fine dispersion of the flexible-

30   coil polymer and rigid-rod polymer.

Because of the fundamental thermodynamic incompatibility of mixtures of

rod-like and coil-like polymers (Flory, Macromolecules, 11:1138-1141 (1978); Roberts,

et al., Chem. Mater., 6:135-145 (1994), which are hereby incorporated by reference), they

phase separate into large domains. Among the consequences of this macrophase

35   separation are poor mechanical properties, poor optical properties such as transparency,

and lack of control and stability in the morphology of the blend. As a novel class of

polymeric surfactants, the rod-coil block copolymers of the present invention function as

compatibilizers of mixtures of rod-like and coil-like polymers by segregating to the

5   interface between the phases in ways similar to how coil-coil block copolymers are

known to compatibilize blends of coil-like polymers (Datta. et al., Polymeric

Compatibilizers, Hamser Publishers, Munich, (1996), which is hereby incorporated by

reference). The compatibilization mechanism is thus accomplished by reducing the

interfacial tension between the rigid-rod polymer and flexible-coil polymer phases and by

10   reducing the tendency of phases/domains to coalesce, both factors leading to reduction in

phase sizes and improved adhesion between the phases. By use of the rod-coil block

copolymers of the present invention in this way to compatibilize mixtures of rigid-rod and

flexible-coil polymers, blends, nanocomposites, and molecular composites with fine

dispersion (smaller phase sizes) are obtained, leading to improved mechanical properties

15   for structural applications and improved optical and transport (barrier) properties. The

present rod-coil block copolymers are thus useful means to control and stabilize the

morphology and properties of blends, nanocomposites. and molecular composites of rod-

like and coil-like polymers.

The present invention also relates to a microstructure, nanostructure, or

20   object including a rod-coil block copolymer which includes a rigid-rod block and a

flexible-coil block, wherein the rod-coil block copolymer forms an organized

mesostructure with a region of one block and a region of the other block.

Another aspect of the present invention is an optical article including a

microstructure, nanostructure or object which includes a rigid-rod block and a flexible-

25   coil block, wherein the rod-coil block copolymer forms an organized mesostructure with

a region of one block and a region of the other block and an optical component, wherein

the microstructure, nanostructure or object is formed as a coating on the optical

component.

The present invention also relates to a method for producing a mesoporous

30   solid. This method involves providing a rod-coil block copolymer comprising a rigid-rod

block and a flexible coil block, mixing the rod-coil block copolymer and a selective

solvent for the flexible coil block which solubilizes that block, permitting the rod-coil

block copolymer to self-assemble into organized mesostructures with a region of the

unsolubilized block and a region of the solubilized block, evaporating the solvent, and

35   permitting the organized mesostructures to self-organize into a mesoporous solid.

Rod-coil block copolymers in a selective solvent for the coil-like polymer

self-organize into hollow spherical micelles having diameters depending on the molecular

weight and composition. Long-range, self-ordering of the micelles produces highly

iridescent periodic mesoporous materials (i.e., photonic crystals- structures that can create and manipulate light signals precisely, transmitting certain wavelengths while blocking others). In particular, aggregation in a selective solvent for the flexible-coil block induces spontaneous micellization, forming thermodynamically stable large micelles (>100nm) which after solvent evaporation produce mesoporous membrane films (Figure 12). The underlying mechanism which produces the periodic (ordered) mesoporous solid film appears to be a type of colloidal crystallization as the micellar particle density increases with increasing concentration due to evaporation. Further solvent evaporation after colloidal crystallization and lattice formation appears to be followed by interdigitation of the flexible coil chains of the corona layer. Investigation of the influence of composition and architecture on the properties of the micellar suspensions and of the mesoporous solids allows the tuning of the geometric and physical properties of these self-assembled periodic mesoporous materials which may find applications such as photonic crystals, separation membranes, drug delivery vehicles, and scaffold for tissue engineering.

Solution cast micellar films consist of multilayers of hexagonally ordered arrays of spherical holes whose diameter, periodicity, and wall thickness depend on copolymer molecular weight and composition. Addition of guest molecules, such as fullerenes, into the copolymer solutions in a selective solvent for the flexible-coil block also regulates the microstructure and optical properties of the mesoporous films. These results demonstrate the potential of direct hierarchical self-assembly of macromolecular components for engineering complex two- and three-dimensional periodic and functional mesostructures, without using templates or using conventional microfabrication techniques.

Because the size, mesostructure, and properties of micellar building blocks can be tailored through copolymer architecture and composition as well as the solution chemistry (McConnell et al., Phys Rev. Lett., 71:2102-2105 (1993); McConnell et al., Macromolecules, 28:6754-6764 (1995); McConnell et al., Macromolecules, 30:435-444 (1997); McConnell et al., Phys. Rev. E., 54:5447-5455 (1996); Webber et al., Solvents and Self-Organization of Polymers, Kluwer Academic, Dordrecht (1996); Webber, J. Phys. Chem. B, 102:2618-2626 (1998); Tuzar et al., in Surface and Colloid Science, 15:1-83, Plenum, New York (1993); Halperin et al., Adv. Polym. Sci., 100:31-71 (1992); Förster et al., Adv. Mater., 10:195-217 (1998); Zhang et al., J. Am. Chem. Soc., 118:3168-3181 (1996); Zhang et al., Science, 268:1728-1731 (1995), which are hereby incorporated by reference), this hierarchical self-assembly approach is general for

5   preparing periodic mesoporous polymeric materials. By combining different micellar building blocks and other colloidal particles, self-assembly of very unusual periodic mesoscopic structures with tailorable functions is possible. In particular, different micellar building blocks and colloidal particles can be incorporated into the walls of the mesoporous solids produced by rod-coil block copolymers. Suitable micellar building

10   blocks include micelles from different rod-coil block copolymers and colloidal particles which include dendrimers, polymer lattices, inorganic semiconductor nanocrystals, such as TiO_2, CdS, CdSe, GaAs, and PbS, silver colloids, gold colloids, and peizoelectric ceramic particles. Besides photonic band gap materials and their associated applications (Yablonovitch, J. Opt. Soc. Am. B., 10:283-295 (1993); Joannopoulos et al., Nature,

15   386:143-145 (1997); Martorell et al., Phys. Rev. Lett., 65:1877-1880 (1990); Miguez et al., Appl. Phys. Lett., 71:1148-1150 (1997), which are hereby incorporated by reference), the ordered micellar films and their self-assembly process may have uses in tissue engineering and biomaterials (Fendler, Membrane Mimetic Chemistry, Wiley, New York (1982), which is hereby incorporated by reference), fabrication of molecular electronic

20   devices (Carter, Ed., Molecular Electronics II, Marcel Dekker, New York (1987), which is hereby incorporated by reference), separation media, sensors, optically tunable and responsive coatings, and processing of "soft" colloidal materials.

      Applications are widespread for a device that selectively filters out certain wavelengths, or colors, of light. Optical data storage and telecommunications rely on

25   transmission and detection of specific wavelengths, and holographic memory systems are expected to do the same. The mesoporous solids of the present invention make possible better light-emitting diodes (LEDs), materials that are increasingly being used to produce more efficient lighting systems. Also possible are special paints that change colors under different light conditions -- perhaps lighter in the harsh glare of sunlight and darker under

30   incandescent light. Another potential application: a super-efficient laser that could produce intense light with a fraction of the energy now required. (Yablonovitch, J. Opt. Soc. Am. B., 10:283-295 (1993), which is hereby incorporated by reference).

      Yet another aspect of the present invention is a method for tissue engineering. This method includes providing a mesoporous solid, adding a cell culture to

35   the mesoporous solid, and allowing the cells to grow on the mesoporous solid under conditions effective to produce an organized tissue layer.

      The present invention also relates to a method for producing a polymer adsorption layer or "brush" on a substrate. This method involves providing a rod-coil

5   block copolymer including a rigid-rod block and a flexible-coil block, mixing the rod-coil
     block copolymer and a selective solvent for one of the blocks to form a solution of rod-
     coil block copolymer and solvent, inserting a substrate into the solution, permitting the
     rod-coil block copolymer to adsorb to the substrate, and removing the substrate from the
     solution under conditions effective to form an adsorption layer of a polymer on the

10   substrate.

            Preferred substrates include glass, plastics, metals, semiconductors (e.g., Si
     wafers with or without an oxide layer) glass coated with indium-tin-oxide (ITO) or
     aluminum or other metal, glass or plastic with a plasma treated surface, mica, patterned
     substrates, and chemical functionalized substrates.

15   In a preferred embodiment, the adsorption layer of a polymer is an
     adsorption layer of a rigid-rod polymer block of a rod-coil block copolymer (Figure 13).

            Aggregation of the rod-coil block copolymers at surfaces produces
     adsorption layers of rigid-rod polymers or so-called polymer brushes. There are no
     literature reports of rigid-rod polymer brushes, although much work has been done in the

20   past 15 years on adsorption layers of flexible coil polymers (Halperin et al., Adv. Polym.
     Sci., 100:31-71 (1992); Tuzar et al., Surface and Colloid Science, 15:1-83 (1993); Weber
     et al., Ed., Solvents and Self-Organization of Polymers, Kluwer Academic, Dordrecht
     (1996); Zhang et al., Science, 272:1777-1779 (1996), which are hereby incorporated by
     reference). The order, precise interfaces, and self-organization capability of the rod-coil

25   copolymers suggest that the resulting adsorption layers (Figure 13) will have many novel
     properties of interest for adhesion and adhesives, surface modification, fluorescent
     surfaces, reflective signs/displays, waveguides, coatings, and photoregulation of surface
     properties (smart surfaces).

            Another aspect of the present invention is a substrate with a polymeric

30   adsorption layer, wherein the adsorption layer is a rod-coil block copolymer including a
     rigid-rod block and a flexible-coil block, wherein one of the blocks of the rod-coil block
     copolymer is adsorbed to the substrate.

            The present invention also relates to an optical article including a
     substrate, a transparent conductor formed as a coating on the substrate, an adsorption

35   layer of a polymer including a rod-coil block copolymer including a rigid-rod block and a
     flexible-coil block formed on the transparent conductor, and a coating formed on the
     surface of the adsorption layer, wherein the adsorption layer allows the emission of
     polarized light.

5   Another aspect of the present invention is a method for encapsulating
guest molecules, macromolecules, or nanoparticles. This method involves providing a
rod-coil block copolymer including a rigid-rod block and a flexible-coil block, mixing the
rod-coil block copolymer with a selective solvent for one of the blocks which solubilizes
that block to form a solution of rod-coil block copolymer and solvent, adding guest

10   molecules, macromolecules, or nanoparticles to the solution, and permitting the rod-coil
block copolymer to self-assemble into mesostructures with a region of the unsolubilized
block and a region of the solubilized block under conditions effective to encapsulate the
guest molecules, macromolecules, or nanoparticles.

          As used herein, guest molecules are defined as molecules deliberately

15   added that are not a solvent or the self-assembling rod-coil block copolymer. Guest
molecules may include oligomers which are defined as polymers including from about 2
to about 20 repeat units.

          As used herein, macromolecules are defined as polymers other than the
self-assembling rod-coil block copolymer. Macromolecules are defined as polymers

20   including from about 20 to about 5000 repeat units.

          As used herein, nanoparticles are defined as particles ranging from about 1
nm to about 100 nm.

          Preferred guest molecules, macromolecules, or nanoparticles include
fullerenes, carbon nanotubes, drug formulations, cosmetic formulations, metal particles,

25   semiconductor particles, and magnetic particles. In a preferred embodiment, the guest
molecule is a fullerene, most preferably C_{60} or C_{70}. Spherical fullerenes (i.e., C_{60}, C_{70})
can be solubilized to a large degree by solutions of the rod-coil block copolymers,
resulting in the encapsulation of large numbers (~10^3 to 10^{10}) of fullerene molecules.

          Encapsulating phenomena associated with micellar aggregates (Halperin et

30   al., Adv. Polym. Sci., 100:31-71 (1992); Tuzar et al., Surface and Colloid Science, 15:1-
83 (1993); Weber et al., Ed., Solvents and Self-Organization of Polymers, Kluwer
Academic, Dordrecht (1996); which are hereby incorporated by reference) are enhanced
in amphiphilic rod-coil block copolymers. In particular, it is possible to package guest
molecules, macromolecules, or even nanoparticles. The reason for this is the large size,

35   stability, and hollow cavity of these aggregates self-organized from rod-coil block
copolymer systems. Such an enhanced encapsulating capacity should be of interest for
pharmaceuticals, cosmetics, detergents, lubricants, and agricultural pesticide

5   formulations. (Benita, Ed., Microencapsulation: Methods and Industrial Applications,

Marcel Dekker, New York (1996), which is hereby incorporated by reference.)

Yet another aspect of the present invention is an organized mesostructure

with an encapsulated guest molecule, macromolecule, or nanoparticle which includes a

rod-coil block copolymer including a rigid-rod block and a flexible-coil block, wherein

10   the rod-coil block copolymer forms an organized mesostructure and a guest molecule,

macromolecule, or nanoparticle, wherein the guest molecule, macromolecule, or

nanoparticle is encapsulated within the mesostructure.

Another aspect of the present invention is a method for solubilizing guest

molecules, macromolecules, or nanoparticles. This method involves providing a rod-coil

15   block copolymer including a rigid-rod block and a flexible-coil block, mixing the rod-coil

block copolymer with a selective solvent for one of the blocks which solubilizes that

block to form a solution of rod-coil block copolymer and solvent, adding guest molecules,

macromolecules, or nanoparticles to the solution, and permitting the rod-coil block

copolymer to self-assemble into mesostructures with a region of the unsolubilized block

20   and a region of the solubilized block under conditions effective to solubilize the guest

molecules, macromolecules, or nanoparticles.

EXAMPLES

Example 1 - Synthesis of Rod-Coil Block Copolymers

25

Materials

Polystyrenes with mono- or di- carboxylic acid-terminated functional

group (PS-COOH, HOOC-PS-COOH), which had a molecular weight (M_w) of 218400,

109200, 32760, 14200, respectively, for PS-COOH, and 54600, 27600, and 13100 for

30   HOOC-PS-COOH, and a polydispersity (M_w/M_n) of 1.05 (Scientific Polymer Products,

Inc., Ontario), were used without further purification. Reagents and solvents, such as 4-

aminoacetophenone, dichloromethane, toluene, trifluoroacetic acid, triethylamine,

ethanol, ethyl acetate, diphenyl phosphate were purchased from Aldrich (Milwaukee, WI)

and were used as received. *m*-Cresol was distilled under vacuum before use for the

35   polymerization. 5-Acetyl-2-aminobenzophenone (**52**) was synthesized according to the

method disclosed in Sybert, et al., Macromolecules, 14:493-502 (1981), which is hereby

incorporated by reference. Poly(ethylene oxide) (PEO) (M_w of 5,000,000, M_w/M_n ~2.8)

5   and polystyrene (M_w of 6,000,000, M_w/M_n ~1.2) were purchased from Polysciences, Inc. (Warrington, PA) and were used as received.

Synthesis

Mono-ketone methylene-terminated polystyrene (**53a**).

10   The end group modification reactions are exemplified by the experiment for the carboxylic acid-terminated PS with a M_w of 32760. A rapidly stirred solution of 100 g (3.18 mmol) of carboxylic acid terminated PS (PS-COOH) and 1.74 g (12.84 mmol) of 4-aminoacetophenone in 500 ml of toluene was heated at reflux for 24 hours in a 2-L flask equipped with a Dean-Stark trap. The solution was diluted with 500 ml of

15   toluene and 100 ml of 5 % aqueous HCl solution was added. The organic toluene layer was extracted twice with 100 ml 5 % aqueous HCl solution, washed with water, and dried with anhydrous magnesium sulfate. The toluene was then removed and the functionalized polystyrene was dried in a vacuum oven at 60 °C for 12 hours. The functionalized polystyrene (**53a**) was purified by twice redissolving in chloroform and

20   precipitating into methanol. The yield was 85%. The end groups of mono-functionalized PS (PS-COOH) with a M_w of 218400, 109200, and 14200, were similarly converted to ketone methylene functional units.

Diketone methylene-terminated polystyrene (**53b**).

25   The end group modification reactions are exemplified by the experiment for the dicarboxylic acid-terminated PS with M_w of 54,600. A rapidly stirred solution of 100 g (1.83 mmol) of dicarboxylic acid-terminated PS (HOOC-PS-COOH, M_w = 54,600) and 2.0 g (7.33 mmol) of 4-aminoacetophenone in 500 mL of toluene was heated at reflux for 24 hours in a 2-L flask equipped with a Dean-Stark trap. The reaction solution was

30   diluted with 500 mL of toluene and 100 mL of 5 % aqueous HCl solution was added. The organic toluene layer was extracted twice with 100 mL of 5 % aqueous HCl solution, washed with water, and dried with anhydrous magnesium sulfate. The toluene was then removed by rotary evaporator and the functionalized polystyrene was dried in a vacuum oven at 60 °C for 12 hours. The functionalized polystyrene (**53**) was purified by twice

35   redissolving in chloroform and precipitating into methanol. The yield was 85 %. The end groups of di-functionalized PS (HOOC-PS-COOH) with M_w of 27600 and 13100 were similarly converted to diketone methylene functional units.

5   Poly(phenylquinoline)-b-polystyrene diblock copolymers (54).

PPQ-b-PS block copolymers (PPQ$_{50}$-b-PS$_{2000}$, PPQ$_{50}$-b-PS$_{1000}$, PPQ$_{50}$-b-
PS$_{300}$, PPQ$_{50}$-b-PS$_{130}$, PPQ$_{10}$-b-PS$_{1000}$, PPQ$_{10}$-b-PS$_{300}$, and PPQ$_{10}$-b-PS$_{130}$ (54a-54g)) were
synthesized by copolymerization of 5-acetyl-2-aminobenzophenone (52) with PS-CONH-
Ph-COCH$_3$ (53a) as shown in Figure 5. The copolymerization is exemplified by the

10   preparation of PPQ$_{50}$-b-PS$_{300}$ (54c), as follows. 2.39 g (10 mmol) of 5-acetyl-2-
aminobenzophenone (52) and 6.31 g (0.2 mmol) of PS-CONH-Ph-COCH$_3$ (53a) were
added to a solution of 5 g of diphenyl phosphate (DPP) and 20 g of freshly distilled m-
cresol in a cylindrical glass flask fitted with a mechanical stirrer, two gas inlets, and a side
arm. The reactor was purged with argon for 10 minutes before the temperature was raised

15   slowly to 140 °C in 2-3 hours. As the viscosity of the reaction mixture increased with
time, small amounts of DPP were added, until a total of 20 g of DPP was reached. The
reaction was maintained at 140 °C for 48 hours under argon. The bright orange solution
product was cooled and precipitated into 500 mL of 10% triethylamine/ethanol mixture.
The final product was purified by soxlet extraction with 10% triethylamine/methanol for

20   48 hours to get rid of the residue m-cresol, DPP, and the un-reacted homopolymer PS,
because homopolymer PS can dissolve in hot methanol. The degree of polymerization of
the PPQ block (N$_A$) in the rod-coil diblock (A$_{N_A}$B$_{N_B}$) was controlled by the stoichiometric
method. Because the condensation reaction yields of copolymerization were 100%, the
polydispersity (M$_w$/M$_n$) of the PPQ blocks was estimated to be around the theoretically

25   expected value of 2 (Odian, Principles of Polymerization, 2nd ed., Wiley, New York,
Chapters 1 and 2 (1981), which is hereby incorporated by reference). 54c: Yield: 100%, [1]
H NMR (C$_6$D$_5$NO$_2$) δ: 1.5–1.6 (m, 2x300H), 2.2 (s, 1x300H), 6.7-6.8 (d, 2x300H), 7.3-
7.4 (m, 3x300H), 7.5 (m, 5x50H), 8.9 (d, 1x50H), 9.2 (s, 1x50H), 9.4-9.6 (d, 1x50H), 9.7
(s, 1x50H). FTIR (NaCl disc, cm^{-1}): 3060, 3025, 2920, 2850, 1677, 1600, 1492, 1451,

30   1346, 1204, 1180, 1134, 1028, 756, 698.

The diblock copolymers of PPQ$_{50}$-b-PS$_{2000}$ (54a), PPQ$_{50}$-b-PS$_{1000}$ (54b), PPQ$_{50}$-b-
PS$_{130}$ (54d), PPQ$_{10}$-b-PS$_{1000}$ (54e), PPQ$_{10}$-b-PS$_{300}$ (54f), and PPQ$_{10}$-b-PS$_{130}$ (54g) were
similarly prepared. 54a: Yield: 100%, [1] H NMR (C$_6$D$_5$NO$_2$) δ: 1.5–1.6 (m, 2x2000H), 2.2
(s, 1x2000H), 6.7-6.8 (d, 2x2000H), 7.3-7.4 (m, 3x2000H), 7.5 (m, 5x50H), 8.9 (d,

35   1x50H), 9.2 (s, 1x50H), 9.4-9.6 (d, 1x50H), 9.7 (s, 1x50H). FTIR (NaCl disc, cm^{-1}): 3060,
3025, 2920, 2850, 1677, 1600, 1492, 1451, 1346, 1204, 1180, 1134, 1028, 756, 698. 54b:
Yield: 100%, [1] H NMR (C$_6$D$_5$NO$_2$) δ: 1.5–1.6 (m, 2x1000H), 2.2 (s, 1x1000H), 6.7-6.8

5   (d, 2x1000H), 7.3-7.4 (m, 3x1000H), 7.5 (m, 5x50H), 8.9 (d, 1x50H), 9.2 (s, 1x50H), 9.4-
9.6 (d, 1x50H), 9.7 (s, 1x50H). FTIR (NaCl disc, cm^{-1}): 3060, 3025, 2920, 2850, 1677,
1600, 1492, 1451, 1346, 1204, 1180, 1134, 1028, 756, 698. **54d**: Yield: 100%, ^{1}H NMR
($C_6D_5NO_2$) δ: 1.5–1.6 (m, 2x130H), 2.2 (s, 1x130H), 6.7-6.8 (d, 2x130H), 7.3-7.4 (m,
3x130H), 7.5 (m, 5x50H), 8.9 (d, 1x50H), 9.2 (s, 1x50H), 9.4-9.6 (d, 1x50H), 9.7 (s,

10   1x50H). FTIR (NaCl disc, cm^{-1}): 3060, 3025, 2920, 2850, 1677, 1600, 1492, 1451, 1346,
1204, 1180, 1134, 1028, 756, 698. **54e**: Yield: 100%, ^{1}H NMR ($C_6D_5NO_2$) δ: 1.5–1.6 (m,
2x1000H), 2.2 (s, 1x1000H), 6.7-6.8 (d, 2x1000H), 7.3-7.4 (m, 3x1000H), 7.5 (m,
5x10H), 8.9 (d, 1x10H), 9.2 (s, 1x10H), 9.4-9.6 (d, 1x10H), 9.7 (s, 1x10H). FTIR (NaCl
disc, cm^{-1}): 3060, 3025, 2920, 2850, 1677, 1600, 1492, 1451, 1346, 1204, 1180, 1134,

15   1028, 756, 698. **54f**: Yield: 100%, ^{1}H NMR ($C_6D_5NO_2$) δ: 1.5–1.6 (m, 2x300H), 2.2 (s,
1x300H), 6.7-6.8 (d, 2x300H), 7.3-7.4 (m, 3x300H), 7.5 (m, 5x10H), 8.9 (d, 1x10H), 9.2
(s, 1x10H), 9.4-9.6 (d, 1x10H), 9.7 (s, 1x10H). FTIR (NaCl disc, cm^{-1}): 3060, 3025, 2920,
2850, 1677, 1600, 1492, 1451, 1346, 1204, 1180, 1134, 1028, 756, 698. **54g**: Yield:
100%, ^{1}H NMR ($C_6D_5NO_2$) δ: 1.5–1.6 (m, 2x130H), 2.2 (s, 1x130H), 6.7-6.8 (d,

20   2x130H), 7.3-7.4 (m, 3x130H), 7.5 (m, 5x10H), 8.9 (d, 1x10H), 9.2 (s, 1x10H), 9.4-9.6
(d, 1x10H), 9.7 (s, 1x10H). FTIR (NaCl disc, cm^{-1}): 3060, 3025, 2920, 2850, 1677, 1600,
1492, 1451, 1346, 1204, 1180, 1134, 1028, 756, 698.

Poly (phenylquinoline)-b-polystyrene-b-poly(phenylquinoline) triblock copolymers (**55**).

25   PPQ-*b*-PS-*b*-PS triblock copolymers (PPQ_{50}-b-PS_{500}-b-PPQ_{50}, PPQ_{50}-b-
PS_{250}-b-PPQ_{50}, and PPQ_{50}-b-PS_{120}-b-PPQ_{50} (**55a-c**)) were synthesized by block
copolymerization of 5-acetyl-2-aminobenzophenone (**52**) with **53b** (CH$_3$CO-Ph-NHCO-
PS-CONH-Ph-COCH$_3$), as shown in Figure 6. The copolymerization is exemplified by
the preparation of PPQ_{50}-b-PS_{500}-b-PPQ_{50} (**55a**), as follows. 2.39 g (10 mmol) of **52** and

30   5.20 g (0.1 mmol) of **53b** (M_w= 54600) were added to a solution of 5 g of diphenyl
phosphate (DPP) and 20 g of freshly distilled *m*-cresol in a cylindrical glass flask fitted
with a mechanical stirrer, two gas inlets, and a side arm. The reactor was purged with
argon for 10 minutes before the temperature was raised slowly to 140 °C in 2-3 hours. As
the viscosity of the reaction mixture increased with time, small amounts of DPP were

35   added, until a total of 20 g of DPP was reached. The reaction was maintained at 140 °C
for 48 hours under argon. The bright orange solution product was cooled and precipitated

5   into 500 mL of 10 % triethylamine/ethanol mixture to wash away the *m*-cresol and DPP.
       The final product was purified by Soxlet extraction with 10 % triethylamine/methanol for
       48 hours to get rid of the residue *m*-cresol, DPP, and the un-reacted homopolymer PS,
       because homopolymer PS can dissolve in hot methanol. The degree of polymerization of
       the PPQ block (N_A) in the rod-coil triblock copolymers ($A_{N_A}B_{N_B}A_{N_A}$) was controlled by

10   the stoichiometric method. Because the condensation reaction yields of copolymerization
       were 100%, the polydispersity (M_w/M_n) of the PPQ blocks was estimated to be around the
       theoretically expected value of 2. **55a** : Yield: 100%, [1] H NMR ($C_6D_5NO_2$) δ: 1.5–1.6 (m,
       2x500H), 2.2 (s, 1x500H), 6.7-6.8 (d, 2x500H), 7.3-7.4 (m, 3x500H), 7.5 (m, 5x100H),
       8.9 (d, 1x100H), 9.2 (s, 1x100H), 9.4-9.6 (d, 1x100H) , 9.7 (s, 1x100H). FTIR (NaCl

15   dics, cm⁻¹): 3060, 3025, 2920, 2850, 1677, 1600, 1492, 1451, 1346, 1204, 1180, 1134,
       1028, 756, 698.

               The copolymers of PPQ$_{50}$-b-PS$_{250}$-b-PPQ$_{50}$ (**55b**) and PPQ$_{50}$-b-PS$_{120}$-b-
       PPQ$_{50}$ (**55c**) were similarly synthesized. **55b**: Yield: 100%, [1] H NMR ($C_6D_5NO_2$)
       δ: 1.5–1.6 (m, 2x250H), 2.2 (s, 1x250H), 6.7-6.8 (d, 2x250H), 7.3-7.4 (m, 3x250H), 7.5

20   (m, 5x100H), 8.9 (d, 1x100H), 9.2 (s, 1x100H), 9.4-9.6 (d, 1x100H) , 9.7 (s, 1x100H).
       FTIR (NaCl disc, cm⁻¹): 3060, 3025, 2920, 2850, 1677, 1600, 1492, 1451, 1346, 1204,
       1180, 1134, 1028, 756, 698. **55c**: Yield: 100%, [1] H NMR ($C_6D_5NO_2$) δ: 1.5–1.6 (m,
       2x120H), 2.2 (s, 1x120H), 6.7-6.8 (d, 2x120H), 7.3-7.4 (m, 3x120H), 7.5 (m, 5x100H),
       8.9 (d, 1x100H), 9.2 (s, 1x100H), 9.4-9.6 (d, 1x100H), 9.7 (s, 1x100H). FTIR (NaCl disc,

25   cm⁻¹): 3060, 3025, 2920, 2850, 1677, 1600, 1492, 1451, 1346, 1204, 1180, 1134, 1028,
       756, 698.

Example 2 - Characterization of Block Copolymers

30   Thermogravimetric analysis (TGA) and differential scanning calorimetry
       (DSC) were done on a DuPont Model 2100 Thermal Analyst based on an IBM PS/2
       Model 60 computer and equipped with a Model 951 TGA unit and a Model 910 DSC
       unit. The DSC thermograms were obtained in nitrogen at a heating rate of 5°C/minute.
       The TGA data were obtained in flowing nitrogen at a heating rate of 10°C/minute. [1]H

35   NMR spectra were taken at 300 MHz, using a General Electric Model QE 300 instrument.
       Block copolymer solutions for ^{1}H NMR spectroscopy were prepared in a dry box, using
       deuterated nitrobenzene($C_6D_5NO_2$) containing gallium chloride. Fourier transform

5 infrared (FTIR) spectra were taken at room temperature using a Nicolet 20SXC FTIR
   spectrometer under nitrogen purge. Samples were either free-standing films or films
   coated on NaCl disks. The FTIR spectra of the parent PPQ and PS homopolymers were
   obtained as the free standing films from formic acid and dichloromethane solutions,
   respectively, whereas the spectra of the rod-coil block copolymers were obtained from
10 films coated on NaCl disks. The free standing films were prepared by removing films
   spin-coated on glass using a sharp razor blade after soaking the films in water for 12
   hours.

   Samples for observation by polarized optical microscopy (POM) and
   fluorescence microscopy (FM) were prepared by allowing several drops of a block
15 copolymer solution in TFA:DCM or TFA:toluene to spread and dry on glass slides. The
   various drying conditions explored are described below and were found not to influence
   the observed morphologies of aggregates (size, shape, and their distributions).
   Observations were done on an Olympus Model BX60 Fluorescence Optical Microscope.
   The glass slides were placed under an optical fluorescence microscope. Optical (bright
20 field, polarized light) and fluorescence images were recorded by a digital camera with 0.5
   inches CCD chips. The images were stored and processed by a PC computer equipped
   with Image Pro. (Media Cybernetics, Silver Spring, MD) software.

   Samples for scanning electron microscopy (SEM) were prepared by
   allowing several drops of a copolymer solution to spread and dry on aluminum substrates.
25 The samples were then coated with a thin layer of 100 Å gold.

   Films of solid aggregates were too scattering in the visible light region to
   obtain normal optical absorption spectra. Dilute solution optical absorption spectra of the
   copolymer samples and those of thin films of block copolymers dispersed (0.1 wt%) in
   poly (ethylene oxide) (PEO) were recorded on a Perkin-Elmer Model Lambda 9
30 UV/VIS/NIR Spectrophotometer at room temperature. For the measurements performed
   on solutions, the solutions were sealed inside 1-mm-path-length quartz cuvet to prevent
   solvent evaporation.

   Photoluminescence (PL) and photoluminescence excitation (PLE) spectra
   were obtained on a Spex Fluorolog-2 spectrofluorimeter. Time-resolved fluorescence
35 spectra were obtained by using a single-photon-counting technique. The solutions of the
   aggregates were similarly sealed inside a 1-mm-path-length quartz cuvet. Thin films and
   solutions of aggregates were measured by using the front face geometry in which samples
   were positioned such that the emission was detected at 22.5° from the incident radiation

5   beam. Further details of the photophysical experimental techniques used here are similar to those we have described in detail elsewhere (Osaheni et al., J. Am. Chem. Soc., 117:7389-7398 (1995), which is hereby incorporated by reference).

Example 3 - Aggregation Experiments

10   Self-assembly of aggregates of the rod-coil block copolymers described in Example 1 was done using various ratios of trifluoroacetic acid (TFA)/dichloromethane (DCM) and TFA/toluene, which are good selective solvents for the rigid-rod block. In these mixed solvents, the rigid-rod PPQ block was protonated and solvated by the TFA, forming a rod-like polyelectrolyte block in solution. Drying drops of dilute solutions (0.5

15   to 1.0 mg/ml) of PPQ-b-PS on substrates produced micelle-like aggregates because DCM and toluene, which are selective solvents for the PS block, had faster evaporation rates than TFA which is a selective solvent for the rigid-rod block. In contrast, thin films of the rod-coil block copolymers similarly prepared from nitrobenzene/GaCl₃ solutions (0.5 to 1 mg/ml), i.e., solutions in a nonselective solvent, did not reveal any characteristic

20   aggregate morphology under optical microscopy. These results suggested that block selective solvents facilitated the self-assembly of the amphiphilic rod-coil block copolymers. Films (~1 to 20 μm thick) resulting from drying dilute solutions of the copolymers or copolymer/solubilized fullerenes on glass slides or aluminum substrates at room temperature (or at high temperature, 95 °C) were investigated as made, or after

25   treating them in 5% triethylamine/ethanol (to remove any trace acids) and drying in a vacuum oven at 60 °C for 24 hours, or after heating to 200 °C for one hour (to ensure complete solvent evaporation). The films were investigated by SEM, POM, and FM microscopies as well as by photoluminescence (PL) spectroscopy. No difference in morphology was observed in the various film samples treated differently after drying.

30   However, the dominant morphology prepared from a particular diblock copolymer was highly dependent on the ratio of TFA:DCM or TFA:toluene of the mixed solvent used. These solid aggregates, when placed in a fresh clear TFA:DCM or TFA:toluene solvent mixtures, redissolved in solution and spontaneously re-assembled into aggregates corresponding to that particular solvent mixture. Such an easy dissolution of solid

35   aggregates and subsequent re-aggregation indicated the thermodynamic stability and equilibrium nature of the aggregates formed by diblock and triblock copolymers.

For real time optical microscopy observations, the dilute copolymer solutions (0.001 to 0.1 wt.%) were sealed inside 6 mm x 50 mm glass tubes. Periodic examinations of these dispersions showed that the aggregates were extremely robust and were stable in solution.

Dilute solutions (0.5 to 1.0 mg/ml) of each rod-coil block copolymer in mixed solvents, TFA:DCM or TFA:toluene at various volume ratios, were used for aggregation studies. Because TFA is a good solvent for PPQ block and protonates its imine nitrogens, whereas the PS block is insoluble in it, micelle-like aggregates (Figure 7) resulted from manipulating the solvent composition. In TFA solvent, PPQ blocks essentially were transformed to polyelectrolytes with positive charges. The electrostatic forces between protonated PPQ blocks and the surrounding negative counter-ions were expected to help stabilize the colloidal structures, just as the charged protein helps stabilize the natural rubber latex. By adding various amount of DCM, which is a selective solvent for PS, to TFA, the polarity and acidity of the solvent mixtures could easily be controlled, thus varying the strength of the hydrogen-bonding, electrostatic forces, and solvophobic effects. The hydrogen-bonding and electrostatic forces increased with the decrease in polarity, whereas the solvophobic effects had just the opposite relationship. For diblock copolymers, micelle-like aggregates can be expected (Figure 14) to result from manipulating the solvent composition. The expected structure of such an aggregate in the TFA solution is an inner PS block surrounded by the protonated PPQ shell. This basic aggregate structure is expected to be retained in the solid state after solvent evaporation, which also deprotonates the PPQ block (Figures 7 and 14). Rod-coil-rod triblock copolymers can either fold to form single loop-layers, or they can form bilayer tape-like structures as shown in Figure 14. Therefore, in selective solvents for the rigid rod blocks, triblock copolymers are expected to either form micelles from single loop-layers as diblock copolymer did, or form vesicles from bilayer tape-like structures (Figure 14). The self-assembly of a rod-coil block copolymer in a selective solvent for the rigid-rod block has not been theoretically investigated (Semenov et al., Sov. Phys. JETP, 63:70-79 (1986); Semenov, Mol. Cryst. Liq. Cryst., 209:191-199 (1991); Halperin, Macromolecules, 23:2724-2731 (1990); Halperin, Europhys. Lett., 10:549-553 (1989); Williams et al., Macromolecules, 25:3561-3568 (1992); Raphael et al., Makromol. Chem.. Macromol. Symp., 62:1-17 (1992), which are hereby incorporated by reference) but is experimentally accessible here because of the differential solubility of PPQ and PS

5   blocks. Self-assembly of discrete aggregates of the rod-coil block copolymers did not

occur from solutions in non-selective solvents, such as nitromethane containing GaCl$_3$.

Four different, micelle-like aggregate morphologies were observed in

PPQ$_{50}$-b-PS$_{300}$ (54c) by OM, FM, and SEM: spheres, lamellae, cylinders, and vesicles

(Figures 15 and 16). The main factors determining morphology were the initial solvent

10   composition (TFA:DCM ratio) and the solution drying rate. The cylindrical aggregates

were obtained from highly polar solvents with TFA/DCM ratio of 9/1. They were

relatively uniform in diameter (1 to 3 μm) but highly polydisperse in length (5 to 25 μm),

coexisting with minor phase-spherical aggregates. Spherical aggregates with a wide

distribution of sizes, typically 0.5 to 10 μm diameters, were observed by rapid drying of

15   solutions on a heated substrate at 95 °C and by preparing aggregates from solutions from

a TFA/DCM ratio of 4/1. Further reducing the TFA/DCM ratio resulted in two more

phases. Relatively flat (2D) lamellae with rough surfaces having diameters in the range

of 5 to 30 μm together with minor phase-donut-shape rings (< 20%) were obtained from a

solution with a solvent ratio of 1:1. Further reducing the solvent ratio to 1/4 led to

20   predominantly (~80%) donut-shape rings, with outer diameters of about 0.5 to 1.0 μm and

wall thickness of about 200 nm, coexisting with a minor phase of lamellae. All these four

morphologies had highly ordered structures with crystalline feature, as evidenced by

Figures 16A and 16C, which were taken under cross-polarizers. In Figure 16D, the

hollow microcavity and closed ends of the cylindrical aggregates were revealed.

25   Aggregates prepared by drying solutions at room temperature had non-spherical

morphologies, and each sample was predominantly (~70%) either lamellae, cylinders, or

vesicles depending on the initial solvent composition; the minor phases in these

morphologies were cylinders, lamellae, or spheres, respectively. Lamellar aggregates had

diameters in the 5 to 30 μm range, the cylinders were relatively uniform in diameter (1 to

30   3 μm) but highly polydisperse in length (5 to 25 μm), and vesicles had outer diameters of

about 0.5 to 1.0 μm and wall thickness of about 200 nm. Similar multiple morphologies

were observed in aggregates prepared from other diblock copolymers, with average sizes

of the aggregates depending on the molecular weight of the block copolymers (Table 1).

Table 1. Typical morphologies from diblock and triblock copolymers, and their sizes.

Copolymer	N_A-N_B or N_A-N_B-N_A	Morphology	
		Type	Size (μm) *
54a	50-2000	Spherical	1-40 (10)
		Lamellar	40
54b	50-1000	Spherical	1-20 (8)
		Cylindrical	Diameter of 2 μm
		Lamellar	30
		Ring	Outer diameter 2μm
54c	50-300	Spherical	1-10 (4)
		Cylindrical	Diameter of 1 μm
		Lamellar	20
		Ring	Outer diameter 1 μm
54d	50-130	Spherical	1-5 (2)
		Cylindrical	Diameter of 0.8 μm
		Lamellar	10
		Ring	Outer diameter 0.8 μm
54e	10-1000	Spherical	1-10 (4)
		Cylindrical	Diameter of 1 μm
		Lamellar	20
		Ring	Outer diameter 1 μm
54f	10-300	Spherical	0.5-5 (3)
		Cylindrical	Diameter of 0.5 μm
		Lamellar	10
		Ring	Outer diameter 0.5 μm
54g	10-130	Spherical	1-10 (1)
		Lamellar	8
55a	50-500-50	Spherical	0.5-200 (27)
55b	50-250-50	Spherical	0.5-80 (16)
55c	50-120-50	Spherical	0.5-15 (2)

*The number inside bracket is the average sizes.

Figure 17 shows some representative morphologies self-assembled from copolymer **54b** (Figures 17A and 17B), **54e** (Figure 17C), **54f** (Figures 17D), and **54g** (Figures 17E and 17F). Spherical aggregates with sizes ranging from 1 - 20 μm were obtained from PPQ_{50}-b-PS_{1000} (**54b**, Figure 17A), which was bigger than those from PPQ_{50}-b-PS_{300} (**54c**) by a factor of about 2 (Figures 16A and B). Cylindrical aggregates prepared from PPQ_{50}-b-PS_{1000} (**54b**, Figure 17B) had a diameter of 2 μm, and length of 2-20 μm, with diameter

5   about twice the size of cylinders prepared from PPQ_{50}-b-PS_{300} (54c). Therefore, the

higher the molecular weight, the bigger the average sizes of the aggregates. This trend

was more clearly shown in Figures 17C to 17F. The lamellae prepared from PPQ_{10}-b-

PS_{1000} (54e) had sizes in the ranges of 20-30 μm, the sizes were reduced to 10-15 μm for

PPQ_{10}-b-PS_{300} (54f), and further down to 5-8 μm for PPQ_{10}-b-PS_{130} (54g). All these

10   aggregates had highly ordered structure, as evidenced by Figure 17E, which was taken

under cross-polarizers. These observations were consistent with theoretical prediction

that morphologies of the aggregates change with the varying molecular weight

(Radzilowski et al., Macromolecules, 26:879-882 (1993); Radzilowski et al.,

Macromolecules, 27:7747-7753 (1994); Wadawski et al., Nature, 369:387 et seq. (1994);

15   Chen et al., Science, 273:343-346 (1996); Chen et al., Macromolecules, 28:1688-1697

(1995), which are hereby incorporated by reference).

Repeated heating of the aggregates to 200 °C, which is above the glass

transition (T_g) of PS blocks (T_g = 100 °C) and below that of PPQ blocks (T_g >350 °C)

(Sybert et al., Macromolecules, 14:493-502 (1981); Agrawal et al., Macromolecules,

20   26:895-905 (1993); Agrawal et al., Chem. Mater., 8:579-589 (1996), which are hereby

incorporated by reference), did not have any effect on the aggregate morphologies, which

demonstrated the robustness of these aggregates. Also, the polydispersity of the rigid-rod

block apparently had no discernible effect on the aggregate morphologies.

Compared to recently observed multiple morphologies in coil-coil block

25   copolymers (Zhang et al., Science, 272:1777-1779 (1996); Zhang et al., Science,

268:1728-1731 (1995); Zhang et al., J. Am. Chem. Soc., 118:3168-3181 (1996), which

are hereby incorporated by reference), the present aggregates were larger by about two

orders of magnitude.

The unusually large sizes of the spherical and cylindrical aggregates,

30   unlike bilayer vesicles and lamellae that could in principle grow to any size (Figure 18),

could not be explained by a simple core-shell structure of conventional block copolymer

micelles (Halperin et al., Adv. Polym. Sci., 100:31-71 (1992); Tirrell, in Weber et al.,

Eds., Solvents and Self-Organization of Polymers, Kluwer Academic, Dordrecht, pp.281-

308 (1996); Tuzar et al., Surface and Colloid Science, 15:1-83 (1993); Weber et al., Eds.,

35   Solvents and Self-Organization of Polymers, Kluwer Academic, Dordrecht, (1996); Gast,

in Weber et al., Eds., Solvents and Self-Organization of Polymers, Kluwer Academic,

Dordrecht, pp. 259-280 (1996); Vagberg et al., Macromolecules, 24:1670-1677 (1991);

5   Semenov et al., Sov. Phys. JETP, 63:70-79 (1986); Semenov, Mol. Cryst. Liq. Cryst.,
     209:191-199 (1991); Halperin, Macromolecules, 23:2724-2731 (1990); Halperin,
     Europhys. Lett., 10:549-553 (1989); Williams et al., Macromolecules, 25:3561-3568
     (1992); Raphael et al., Makromol. Chem.. Macromol. Symp., 62:1-17 (1992); Zhang et
     al., Science, 272:1777-1779 (1996); Zhang et al., Science, 268:1728-1731 (1995); Zhang

10   et al., J. Am. Chem. Soc., 118:3168-3181 (1996), which are hereby incorporated by
     reference). The main difficulty was that the rod-coil block copolymer chains from which
     the aggregates were assembled had on average fully extended lengths of at most 500 nm
     for PPQ_{50}-b-PS_{2000} (54a), and much less for the others, e.g., ~100 nm for PPQ_{50}-b-PS_{300}
     (54c). From x-ray diffraction data on oligoquinolines the repeat unit length of PPQ is

15   0.64 nm. The repeat unit length of extended chain PS was estimated to be ~0.226 nm.
     Therefore, the maximum extended chain lengths of PPQ_{50}-b-PS_{300} (54c) and PPQ_{10}-b-
     PS_{300} (54f) would be ~100 and ~74 nm, respectively. Spherical and cylindrical
     aggregates of about 200 nm diameter would thus be expected if solid PS-core/PPQ-shell
     assemblies were formed for PPQ_{50}-b-PS_{300} (54c). In contrast, the observed aggregates

20   were about 10 to 50 times larger (Figures 15-17). To account for the size difference, the
     observed spherical and cylindrical aggregates were thought to form large hollow cavities.
     An aggregate structure in accord with this hypothesis is cavity-core/PS-inner shell/PPQ-
     outer shell (Figure 7 and 14). For a typical 5-μm diameter spherical aggregate, 89% of its
     total volume of 65 μm^3 would be empty. The driving force for the large size and hollow

25   cavity of these aggregates appeared to be a more efficient packing of the rigid-rod blocks
     and, consequently, a more ordered and stable aggregate structure. All the different
     aggregates under cross-polarizers showed that they were highly ordered with crystalline
     features. The aggregation number, N_o, or number of rod-coil block copolymer chains per
     aggregate, was estimated to be 1.5 x 10^8 for a hollow sphere with diameter of 5 μm,

30   assuming the density of the spherical aggregates is 0.14 g/cm^3. The aggregation number
     for cylindrical aggregates with diameter of 1 μm and length of 10 μm was similarly
     estimated to be 3x10^8. The aggregation number N_o can also be estimated by the amount
     of the copolymers consumed for construction of various aggregates. For example, about
     2x10^5 discrete spherical aggregates/mm^2 was measured from a photomicrograph taken

35   from a 1-mg diblock copolymer PPQ_{50}-b-PS_{300} (54c) covering a total area of 5 cm^2.
     Thus, one gets 2.4x10^{-16} mole diblock/aggregate (or 10^{-8} mg diblock/aggregate) or N_o =
     1.5x10^8. Similar procedures for cylindrical aggregates gave 2x10^4 aggregates/mm^2 from a

5   photomicrograph taken on a 0.2-mg diblock copolymer PPQ_{50}-b-PS_{300} (**54c**) covering a 5-cm^2 area. From this, one gets 4.8×10^{-15} mole diblock/aggregate or $N_o = 3 \times 10^8$. The aggregation numbers estimated by these two different methods were in perfect agreement.

Aggregate luminescence of the diblock copolymers (**54a-54g**) and the triblock copolymers (**55a-55c**) was explored as a means of probing the molecular packing

10   of the luminescent rigid-rod PPQ blocks in the different aggregate morphologies. Different photoluminescence (PL) emission and excitation (PLE) spectra were observed for spherical, lamellar, and cylindrical aggregates self-assembled from diblock copolymers **54a-54g** (**54c**, Figure 19) and vesicles from triblock copolymer **55a-55c**. For comparison, PLE and PL spectra of PPQ homogeneously dispersed in poly(ethyl oxide)

15   (PEO) matrix (0.1 wt.%) were also obtained. (Table 2)

Table 2. Photophysical parameters of aggregates from diblock and triblock copolymers.

Copolymer /polymer	PPQ/PEO Single-chain	Diblock copolymers 3a-3g				Triblock copolymers 55a-55c
		spherical	cylindrical	lamellar	Ring-like	
PL λ_{max} (nm)	460	454	594	576	580	610
PLE λ_{max} (nm)	390	388	406, 422, 460	406, 422, 460	406, 422, 460	406, 422, 475
Lifetime (τ_1)	1.1	0.93	0.38	0.34	0.35	0.36
Lifetime (τ_2)	4.7	—	3.5	2.6	2.5	2.8

The PL spectrum of PPQ/PEO solid solution gave rise to an emission band centered at

20   460 nm, which was assigned to PPQ single-chain emission. The corresponding PLE spectrum, when monitored at 460 nm, gave rise to an absorption band centered at 390 nm, which was identical to the absorption spectrum obtained from UV-vis experiments. Spherical aggregates from diblock copolymers exhibited a blue emission band centered at 454 nm, whereas the PLE spectrum showed an absorption band with a peak at 388 nm,

25   slightly blue-shifted to the emission from the PPQ single chain. In contrast, both lamellar and cylindrical aggregates from diblock and vesicles from triblock copolymers had broad emission bands with peaks at 576, 594 nm, and 610nm, respectively, and PLE spectra of those when monitored at emission peaks gave rise to spectra which were totally different

5   to the PLE spectrum of PPQ/PEO solid solution. The PLE spectra showed a peak at 422 nm and a shoulder peak at 406 nm and ~460 nm. The extensive morphology studies of aggregates revealed that all the aggregates had highly ordered crystalline structures (Figures 16, 17, 20, and 21), suggesting that in all these aggregates, a high degree of ordered packings of PPQ blocks took place. Therefore, the PL and PLE spectra showed

10   that the PPQ blocks in spherical aggregates self-assembled from diblock copolymers formed H-aggregates, whereas the PPQ blocks in cylindrical, lamellar, donut-ringlike aggregates from diblock copolymers and vesicles from triblock copolymers formed J-aggregates (Shimomura et al., J. Am. Chem. Soc., 109:5175-5183 (1987), which is hereby incorporated by reference). The slight differences in PL and PLE spectra of the J-

15   aggregates could be caused by the differences in tilted angles of the PPQ blocks (Figure 22). The different molecular packing of PPQ blocks in the spherical, lamellar and cylindrical aggregates from diblock together with vesicles form triblock was confirmed by the time-resolved PL studies (Figure 19). Time-resolved PL decay dynamics of the fluorescent PPQ block in the different aggregate morphologies evidenced different

20   excited-state lifetimes (Figures 19 and 23B). Compared to the PPQ dilute solid solution, which exhibited two lifetimes (1.1 and 4.7 ns), the PL decay dynamics of PPQ blocks in the spherical aggregates from diblock copolymer was approximately described by a single lifetime of 0.93 ns. However, in the lamellar and cylindrical aggregates and vesicles, biexponential lifetimes of 0.38 and 3.5 ns, 0.34 and 2.6 ns, and 0.36 and 3.0 ns,

25   respectively, best fit the decay dynamics. These results suggested that the observed morphology-dependent emission properties of the block copolymer aggregates reflected the varying molecular packing of the fluorescent rigid-rod blocks.

      SEM microscopy was used to confirm the proposed structures of the spherical and cylindrical aggregates and provide additional information of the large cavity

30   inside the aggregates. Figure 24 shows the SEM of the spherical aggregates from diblock copolymer **54c** (Figures 24A, 24B, 24E, 24F) and **54f** (Figures 24C, 24D) prepared from TFA/DCM (7/1, v/v) solutions with copolymer concentration of 0.5 wt.%. Spherical aggregates with wide size distribution, with size in the range of 1-10 μm were observed for copolymer **54c**, whereas the spherical aggregates from **54f** had typical sizes in the

35   range of 0.5-5 μm. These spherical aggregates had a very smooth surface and 3-D spherical shapes. Figure 24E shows a spherical aggregate prepared from copolymer **54c** with a defect hole, and the magnified version of defect area of Figure 24E is shown in

Figure 24F. That the spherical aggregate is indeed hollow inside and can be seen clearly, consistent with the proposed model for the spherical aggregates.

Fluorescence photomicrographs (Figures 25 and 26) confirmed the aggregate sizes and shapes observed in OM and SEM for the diblock copolymers and revealed that the fluorescent rigid-rod blocks were located at the outer shells of the aggregates, as depicted in the model of Figure 7. The hollow microcavity and closed ends of the cylindrical aggregates were also revealed (Figure 25C). The entire ~200 nm bilayer thickness of each vesicle appeared to fluoresce because the ~140 nm separation between the PPQ blocks in the bilayers was below the resolution limit (Figure 25D). Also, because of three-dimensional (3-D) symmetry and uniformity of emission, the microcavity of the spherical aggregates could not be directly observed (Figure 25A) but could be inferred from that of similarly formed cylinders (Figure 7). The 3-D nature of the spherical aggregates could be clearly distinguished from the relatively flat (2-D) lamellae, which have rough surfaces. Figure 26 shows the fluorescence photomicropraphs of typical aggregates, revealing remarkably clear images of large micellar aggregates (spheres, lamellae, cylinders) by virtue of the intrinsic fluorescence of the rod-like block. These self-assembled nonbiological aggregates were in the size range (albeit not the complexity) of cellular biology. Furthermore, they had well-defined 3-D shape and were larger than micelles from conventional surfactants and coil-coil block copolymers by factors of 100 and 5000, respectively (Halperin et al., Adv. Polym. Sci., 100:31-71 (1992); Tuzar et al., Surface and Colloid Science, 15:1-83 (1993); Weber et al., Ed., Solvents and Self-Organization of Polymers, Kluwer Academic, Dordrecht (1996); Zhang et al., Science, 272:1777-1779 (1996); Chen et al., Science, 273:343-346 (1996); Jenekhe et al., Science, 279:1903-1907 (1998), which are hereby incorporated by reference). Because of the imprinted instructions for self-organization with well-defined rod-coil interfaces, novel highly ordered 3-D aggregates, unlike conventional surfactant or block copolymer micelles, were formed (Figure 7). Examples of 3-D shaped objects that could be prepared by macromolecular self-assembly are shown in Figure 27.

Compared to multiple morphologies (spherical, cylindrical, rings, and lamellar) self-assembled from diblock copolymers, triblock copolymers arranged as only one type morphology, i.e., spherical micelles under similar conditions, and the size of which was an order of magnitude larger than those of diblock copolymers. Figure 20 shows the polarized optical micrographs and fluorescence micrographs of triblock copolymers (55a, 55b, and 55c) prepared from TFA/DCM solutions with triblock

copolymer concentration of 0.1 wt.%. All of the samples were prepared by spreading the solvents on hot glass substrates (90 °C). Only spherical micelles were formed with sizes ranging from 0.5 μm to 200 μm. For triblock copolymer PPQ_{50}-b-PS_{500}-b-PPQ_{50} (55a), perfect spherical micelles with sizes ranging from 20 - 40 μm were observed. However, small spherical micelles with a size of 1 μm to 5 μm (10%) and very large spherical micelles with sizes ranging from 40 μm to 200 μm were also observed (10%). The average size of spheres from copolymer PPQ_{50}-b-PS_{500}-b-PPQ_{50} (55a) was 27 μm. Spherical aggregates self-assembled from triblock copolymer PPQ_{50}-b-PS_{250}-b-PPQ_{50} (55b) had much narrower size distribution, with typical sizes in the range of 10 - 20 μm (90%), and the minor phase was very small spherical aggregates with sizes from 1 μm to 5 μm (10%), giving an average size of 16 μm. Triblock copolymer PPQ_{50}-b-PS_{120}-b-PPQ_{50} (55c) also arranged as spherical aggregates in solid state, with sizes ranging from 1 - 5 μm, with structures having severe defects with many holes developed in the micelles. The spherical aggregates from copolymers PPQ_{50}-b-PS_{500}-b-PPQ_{50} and PPQ_{50}-b-PS_{250}-b-PPQ_{50} (55a and 55b) formed similar sizes arranged closed-packed in substrates in a hexagonal manner. All the spherical aggregates (with or without defects) had highly ordered structures, as indicated in images taken under cross polarizers (Figures 20A, 20C, and 20E).

The morphologies of the triblock copolymers prepared from different processing temperatures (from 20 °C to 90 °C), copolymer concentrations (0.01 – 0.5 wt%), and solvent ratios of TFA:DCM (from 9/1 to 1/9) were also investigated. No differences in size, shape, or hierarchical arrangement of spherical aggregates was observed for the various processing conditions, in sharp contrast to that of diblock copolymers, whose morphologies were highly dependent on the solvent ratio. For the samples prepared from solutions with very low copolymer concentrations (< 0.005 wt.%), no spherical aggregates were observed under optical microscope, probably due to the fact that the size of the aggregates was too small to be detected by optical microscopy. The size of the spherical micelles was mainly determined by the length of the coil. As D_p of PS decreased from 500 to 250, then to 120, the average diameter of spherical micelles correspondingly decreased from 27 μm, to 16 μm, and then to 2 μm, and no correlation could be found between the size and temperature or between size and solvent ratio. Although for each triblock, spherical aggregates had size distribution, the aggregates with similar sizes tended to stay together, and arranged in a hexagonal manner.

5   The aggregation number for each aggregate was also estimated. For **55a**, 0.5-g solution with copolymer concentration of 0.1 wt.% can cast a film with area of 2 cm^2. In this area, average density of the micelles with typical diameter of 30 μm was about 1.5 x 10^4 /cm^2. Therefore the aggregation number was calculated to be 3.3 x 10^{10}. The aggregation number can also be estimated from density. Assuming the micelle has

10   90 % porosity, the density of the micelles is close to 0.14 g/cm^3. As the volume for each micelle is 1.4 x10^4 μm^3, aggregation number will be 1.5 x10^{10}, very close to that estimated from the other method (see above). The aggregation number for **55b** (diameter of 10 μm) and **55c** (diameter of 2 μm) can be similarly estimated. The aggregation number was 5.6 x 10^8, and 4.4 x 10^6, respectively.

15   Figure 28 shows the SEM micrographs of triblock copolymers **55a**, **55b** and **55c** prepared from TFA/DCM solutions with triblock copolymer concentrations of 0.5 wt.%. All the samples were prepared by slowly evaporating the solvents at room temperature. For triblock copolymer PPQ_{50}-b-PS_{500}-b-PPQ_{50} (**55a**) (Figures 28A and 28B), perfect spherical aggregates with sizes ranging from 20 - 40 μm were observed,

20   however, large spherical micelles with sizes ranging from 40 μm up to 200 μm were also observed (20%). These large spherical aggregates (40 μm-200μm) had flattened shapes (Figures 28A and 28B). Samples from triblock copolymer PPQ_{50}-b-PS_{250}-b-PPQ_{50} (**55b**) exhibited perfect spherical micelles with typical sizes in the range of 10 - 20 μm (Figure 28C). Triblock copolymer PPQ_{50}-b-PS_{120}-b-PPQ_{50} (**55c**) also arranged as spherical

25   micelles in solid state; however, severe defects, such as holes with sizes ranging from 0.5 μm to 1 μm, developed all through the structures (Figure 28D). Figures 28E and 28F show the SEM micrographs of broken spherical aggregates from copolymers **55a** and **55b**, respectively. The microcavity inside the spherical micelles was clearly revealed. The wall thickness of the aggregate prepared from PPQ_{50}-b-PS_{500}-b-PPQ_{50} (**55a**) varied

30   from 340 nm to 1100 nm, whereas the wall thickness varied from 250 nm to 540 nm for copolymer PPQ_{50}-b-PS_{250}-b-PPQ_{50} (**55b**). Because the extended lengths for copolymer **55a** and **55b** were 180 nm and 120 nm, respectively, it appeared that the wall of the aggregates needed to be at least 2 to 6 extended copolymer molecules in order to reach the necessary thickness. Spherical aggregates from solutions with lower copolymer

35   concentrations (0.1 wt.%, 0.05 wt.%, and 0.01 wt.%) were also prepared. SEM studies of these samples revealed that spherical aggregates in the range of 200 nm to 1000 nm were also present, coexisting with the aggregates with sizes larger than 1 μm. About 5-10 % of

5   the spheres whose sizes were in the range of 100 to 1000 nm were observed in the sample
       prepared from 0.1 and 0.5 wt.% solutions. In samples prepared from 0.01 wt.% solution,
       the numbers of the spherical aggregates with sizes in the range of 200 to 1000 nm
       increased to almost 20 %. These results suggested that the concentration of the solution
       had significant effects on the size of the aggregates.

10   The spherical aggregates self-assembled from triblock copolymers could
       not be similarly explained as aggregates with inner-shell PS/outer-shell-PPQ as diblock
       copolymer could. The main difficulty was in the discrepancy of the wall thickness. If the
       triblock copolymer folds over and forms a loop-single layer, because the lengths of the
       triblock copolymers were all less than 180 nm, spherical aggregates with at most 90-nm

15   thick walls would be expected. However, extensive studies revealed that the wall
       thickness varied from 250 nm to 1100 nm, indicating several layers were present and
       constituted the wall. Therefore, the spherical aggregates self-assembled from triblock
       copolymers were vesicles which had one or several bilayer structures forming the wall.
       Although not wishing to be bound by theory, because no other morphologies except

20   vesicles were obtained, a large portion of triblock copolymers may have folded to form a
       single layer, serving as the curvature-inducing factor to let bilayers form vesicles instead
       of lamellae (Szleifer et al., Proc. Natl. Acad. Sci. USA, 95:1032-1037 (1998); Safran et
       al., Science, 248:354-356 (1990); Dan et al., Europhys. Lett., 21:975 et seq. (1993); Porte
       et al., J. Chem. Phys., 102:4290 et seq. (1993), which are hereby incorporated by

25   reference). In fact, the aggregates formed by copolymer PPQ_{50}-b-PS_{120}-b-PPQ_{50} (55c)
       suggested that bilayer structures were the central building units. The spherical structure
       with many holes developed within was a new structure called "perforated vesicles" or
       sponge phase, arising from the need to avoid edges by making a continuous web of
       bilayer in a sponge-like structures (Hecht et al., Macromolecules, 28:5465-5476 (1995);

30   Roux et al., J. Phys. Chem., 96:4174-4187 (1992); Hoffmann et al., Langmuir, 8:2629-
       2638 (1992), which are hereby incorporated by reference). "Perforated vesicles" or
       sponge phases have been reported in several systems (Safran et al., Science, 248:354-356
       (1990); Dan et al., Europhys. Lett., 21:975-980 (1993); Porte et al., J. Chem. Phys.,
       102:4290-____ (1993), which are hereby incorporated by reference). Because only the

35   aggregates with sizes ranging from 1 – 15 μm self-assembled from copolymer PPQ_{50}-b-
       PS_{120}-b-PPQ_{50} (55c) into perforated vesicles, two factors, both large curvature of the

5   vesicles and the difficulty in folding to form single layers, might attribute to the formation
     of the sponge phase.

            Transmission electron microscopy (TEM) technique was also used to
     study the aggregates self-assembled from diblock and triblock copolymers. The samples
     were prepared by dipping copper grids into 0.1 wt.% solutions at room temperature, then

10   drying under a mild flow of air. Because large aggregates (>1 μm) are too heavy to hold
     by the thin copolymer films formed between the grids, only small aggregates could be
     detected. Figure 29 shows typical TEM images from diblock copolymer PPQ_{10}-b-PS_{300}
     (54f) (Figure 29A), PPQ_{50}-b-PS_{300} (54c) (Figure 29B) and triblock copolymer PPQ_{50}-b-
     PS_{250}-b-PPQ_{50} (55a) (Figure 29C) and PPQ_{50}-b-PS_{500}-b-PPQ_{50} (55b) (Figure 29D).

15   Spherical aggregates prepared from diblock PPQ_{10}-b-PS_{300} (54f) and PPQ_{50}-b-PS_{300} (54c)
     in the range of 100 to 100 nm were clearly revealed in Figures 29A and 29B, whereas
     spherical aggregates with sizes varying from 150 nm to 800 nm were shown in Figures
     29C and 29D. Based on this information, it seemed that the molecular packing in diblock
     and triblock copolymer was different, as evidenced from Figure 29A and Figure 29D.

20   The spherical aggregates from triblock copolymers were more structured; a concentric
     ring-like image was revealed in TEM. It also seemed that folding did occur in triblock
     copolymers. The smallest size of the vesicles shown in Figures 29C and 29D was about
     150 nm. Because the fully extended length for triblock PPQ_{50}-b-PS_{500}-b-PPQ_{50} (55a) and
     PPQ_{50}-b-PS_{250}-b-PPQ_{50} (55b) was about 180 nm and 120 nm, respectively, the results

25   suggested that the folded loop-single layer (Figure 14) was the main building unit for the
     vesicles (<600 nm).

     Example 4 - Some Characterization Results

            The synthetic approaches outlined in Figures 5 and 6 ensured that the

30   desired rod-coil block copolymer structures (54a-54g and 55a-55c) were obtained. The
     composition of the diblocks $A_{N_A}B_{N_A}$ and triblocks $A_{N_A}B_{N_B}A_{N_A}$ was controlled by the
     stoichiometric method, where A and B were the PPQ and PS repeat units, respectively.
     Various techniques, including solvent extraction, ^1H NMR and FTIR spectroscopies,
     DSC, and TGA were used to confirm the proposed structures and compositions. To

35   establish that the copolymer samples were rod-coil block copolymers and not physical
     blends, Soxhlet extraction using refluxing ethyl acetate, which is a selective solvent for
     the coil-like block (PS), was performed on PPQ_{50}-b-PS_{130} (54d) and PPQ_{50}-b-PS_{120}-b-

5   PPQ$_{50}$ (**55c**). The yields were higher than 95% after 24 hours extraction, whereas continued extraction past this time resulted in no additional weight loss, indicating that all the flexible coil blocks in the sample were chemically bonded to the rigid-rod PPQ.

TGA thermograms of the rod-coil block samples are shown in Figures 30 and 31. TGA thermograms of the PPQ and PS homopolymers were also obtained for

10 comparison. The decomposition temperatures of PPQ and PS were 600 °C and 400 °C, respectively. TGA thermograms of the block copolymers showed a two-step decomposition in flowing N$_2$. The onset of the first thermal decomposition of the rod-coil blocks was 420 °C for **54c** and **54d**, 400 °C for **54a, 54b, 54e-54g**, and 410 °C for **55a-55c**, which was assigned to the decomposition of the flexible-coil PS block. (Figures 31A

15 and 31B). The slightly improved thermal stability of the PS block in the rod-coil block copolymers compared to the parent PS homopolymer can be understood as a consequence of the tethering of the former chains onto rigid-rod chains. After the decomposition of the flexible-coil blocks, the PPQ blocks were stable until 600 °C, which was identical to the decomposition temperature of the PPQ homopolymer. Observation of two characteristic

20 decomposition temperatures indicated that the samples were block copolymers and not random copolymers. The weight losses of block copolymers in the 400 to 600 °C ranges are shown in Tables 3 and 4, below.

Table 3. Proton NMR, T$_g$ and TGA data for copolymers 55a-55c and PPQ and PS homopolymers.

Polymer/ Copolymer	Chemical Shift (δ)	Glass transition temperature (Tg) (°C)	Number of repeat units (N$_A$)		Weight loss during 400 - 600 °C	
			Calculated	Measured	Calculated	Measured
PPQ	7.5, 8.9, 9.2, 9.4-9.6, 9.7	>400	--	--	0	0
PS	1.5-1.6, 2.2, 6.7-6.8, 7.3-7.4	100	--	--	100	100
55a QSQ-1	1.5-1.6, 2.2, 6.7-6.8, 7.3-7.4, 7.5, 8.9, 9.2, 9.4-9.6, 9.7	114	50	50	69.4	70
55b QSQ-2	1.5-1.6, 2.2, 6.7-6.8, 7.3-7.4, 7.5, 8.9, 9.2, 9.4-9.6, 9.7	114	50	52	53.2	51
55c QSQ-3	1.5-1.6, 2.2, 6.7-6.8, 7.3-7.4, 7.5, 8.9, 9.2, 9.4-9.6, 9.7	>114	50	50	35.3	35

5

- 47 -

Table 4. Proton NMR, T$_g$ and TGA data for copolymers 54a-54c.

Polymer/ Copolymer	Chemical Shift (δ)	Glass transition temperature (Tg) (°C)	Number of repeat units (N$_A$)		Weight loss during 400 - 600 °C	
			Calculated	Measured	Calculated	Measured
54a 50-2000	1.5-1.6, 2.2, 6.7-6.8, 7.3-7.4, 7.5, 8.9, 9.2, 9.4-9.6, 9.7	100	50	50	94.8	94
54b 50-1000	Same as above	100	50	50	90.1	90
54c 50-300	Same as above	100	50	50	73.2	73
54d 50-130	Same as above	100	50	50	54.1	53
54e 10-1000	Same as above	100	10	10	97.8	97
54f 10-300	Same as above	100	10	12	93.2	92
54g 10-130	Same as above	100	10	12	85.5	83

5

5   The measured weight losses in the 400 to 600 °C ranges and hence estimated N_A, were in

excellent agreement with the calculated composition of block copolymers. The 4 %

difference between the expected block copolymer composition in PPQ_{50}-b-PS_{250}-b-PPQ_{50}

(**55b**) and that estimated from TGA data can be accounted for by the residual weight of

the PS block in the 400 to 600 °C range and was well within the experimental accuracy of

10   TGA analysis for composition determination.

        The DSC thermograms of the rod-coil block copolymers, and those of the

two parent homopolymers were also obtained. PS homopolymer had a glass transition

temperature (T_g) at 100 °C. No crystalline melting or T_g was observed in PPQ before

reaching its decomposition, consistent with the excellent thermal stability and high

15   modulus of rigid rod-like conjugated polyquinolines. The DSC thermograms of the

diblock copolymers **54a-54g** were essentially superpositions of those of the two parent

homopolymers, exhibiting only a glass transition at 100 °C. However, the DSC

thermograms of triblock copolymers **55a-c** behaved quite differently. The DSC

thermograms of PPQ_{50}-b-PS_{500}-b-PPQ_{50} (**55a**) and PPQ_{50}-b-PS_{250}-b-PPQ_{50} (**55b**) in the

20   first scan showed a second-order transition with temperature at 114 °C, and subsequent

scans of the samples were identical to those of the initial scans. The DSC thermogram of

PPQ_{50}-b-PS_{120}-b-PPQ_{50} (**55c**) showed a straight line from -50 to 400 °C; no discernible

transition was observed. Compared to polystyrene homopolymer, triblock copolymers

PPQ_{50}-b-PS_{500}-b-PPQ_{50} (**55a**) and PPQ_{50}-b-PS_{250}-b-PPQ_{50} (**55b**) exhibited an enhanced

25   glass transition temperature by 14 degrees. Copolymer PPQ_{50}-b-PS_{120}-b-PPQ_{50} (**55c**),

which had the shortest coil block length (Dp ~ 120), exhibited no glass transition at all in

the temperature range of -50 to 400 °C, indicating its glass transition temperature was

higher than 400 °C. These results suggested that the tethering of both ends of the flexible

PS chains to rigid-rod blocks had tremendous effects on the glass transition of the PS; the

30   movement of the PS was severely limited by the anchors on the ends. As the

enhancement of T_g in conventional coil-coil triblock copolymers was not observed, nor in

PPQ-PS diblock copolymers, which had numbers of PS repeat units (D_p) ranging from

2000 to 130, close to the D_p of PS in triblock copolymers (500 to 120), two factors, both

the tethering of the PS on both ends and the rigid rod-like nature of the blocks PS was

35   tethered to, are believed to have contributed to the enhancement of the glass transition

temperature.

        ^{1}H NMR spectra of **54a-54g** and **55a-55c** in deuterated nitrobenzene

containing $AlCl_3$ were obtained and assigned to the proposed structures by comparison

5   with those of the PPQ and PS homopolymers. ^{1}H NMR spectra of copolymers were

essentially superpositions of those of two parent components, PPQ and PS. Figure 32

shows a typical ^{1}H NMR spectrum of copolymer PPQ_{50}-b-PS_{500}-PPQ_{50} (55a). The

protons of the PPQ block appeared as resonances at 9.7, 9.4-9.6, 9.2 and 8.9 ppm, which

were assigned to the protons of the quinoline ring. Protons of the side group phenyl ring

10 appeared at 7.5 ppm, overlapping with the signals from the nitrobenzene solvent. Protons

of the PS block had resonances at 7.3-7.4 and 6.7-6.8 ppm, assigned to the phenyl ring,

and at 1.5-1.6 and 2.2 ppm due to resonances of the protons of the methylene units.

Comparison of the integral of PPQ proton resonances in the range 8.8-9.8 ppm to that of

the methylene units in the range of 1.5-2.2 ppm, gave the average repeat units of PPQ in

15 54a-54d as around 50, 54e-54g as around 10, and 55a-55c as around 100, respectively.

These results were in good agreement with the proposed block copolymer composition.

FTIR spectra were also obtained as an independent check for the

molecular structure of the rod-coil block copolymers. (Figure 33) The FTIR spectra of

the rod-coil block copolymer samples were essentially superpositions of the spectra of the

20 parent PS and PPQ homopolymers. There were significant differences between the

vibrational spectra of PS and PPQ homopolymers and hence their contributions to the

FTIR spectra of the block copolymers 54a-g and 55a-c. For example, the vibrational

bands at 2922 and 2949 cm^{-1}, which can be assigned to aliphatic C-H stretching in PS,

were absent in the FTIR spectrum of PPQ homopolymer. On the other hand, the strong

25 bands at 1346 and 1028 cm^{-1} were characteristic of the quinoline ring of the PPQ block.

The FTIR results in conjunction with the ^{1}H NMR spectra, DSC and TGA thermograms,

and other characterizations of the rod-coil block copolymer samples confirmed their

proposed structures and compositions.

For all the diblock and triblock copolymers, it seemed that aggregates were

30 spontaneously formed in solutions with concentration of 0.01 to 0.5 wt.%. No size

difference was observed for various copolymer concentrations, although for lower

concentration, the density of the aggregates was much less. For very dilute solutions with

concentrations equal to or below 0.001 wt.%, no discernible aggregates were observed,

suggesting that concentration of 1×10^{-7} M probably was the critical concentration for

35 forming aggregates with size larger than 1 μm. Spherical aggregates prepared from

diblock copolymer PPQ_{50}-b-PS_{1000} (54b) with size in the range of 1 to 20 μm (Figure

21A), and cylindrical aggregates from diblock copolymer PPQ_{50}-b-PS_{300} (54c) with

5   diameter of 1 μm and length of 1 to 20 μm (Figure 21B), were observed. Under cross-polarizers, no structures could be revealed probably due to the fact that the wall of the structure was too thin. Vesicles formed from triblock copolymer PPQ_{50}-b-PS_{500}-b-PPQ_{50} (55a) had size ranges of 5 μm to 120 μm (Figures 21C, 21D, and 21E), whereas vesicles from copolymer PPQ_{50}-b-PS_{250}-b-PPQ_{50} (55b) (Figure 21F) and PPQ_{50}-b-PS_{120}-b-PPQ_{50}

10   (55c) had sizes in the range of 1 to 100 μm, and 1 to 15 μm, respectively. The vesicles from triblock copolymers PPQ_{50}-b-PS_{500}-b-PPQ_{50} (55a) and PPQ_{50}-b-PS_{250}-b-PPQ_{50} (55b) were perfect; no flat or elongated shapes were observed. However, vesicles from copolymer PPQ_{50}-b-PS_{120}-b-PPQ_{50} (55c) had severe deformities in the structures, with holes developed all through the structures. All the vesicles (with or without defects)

15   seemed to have highly ordered structures, as evidenced by the images taken under cross polarizers (Figure 21C). All these results were consistent with the observation from the samples in solid state. The only exception was that no vesicle with a flattened shape was observed for triblock copolymer PPQ_{50}-b-PS_{500}-b-PPQ_{50} (55a) in solutions, as evidenced by the studies when the tubes were rotated. This indicated that the vesicles with a

20   flattened shape (Figures 28A and 28B) were caused by inadequate mechanical strength of the spherical structures.

        The aggregates in solutions were colloidal stable; they remained intact and had no tendency to precipitate or coagulate after standing for several weeks at 20 °C. The spherical aggregates from diblock copolymers had similar optical transparency,

25   suggesting they had the same wall thickness. In contrast, vesicles prepared from triblock copolymers had at least three types of wall-thickness: thin-wall, medium-wall, and thick-wall (Figures 21C-21F). These vesicles with different wall-thickness appeared in all the sizes and the vesicles with the thinnest wall had the same optical transparency as the aggregates self-assembled from diblock copolymers (Figure 21A). If the solutions were

30   perturbed, the vesicles began to move against each other and no attraction or repulsion was observed between two aggregates when they moved closer. When two aggregates were in contact range no merging of the aggregates or deforming of one or two aggregates were observed.

        The driving force for the large size and hollow cavity of aggregates

35   appeared to be a more efficient packing of the rigid-rod blocks and, consequently, a more ordered and stable aggregate structure. All the different aggregates under cross-polarizers showed that they were highly ordered with crystalline features. The different building

5   units for the spherical aggregates from diblock and from triblock copolymers led to the many differences between the aggregates from diblock and triblock copolymers. Such differences included the fact that the size of the latter was about an order of magnitude larger and the presence of multiple wall thicknesses of the aggregates from the triblock copolymers.

10

Example 5 - Solubilization Studies

Materials

The two copolymer compositions of poly(phenylquinoline)-*block*-

15   polystyrene used in this study, denoted here as PPQ_{50}-b-PS_{300} (**54c**) and PPQ_{10}-b-PS_{300} (**54f**), were synthesized by coupling functionalized polystyrene (PS) with the PPQ monomer, 5-acetyl-2-aminobenzophenone (Sybert et al., Macromolecules, 14:493-502 (1981), which is hereby incorporated by reference), followed by polycondensation synthesis of the PPQ block. The starting monofunctionalized PS had a reported number average degree of polymerization of 300 and a polydispersity of 1.05 (Aldrich,

20   Milwaukee, WI). The number average degree of polymerization of the PPQ blocks was determined from ^{1}H NMR spectra, thermal analysis, and other data.

Analytical grade solvents trifluoroacetic acid (TFA), dichloromethane (DCM), carbon disulfide (CS_2), and toluene were purchased from Aldrich (Milwaukee,

25   WI) and were used as received. Fullerene molecules C_{60} (TCI, 99.9 %) and C_{70} (Aldrich, Milwaukee, WI 99 %) were used as received. Poly(ethylene oxide) (PEO) (M_w of 5,000,000, M_w/M_n ~2.8), poly(methyl methacrylate) (M_w of 350,000, M_w/M_n ~1.15) and polystyrene (M_w of 6,000,000, M_w/M_n ~1.2) were purchased from Polysciences, Inc. (Warrington, PA) and were used as received.

30

Micellization and Solubilization Procedures

Copolymer solutions of PPQ-*b*-PS block copolymers (PPQ_{50}-b-PS_{300} (**54c**) and PPQ_{10}-b-PS_{300} (**54f**)) (0.5 to 1 mg/ml) used for the solubilization studies were prepared by dissolving each copolymer in various TFA/DCM or TFA/toluene mixtures of

35   9/1, 7/1, 1/1, and 1/4 solvent volume ratios. The resulting solutions had concentrations of 0.35 to 3.5 mg/ml (0.05 to 0.5 wt.%) of diblock copolymers. The critical micelle concentration (cmc) of PPQ-PS block copolymers in these binary solvents was unknown, but much less than order 10^{-3} wt.%. A known amount of fullerene (C_{60} or C_{70},) was then

5   added to the pre-made copolymer solutions. Alternatively, fullerene/copolymer solutions were prepared by adding know amounts of solid polymer and fullerene to the binary TFA/DCM or TFA/toluene at the same time to achieve solutions with similar concentrations. Fullerene/copolymer solutions were also prepared by mixing a solution of fullerene in DCM or in toluene with a pre-made copolymer solution. Different weight

10   ratios of fullerene to copolymer were employed, ranging from 0.1 to 50 wt.%. The fullerene/copolymer solutions were then stored for at least 2 days to equilibrate before assessment of solubilization and preparation of fullerene/block copolymer aggregates.

    Films (~1 to 20 μm thick) resulting from drying the dilute solutions of block copolymer/solubilized fullerenes on glass slides at room temperature were

15   investigated as made. or after treating them in 5 % triethylamine/ethanol (to remove any trace acids). and drying in a vacuum oven at 60 °C for 24 hours. The films were investigated by polarized optical and fluorescence microscopies as well as by UV-Vis absorption and photoluminescence spectroscopies.

    Preliminary experiments on the release of encapsulated fullerencs were

20   done by placing dried fullerene/copolymer aggregates in either good solvents for the rigid-rod PPQ block (fresh, clear, 1:1 TFA:DCM or TFA:toluene solvent mixtures) or good solvents for the coil-like PS block (pure DCM or toluene). Release of encapsulated fullerene was monitored by optical absorption spectroscopy to track any absorption signals of fullerene in solution.

25   Absorption spectra of solutions (0.1 wt.%) of fullerene C_{60} and C_{70} in CS_2 were obtained using a quartz cuvet which was sealed by wax to prevent solvent evaporation. Absorption spectra of the pure PPQ_{50}-b-PS_{300} (54c) and PPQ_{10}-b-PS_{300} (54f) were similarly obtained in 1:1 TFA:DCM solutions at 0.1 wt.% which was orders of magnitude larger than their cmc. These were used as the reference spectra for comparing

30   the absorption spectra of solubilized fullerene/block copolymer micelles. The UV-Vis absorption spectra of all fullerene/PPQ-PS dispersions were obtained in a 1-mm cuvet at room temperature (25 °C) and were used to estimate the solubilization capacities of the fullerene/PPQ-PS systems. For this purpose, the absorbance of each UV-Vis spectrum was normalized at a characteristic C_{60} or C_{70} absorption band. The normalized

35   absorbance was then plotted as a function of the amount of fullerene added to a dispersion. The saturation of the normalized absorbance versus fullerene loading provided an estimate of the maximum amount that was solubilized.

The normalized absorbance X of solutions of C_{60}/diblock copolymers at 330 nm was given by $X= C \bullet N_A \bullet [A_{330}-A^{\circ}_{330}]/[A_{422}-A^{\circ}_{422}]$, where X is proportional to C_{60} solubilized per diblock copolymer chain in solution, C is a constant, which is the ratio of the absorption coefficients of the PPQ block at 422 nm and C_{60} at 330 nm, N_A is the number of repeat units of PPQ in the diblock copolymer, and A_{330} and A_{422} are the absorbances at 330 and 422 nm, respectively. A°_{330} is the calculated absorbance of PPQ at 330 nm whereas A°_{422} is the calculated absorbance of C_{60} at 422 nm. Because of the negligible absorbance of C_{60} at 422 nm, $A^{\circ}_{422} = 0$. For solutions of C_{70}/diblock copolymers, the normalized absorbance was $Y= C \bullet N_A \bullet [A_{473}-A^{\circ}_{473}]/[A_{335}-A^{\circ}_{335}]$, where Y is proportional to C_{70} solubilized per diblock copolymer chain, C is a constant, which is the ratio of the absorption coefficients of PPQ at 335 nm and C_{60} at 473 nm, N_A is the number of repeat units of PPQ in the diblock copolymer, and A_{335} and A_{473} are the absorbances at 335 and 473 nm, respectively. A°_{335} is the calculated absorbance of C_{60} at 335 nm whereas A°_{473} is the calculated absorbance of PPQ at 473 nm. Because of the negligible absorbance of PPQ at 473 nm, $A^{\circ}_{473} = 0$.

Films of solid aggregates were too scattering in the visible region to obtain normal optical absorption spectra. Dilute solution optical absorption spectra of the pure fullerene and fullerene/copolymer samples, and those of thin films of block copolymers dispersed (0.1 wt%) in poly(ethylene oxide) (PEO) were recorded on a Perkin-Elmer Model Lambda 9 UV/VIS/NIR Spectrophotometer. All spectra were obtained at room temperature (25 °C).

Samples for observation by polarized optical microscopy (POM) and fluorescence microscopy (FM) were prepared by allowing several drops of a fullerene/block copolymer solution in TFA:DCM or TFA:toluene to spread and dry on glass slides. The various drying conditions explored were described above and were found not to influence the observed morphologies of aggregates (size, shape, and their distributions). Observations were made on an Olympus Model BX60 Fluorescence Optical Microscope and optical (bright field, polarized light) and fluorescence images were recorded by a digital camera.

Photoluminescence (PL) and photoluminescence excitation (PLE) spectra were obtained on a Spex Fluorolog-2 spectrofluorimeter. Thin films of aggregates were measured by using the front face geometry in which samples were positioned such that the emission was detected at 22.5° from the incident radiation beam. Further details of

5   the photophysical experimental techniques used here are similar to those we have
described in detail elsewhere (Osaheni et al., J. Am. Chem. Soc., 117:7389-7398 (1995);
Jenekhe et al., Science, 265:765-768 (1994), which are hereby incorporated by reference).
       The DSC thermograms were obtained on a Du Pont Model 2100 Thermal
Analyst based on an IBM PS/2 Model 60 computer and equipped with a Model 910 DSC
10   unit. The DSC thermograms of samples were obtained in nitrogen at a heating rate of
10 °C/min. Samples for DSC measurements were prepared by casting films of
fullerene/PPQ$_{50}$-b-PS$_{300}$ (54c) solutions in TFA/DCM (1/1, v/v) onto glass slides and
carefully removing vacuum dried fullerene-containing aggregates from glass slides into
DSC sample pans by using a sharp razor blade. Before the aggregates were removed
15   from the glass slides, they were observed by an optical microscope to ascertain their
spherical micellar morphology. In the case of fullerene/polystyrene and
fullerene/poly(methyl methacrylate) samples, drops of solutions in CS$_2$ were dried
directly in aluminum DSC pans.

20   *Micellar Solubilization of Fullerenes.*
       PPQ-PS solutions in the two binary solvent systems TFA/DCM and
TFA/toluene were previously shown to undergo self-organization to produce hollow
spheres, tubules and other aggregates (See Examples 3-4; Jenekhe et al., Science,
279:1903-1907 (1998), which is hereby incorporated by reference). Both solvent systems
25   were selective for the PPQ block and were highly polar. Both C$_{60}$ and C$_{70}$ were insoluble
in pure TFA or TFA/DCM or TFA/toluene mixtures (4/1 to 1/4, v/v) even though the
fullerenes were slightly soluble in pure DCM (0.192 mg/g) and pure toluene (3.16 mg/g).
Both C$_{60}$ and C$_{70}$ readily dissolved in these binary solvents at room temperature (25 °C)
when either PPQ$_{50}$-b-PS$_{300}$ (54c) or PPQ$_{10}$-b-PS$_{300}$ (54f) was present as illustrated in
30   Figure 34. Optical absorption experiments on the resulting solutions showed strong
characteristic fullerene absorption bands (Dresselhaus et al., Science of Fullerenes and
Carbon Nanotubes, Academic Press, San Diego, California (1996); Hirsch et al., The
Chemistry of the Fullerenes, Georg Thieme Verlag, Stuttgart (1994), which are hereby
incorporated by reference), indicating the presence of fullerene in solution and hence
35   evidence of enhanced solubility facilitated by the amphiphilic block copolymers.
       Figure 35 shows the absorption spectra of TFA/DCM solutions of pure
PPQ$_{50}$-b-PS$_{300}$ (54c) (Figure 36A), PPQ$_{50}$-b-PS$_{300}$ (54c) with 5 wt % C$_{60}$ (Figure 35B),

5   together with the spectrum of pure C_{60} in CS_2 (Figure 35C). The spectrum of C_{60}/PPQ$_{50}$-
b-PS$_{300}$ blend solution showed absorption bands characteristic of the two components, C_{60}
and the diblock copolymer PPQ$_{50}$-b-PS$_{300}$ (54c). The absorption band in the 370-460 nm
region with maxima at 405 nm was due to the PPQ block of the copolymer. The sharp
peak at 330 nm was due to the optical transition of C_{60}. The magnified version of the

10   blend spectrum in the 400-700 nm region is shown as the insert of Figure 35. The
absorption bands with λ_{max} at 540 and 600 nm were characteristic absorption bands of
C_{60}. Figure 36 shows the absorption spectra of 5 wt.% C_{70}/PPQ$_{50}$-b-PS$_{300}$ and 5.wt %
C_{70}/PPQ$_{10}$-b-PS$_{300}$ in TFA/DCM and C_{70} in CS_2. The characteristic C_{70} absorptions at
335, 383 and 473 nm and PPQ-PS absorption centered at 405 nm were observed in the

15   C_{70}/PPQ-PS solution spectra which could be readily deconvoluted into the component
spectra. The fact that the absorption spectra of the C_{60}/PPQ$_{50}$-b-PS$_{300}$ and C_{70}/PPQ$_{50}$-b-
PS$_{300}$ solutions were a superposition of the two chromophoric components (fullerene and
pure diblock copolymer) suggested that there was no ground state electronic interaction
between the fullerenes and the conjugated PPQ segments. This was to be expected since

20   the fullerenes C_{60} and C_{70} were strong electron accepting molecules (Dresselhaus et al.,
Science of Fullerenes and Carbon Nanotubes, Academic Press, San Diego, California
(1996); Hirsch et al., The Chemistry of the Fullerenes, Georg Thieme Verlag, Stuttgart
(1994); Adreoni, ed., The Chemical Physics of Fullerenes 10 (and 5) Years Later, Kluwer
Academic Publishers, Dordrecht, The Netherlands (1996); Hebard et al., Nature, 350:600-

25   601 (1991); Zakhidov et al., Phys. Lett., 205:317-326 (1995); Kajii et al., Synth. Met.,
86:2351-2352 (1997); Sariciftci et al., Science, 258:1474-1476 (1992); Sariciftci et al.,
Appl. Phys. Lett., 62:585-587 (1993); Wang, Nature, 356:585-587 (1992); and Wang et
al., J. Phys. Chem., 101:5627-5638 (1997), which are hereby incorporated by reference)
as are the conjugated polyquinolines (Sybert et al., Macromolecules, 14:493-502 (1981);

30   Agrawal et al., Macromolecules, 26:895-905 (1993); Agrawal et al., Chem. Mater.,
8:579-589 (1996); Agrawal et al., J. Phys. Chem., 96:2837 et seq. (1992); Jenekhe et al.,
Chem. Mater., 9:409 et seq. (1997), which are hereby incorporated by reference).
Therefore, absorption spectroscopy could be used to quantify the solubilization capacity
of fullerenes in the block copolymer solutions.

35   All solubilization studies and solution optical absorption measurements
were done on the four basic systems: C_{60}/PPQ$_{50}$-b-PS$_{300}$, C_{60}/PPQ$_{10}$-b-PS$_{300}$, C_{70}/PPQ$_{50}$-b-
PS$_{300}$, and C_{70}/PPQ$_{10}$-b-Ps$_{300}$. In addition to the two different approaches to preparing

5 solubilized fullerene/block copolymer solutions illustrated in Figure 34, i.e., addition of
solid fullerene to a pre-existing copolymer solution and addition of both fullerene and
block copolymer to the solvent mixture, fullerene/PPQ-PS solutions were also prepared
by mixing a solution of fullerene in DCM with a pre-made copolymer solution. No
discernible differences were observed between the three methods. Similar solution

10 absorption spectra and, subsequently, similar aggregate morphologies were obtained.
This suggested that the observed solubilization behavior was likely near equilibrium
conditions.

Normalized absorbancies of the characteristic fullerene absorption bands
were used as measures of the relative amounts of fullerene solubilized in the block

15 copolymer solutions. Figure 37A shows plots of normalized C_{60} absorbance at 330 nm
versus C_{60} loading into the solution (mg C_{60} per g diblock copolymer in solution). The
relative amount of solubilized C_{60} increased linearly with the fullerene loading of the
diblock copolymer solutions, reaching saturation at a loading of about 200 mg/g. This
was taken as the solubilization capacity of the block copolymer solutions. The C_{60}

20 solubilization characteristics of PPQ_{50}-b-PS_{300} (54c) and PPQ_{10}-b-PS_{300} (54f) were
essentially identical as were the different copolymer concentrations (Figure 37A).
Similar data of normalized absorbance versus loading for C_{70} are shown in Figure 37B. A
solubilization capacity of ~200 mg fullerene –C_{70}/g diblock copolymer was obtained.
This was identical to the C_{60} result. The solubilization capacity of 200 mg/g translated to

25 11.8 and 9.2 solubilized C_{60} molecules per diblock chain for PPQ_{50}-b-PS_{30} (54c) and
PPQ_{10}-b-PS_{300} (54f), respectively. Similarly, the maximum amount of solubilized C_{70}
molecule per diblock chain of PPQ_{50}-b-PS_{300} and PPQ_{10}-b-PS_{300} were 10.1 and 7.9,
respectively.

The measured solubilization capacity of 200 mg of solubilized fullerene

30 (C_{60} or C_{70}) per gram of diblock copolymer represented a solubility enhancement by
factors of 1040 and 63 compared to the solubilities in pure dichloromethane and toluene,
respectively. The best previously reported, organic solvent for C_{60} was 1-
chloronaphthalene which had a solubility limit of 42.7 mg/g at room temperature (22 °C)
(Dresselhaus et al., Science of Fullerenes and Carbon Nanotubes, Academic Press, San

35 Diego, California (1996); Ruoff et al., J. Phys. Chem., 97:3379 et seq. (1993); Sivaraman
et al., J. Org. Chem., 57:6077 et seq. (1992), which are hereby incorporated by reference).
The large enhancement of fullerene solubility in organic solvents by amphiphilic block

5   copolymer micelles that was demonstrated is thus very promising for potential applications in the large scale extraction, purification, and processing of fullerenes (Dresselhaus et al., Science of Fullerenes and Carbon Nanotubes, Academic Press, San Diego, California (1996); Hirsch, The Chemistry of the Fullerenes, Georg Thieme Verlag, Stuttgart (1994), which are hereby incorporated by reference).

10   In preliminary experiments on the release of encapsulated fullerenes, PPQ-PS micellar aggregates containing 1 and 5 wt.% fullerenes C_{60} and C_{70} from TFA/DCM and TFA/toluene solutions were dried and then placed in pure DCM or toluene, which are good solvents for PS block, for several days. Release of any encapsulated fullerene was not observed by optical absorption spectroscopy which did not detect any absorption

15   signals of fullerene in solution. Subsequent examination of these aggregates by optical microscopy showed that there was no change in the morphology, before and after their immersion in the aprotic organic solvents. However, when similarly dried aggregates were immersed in TFA/DCM or TFA/toluene solvent mixture (1/1, v/v), they dissolved and progressively released fullerene into solution as judged by absorption spectroscopy

20   which revealed and could be used to track the fullerene absorption signal in solution. The preliminary indication is that the release could be triggered and controlled by pH.

              Given the novel hollow structure and very large sizes of PPQ-PS micelles and some of the unusual features of their solubilization of fullerenes, it was not obvious that current theories of block copolymer micellization and solubilization could explain the

25   experimental results (Nagarajan et al., Macromolecules, 22:4312 et seq. (1989); Nagarajan et al., J. Chem. Phys., 90:5843 et seq. (1989); Hurter et al., Macromolecules, 26:5030 et seq. (1993); Hurter et al., Macromolecules, 26:5592 et seq. (1993); Linse, Macromolecules, 27:2685 et seq. (1994); Cogan et al., Langmuir, 8:429 et seq. (1992); and Xing et al., Macromolecules, 30:1711 et seq. (1997), which are hereby incorporated

30   by reference). One basic issue was whether the observed solubilization of fullerenes by PPQ-PS diblock copolymer assemblies was a micellar solubilization phenomenon (Solvents and Self-Organization of Polymers, Webber et al., Eds., Kluwer Academic Publishers, Dordrecht, The Netherlands (1996), which is hereby incorporated by reference) or vesicle-like trapping (Vesicles, Rosoff, Ed., Marcel Dekker, New York

35   (1996), which is hereby incorporated by reference), or a hybrid of both. Arguing in favor of a micellar mechanism included the similarity of the solubilization capacity regardless of the self-assembly path (Figure 34) which implied that the solubilized fullerene/PPQ-PS assemblies were thermodynamically very stable structures; as will be shown below,

5 fullerene solubilization caused major changes in the physical size, aggregation number, shape, and molecular packing of PPQ-PS aggregates. On the other hand, independence of solubilization capacity from copolymer concentration in solution and from the PPQ block length (N_A~10 and 50) was not a common feature of block copolymer micelle solubilization (Nagarajan et al., Macromolecules, 22:4312 *et seq.* (1989); Nagarajan et al.,

10 J. Chem. Phys., 90:5843 *et seq.* (1989); Hurter et al., Macromolecules, 26:5030 *et seq.* (1993); Hurter et al., Macromolecules, 26:5592 *et seq.* (1993); Linse, Macromolecules, 27:2685 *et seq.* (1994); Cogan et al., Langmuir, 8:429 *et seq.* (1992); and Xing et al., Macromolecules, 30:1711 *et seq.* (1997), which are hereby incorporated by reference) but may reflect the hollow cavity of these assemblies. Nevertheless, some aspects of the

15 results could be rationalized in terms of micellar solubilization theory for block copolymers (Nagarajan et al., Macromolecules, 22:4312 *et seq.* (1989); Nagarajan et al., J. Chem. Phys., 90:5843 *et seq.* (1989); Hurter et al., Macromolecules, 26:5030 *et seq.* (1993); Hurter et al., Macromolecules, 26:5592 *et seq.* (1993); Linse, Macromolecules, 27:2685 *et seq.* (1994); Cogan et al., Langmuir, 8:429 *et seq.* (1992); and Xing et al.,

20 Macromolecules, 30:1711 *et seq.* (1997), which are hereby incorporated by reference). From the known solubility parameters of fullerene-C_{60} (δ_f) (Dresselhaus et al., Science of Fullerenes and Carbon Nanotubes, Academic Press, San Diego, CA (1996), which is hereby incorporated by reference) and polystyrene (δ_{ps}) (Polymer Handbook, Brandrup et al., Eds., 3rd ed., Wiley, New York Chapter V, pp. 77-86 (1989), which is hereby

25 incorporated by reference) which were 10 and 8.7 to 9.9 at 25 °C, respectively, the Flory-Huggins interaction parameter $\chi_{f, ps}$ expressed in terms of the solubility parameters (Nagarajan et al., Macromolecules, 22:4312 *et seq.* (1989); Nagarajan et al., J. Chem. Phys., 90:5843 *et seq.* (1989), which are hereby incorporated by reference) $\chi_{f, ps} = (\delta_f - \delta_{ps})^2 v_f/k_B T$ was as small as 0.015, where v_f is molar volume, k_B is the Boltzmann's

30 constant, and T= 298K. This suggested that there was strong interaction between the fullerene and the PS blocks. Prior investigations of C_{60} solubility in many organic solvents had shown that the largest solubilities were observed in solvents with solubility parameters close to that of C_{60} (Dresselhaus et al., Science of Fullerenes and Carbon Nanotubes, Academic Press, San Diego, CA (1996); Ruoff et al., J. Phys. Chem., 97:3379

35 *et seq.* (1993); Sivaraman et al., J. Org. Chem., 57:6077 *et seq.* (1992), which are hereby incorporated by reference).

5   *Block Copolymer Aggregates with Encapsulated Fullerenes.*

The morphology of fullerene-containing block copolymer aggregates which were dried from solutions was extensively investigated. Unlike the multiple aggregate morphologies (hollow spheres, tubules, lamellae, and doughnuts) observed in the pure PPQ_{50}-b-PS_{300} (**54c**) and PPQ_{10}-b-PS_{300} (**54f**) diblock copolymers (See Examples

10   3-4; Jenekhe et al., Science, 279:1903-1907 (1998), which is hereby incorporated by reference), solid films from all fullerene-containing copolymer solutions with fullerene/copolymer ratios of 0.1 to 6 wt % showed only spherical aggregates. Films cast from solutions with fullerene concentration below this range were similar to the pure diblock copolymer solutions in exhibiting multiple aggregate morphologies. This meant

15   that the solubilized fullerenes at this dilute loading were encapsulated in some of the aggregates without influencing the block copolymer self-organization process in solution. At fullerene loading of 7 wt.% or higher, the solid films showed mixed morphologies consisting of spherical aggregates with encapsulated fullerene as well as needle-like crystals of the pure C_{60} or C_{70}.

20   Figures 38-40 show the typical morphologies of PPQ_{50}-b-PS_{300} (**54c**) aggregates with encapsulated fullerenes revealed by optical and fluorescence microscopies. Figure 38 shows the fluorescence (Figure 38A-B) and polarized optical (Figure 38C) micrographs of a 0.1 wt.% C_{70}/PPQ_{50}-b-PS_{300} copolymer sample. Only spherical aggregates, with a typical diameter of about 10 μm, were observed. The

25   spherical aggregates had highly ordered structures as indicated by the polarized optical micrographs such as that shown in Figure 38C. Compared to the typical spherical aggregates of pure PPQ_{50}-b-PS_{300} (**54c**) which were about 5 μm in diameter, an enlargement of about a factor of 2 resulted from C_{70} encapsulation, even at this low loading level. Also, these aggregates with encapsulated C_{70} were not very perfect

30   spheres, having many rough surfaces and edges. In contrast, the empty hollow spheres from all the diblock copolymers had perfectly round geometry and very smooth surfaces when compared on the same size scale. Figure 38D shows a typical morphology of fullerene-C_{60} encapsulated in PPQ_{50}-b-PS_{300} (**54c**) at 0.1 wt.% loading. The spherical aggregates were very similar in size, shape and size uniformity to the PPQ_{50}-b-PS_{300} (**54c**)

35   aggregates containing 0.1 wt.% C_{70}.

Figures 39 and 40 show the photomicrographs of 1% C_{60}/PPQ_{50}-b-PS_{300} and 6% C_{60}/PPQ_{50}-b-PS_{300} samples, respectively. The average diameter of the aggregates

5   in Figure 39 was 20 μm. Fluorescence imaging showed the aggregates to be bright red in color (Figures 39A, B). Under crossed polarizers, the same aggregates showed yellow-brown color (Figure 39C). At a loading of 6 wt.% C_{60}, the average diameter of the highly spherical aggregates of Figure 40 was 30 μm. These aggregates were relatively uniform in size distribution and they had highly ordered structures with deep reddish-brown color

10   under crossed polarizers.

        Optical microscopy observation of films cast from solutions with high solubilized fullerene loading ($\geq$ 7 wt.% C_{60} or C_{70} in PPQ_{50}-b-PS_{300}) showed the coexistence of the discrete spherical aggregates observed at smaller fullerene loading with needle-like and continuous fullerene phases. Optical micrographs of PPQ_{50}-b-PS_{300}

15   copolymer with 8 and 10 wt.% solubilized C_{60} are shown in Figure 41. In addition to spherical aggregates with average diameters in the 10-20 μm range, large needle-like phases (up to 10-20 μm wide x 200 μm long) characteristic of the pure C_{60} were also observed.

        Figure 42 shows the average aggregate diameter, measured from the

20   optical and fluorescence micrographs, as a function of fullerene loading in the four different fullerene/PPQ-PS systems. One main feature of the data was that at all fullerene loadings, C_{70}/PPQ_{50}-b-PS_{300} aggregates had the largest sizes. However, there was no clear difference in size between the C_{70} – and C_{60} – containing aggregates of PPQ_{10}-b-PS_{300}. These results suggested that there was both an effect of fullerene size on the

25   fullerene/PPQ-PS aggregates size ($C_{70} > C_{60}$) as well as a dependence on the rod-like block length (PPQ_{50}-b-$PS_{300} > PPQ_{10}$-b-PS_{300}). Another notable feature of the data was the trend of aggregate size with fullerene loading. Increase of diameter with encapsulated fullerene amount was observed to peak at about 60-70 mg/g which was followed by a factor of 2-3 decrease in size at fullerene loadings greater than 70 mg/g. The apparent 70-

30   mg/g transition point may be regarded as the encapsulation capacity of the fullerenes in the block copolymer assemblies; that is, the maximum fullerene loading level where complete sequestering inside the spherical block copolymer aggregates is ensured as evidence by the morphological observations (Figures 38-41). Since this loading level (70 mg/g) was much smaller that the amount of fullerene that could be solubilized (200 mg/g)

35   as determined by solution absorption spectroscopy, this raised questions about the origin for this difference. One possibility was that the excess fullerene molecules outside the spherical aggregates (see for example Figure 41) were originally solubilized inside the

5   nonspherical aggregates (tubules, lamellae, doughnuts) which were distabilized. Another possibility was that some of the fullerene molecules in solution exhibited colloidal interactions with the block copolymer molecules and micelles.

The aggregation number N_o of the self-organized fullerene/PPQ-PS assemblies was estimated from optical and fluorescence micrographs taken over large

10   areas in conjuction with mass balance. For example, for the 6 wt.% C_{60}/PPQ$_{50}$-b-PS$_{300}$ assembly, 10^3 spherical aggregates per mm^2 area was measured from a photomicrograph taken from a 0.2 mg sample covering a 5 cm^2 area. This information translated to 9.6×10^{-15} mole PPQ$_{50}$-b-PS$_{300}$ diblock/aggregate or $N_o = 6 \times 10^9$. Furthermore, the 6 wt.% C_{60} or 64 mg/g encapsulated was equivalent to 3.7 C_{60} molecules per PPQ$_{50}$-b-PS$_{300}$ diblock

15   chain which in combination with N_o meant that about 2.2×10^{10} fullerene-C_{60} molecules were encapsulated inside each aggregate of Figure 40. Similar estimates of the number of C_{60} encapsulated in the PPQ$_{50}$-b-PS$_{300}$ spherical micelles at 0.1 and 3 wt.% fullerene loading were 4×10^8 and 2×10^9, respectively. Since a similar estimate of N_o for the empty PPQ$_{50}$-b-PS$_{300}$ was 1.5×10^8, these results suggested that fullerene solubilization and

20   encapsulation enhanced the aggregation number by factors of 2.7, 13, and 150 respectively at 0.1, 3, and 6 wt.% C_{60} loading. Although such an enhancement of N_o was qualitatively consistent with the predictions of current theories for solubilization by micelles formed by coil-coil block copolymer (Nagarajan et al., Macromolecules, 22:4312 et seq. (1989); Nagarajan et al., J. Chem. Phys., 90:5843 et seq. (1989); Hurter et

25   al., Macromolecules, 26:5030 et seq. (1993); Hurter et al., Macromolecules, 26:5592 et seq. (1993); Linse, Macromolecules, 27:2685 et seq. (1994); Cogan et al., Langmuir, 8:429 et seq. (1992); and Xing et al., Macromolecules, 30:1711 et seq. (1997), which are hereby incorporated by reference),[7-11] it remains to establish their applicability to the unusually large micelles of PPQ-PS block copolymers. Compared to the typical N_o

30   values of 50-100 for coil-coil block copolymer micelles (Solvents and Self-Organization of Polymers, Webber et al., Eds., Kluwer Academic Publishers, Dordrecht, The Netherlands (1996), which is hereby incorporated by reference), the aggregation number of the present PPQ-PS rod-coil block copolymer micelles was about 6 to 7 orders of magnitude larger.

35   To further shed light on the nature of PPQ-PS aggregates with encapsulated fullerenes, differential scanning calorimetry (DSC) was done on fullerene-C_{60}/PPQ$_{50}$-b-PS$_{300}$ aggregates and control samples of pure C_{60}, PS homopolymer, C_{60}/PS blend, and C_{60}/poly(methylmethacrylate) blend. Figure 43A shows the DSC scans of PS

5   homopolymer (curve 1, the first and subsequent scans were identical), revealing a glass

transition (T_g) at 373 K which was in accord with literature values. The repeated DSC

scans of C_{60} were identical (curve 2) to that shown in Figure 43A. The observed sharp

endotherm at 259 K has previously been seen and assigned to the orientational phase

transition of C_{60} from the simple cubic (sc) crystalline form which exists below 259 K to

10   the face-centered cubic (fcc) crystalline form above 259 K (Dresselhaus et al., Science of

Fullerenes and Carbon Nanotubes, Academic Press, San Diego, CA (1996), which is

hereby incorporated by reference). The PPQ homopolymer does not exhibit any DSC

transitions below 673 K. Also shown in Figure 43A is the first DSC scan of 3 wt.%

C_{60}/PPQ_{50}-b-PS_{300} (curve 3) which revealed two second-order transitions with onset

15   temperatures at 273 and 375 K, respectively. These two transition temperatures shifted

slightly during subsequent scans, 269 and 374 K for the second run and 282 and 374 K

for the third scan. It is noteworthy that the sc→fcc phase transition of pure C_{60} at 259 K

was not observed in the DSC scan of C_{60}/PPQ_{50}-b-PS_{300} aggregates. The aggregate

transition at 374-375 can be easily interpreted as the T_g of the PS block (Polymer

20   Handbook, Brandrup et al., Eds., 3rd ed., Wiley, New York, Chapt. V, pp. 77-86 (1989),

which is hereby incorporated by reference).[38] However, the aggregate second-order

transition near 273 K was new and must be carefully assigned.

The DSC scan of a 1 wt.% C_{60}/PS sample is shown in Figure 43B,

revealing two second-order transitions at 274 and 373 K during the first run. The 373-K

25   transition corresponded to the T_g of PS. The transition at 274 K shifted slightly to 270 K

in subsequent scans. Similarly, the repeated DSC scans of C_{60} dispersed in

poly(methylmethacrylate) (PMMA) (~1 wt % C_{60}) gave a second-order transition at 270

K as well as the T_g transition of the polymer at 377 K (Polymer Handbook, Brandrup et

al., Eds., 3rd ed., Wiley, New York, Chapt. V, pp. 77-86 (1989), which is hereby

30   incorporated by reference)[38]. The characteristic sc→fcc crystalline transition of pure C_{60}

was not observed in either of the DSC scans of this fullerene in an amorphous polymer

matrix (PS or PMMA). These results suggested that the new second-order transition at

270 K in the DSC scan of $C_{60}/PPQ_{50}PS_{300}$ aggregates was characteristic of isolated or

amorphous C_{60} dispersed in a polymer matrix. From these results it can also be concluded

35   that the C_{60} molecules encapsulated inside the block copolymer micelles were not

crystalline and that at least some of them were close to and homogeneously dispersed in

5   the PS block. This also supported the micellar mechanism of fullerene solubilization and
     encapsulation by PPQ-PS aggregates.

          In addition, TGA thermograms of block copolymer samples PPQ_{50}-b-PS_{300}
     (54c) and PPQ_{10}-b-PS_{300} (54f) and the PPQ and PS homopolymers at 10 °C/minute in N_2
     are shown in Figure 46.

10   These studies of the morphology of self-organized fullerene/diblock
     copolymer aggregates in comparison with the empty micelles clearly revealed the
     profound effects of fullerene solubilization and encapsulation on the physical size and
     aggregation number. The observed increase in diameter of the fullerene/PPQ-PS
     spherical aggregates correlated well with an amount of fullerene loading up to 70 mg/g

15   and the underlying accommodation of more diblock chains per micellar aggregate. The
     previously discussed solubilization results together with the morphological observations
     and DSC results supported the model structure of the rod-coil block copolymer micelles
     with encapsulated fullerene molecules shown in Figure 34. This structure assumed that
     the hollow cavity as well as the inner PS shell were partially filled with fullerene

20   molecules whereas the rigid-rod PPQ outer shell was free of fullerenes.

     Effect of Encapsulated Fullerenes on Block Copolymer Assemblies.

          The intrinsic electroactive and photoactive properties of PPQ-PS block
25   copolymers (Agrawal et al., Macromolecules, 26:895-905 (1993); Agrawal et al., Chem.
     Mater., 8:579-589 (1996); Agrawal et al., J. Phys. Chem., 96:2837 *et seq.* (1992); Jenekhe
     et al., Chem. Mater., 9:409 *et seq.* (1997), which are hereby incorporated by reference)
     were exploited to probe molecular packing and the effects of encapsulated solubilizates
     on the molecular packing of the block copolymer assemblies. In particular, the focus was

30   on the molecular packing of the conjugated rigid-rod PPQ block whose relative
     fluorescence quantum yield was orders of magnitude larger than those of the fullerenes
     (C_{60}, C_{70}). It was also noteworthy that the emission bands of the fullerenes were in the
     near infrared region, which was far away from where PPQ-PS aggregates emit, so that
     there was no possible interference from their fluorescence bands. As a reference

35   chromophore, the photoluminescence emission (PL) and excitation (PLE) spectra of the
     isolated PPQ_{50}-b-PS_{300} chain in the form of a dilute blend film [0.1 wt % PPQ_{50}-b-PS_{300} in
     poly(ethylene oxide) (PEO)] was investigated. The PL spectrum of such an isolated

5   PPQ$_{50}$-b-PS$_{300}$ chain had a peak at 466 nm (when excited at 380 nm) and a PLE spectrum
       with an absorption maximum at 390 nm when monitoring emission at 460 nm.

                      Figure 44A shows the PL and PLE spectra of a film of spherical PPQ$_{50}$-b-
       PS$_{300}$ aggregates without any fullerene. These spherical aggregate spectra were very
       similar to those of the isolated PPQ$_{50}$-b-PS$_{300}$ single chain except that they were slightly
10   blue shifted. The aggregate PL spectrum had a peak at 454 nm whereas the PLE
       spectrum had a peak at 388 nm. Incorporation of fullerene molecules in PPQ$_{50}$-b-PS$_{300}$
       aggregates resulted in dramatic changes in the aggregate photophysical properties as
       exemplified by Figure 44B which shows the PL and PLE spectra of a film of 1 wt.%
       C$_{60}$/PPQ$_{50}$-b-PS$_{300}$. Two emission bands at ~430 and ~600 nm were observed in the PL
15   spectrum. The 430-nm emission band was blue-shifted compared to that of spherical
       PPQ$_{50}$-b-PS$_{300}$ aggregate without any C$_{60}$ since the excitation spectra were similar
       whereas the 600-nm band was new. The PLE spectrum monitored at 480 nm gave an
       absorption band centered at 388 nm, slightly narrower (full width at half maximum of 62
       versus 72 nm) than the spectrum of the empty PPQ$_{50}$-b-PS$_{300}$ aggregates. However, the
20   PLE spectrum monitored at 600 nm showed entirely new absorption characteristics with
       peaks at 426 and 480 nm. These results suggested that the 430-nm and 600-nm emission
       bands come from different emitting species. Direct excitation of the fullerene-PPQ$_{50}$-b-
       PS$_{300}$ aggregate at 480 nm gave an emission band that was the same as the 600-nm PL
       band. Figure 44C shows the PL and PLE spectra of aggregates of 5 wt.% C$_{60}$/PPQ$_{50}$-b-
25   PS$_{300}$. Only one emission band at 600 nm was observed regardless of the excitation
       wavelength. The corresponding PLE spectrum monitored at 600 nm showed absorption
       peaks at 429 and 506 nm. In fact, similar investigations of other compositions of
       encapsulated C$_{60}$ in PPQ$_{50}$-b-PS$_{300}$ between 0.1 and 5 wt.% of C$_{60}$ showed a progressive
       evolution of the photophysical properties with fullerene loading.

30   These spectral features of the absorption and emission properties of
       fullerene/PPQ-PS assemblies can best be understood within the framework of H- and J-
       aggregation (Kasha, Radiation Research, 20:55 et seq. (1963); Czikkely et al., Chem.
       Phys., 6:11 et seq. (1970); Fidder et al., Phys. Stat. Sol. B., 188:285 et seq. (1995);
       Hochstrasser et al., Photochem. Photobiology, 3:317 et seq. (1964); Chen et al., J. Am.
35   Chem. Soc., 118:2584 et seq. (1996); Gratzel et al., Chem. Phys., 193:1 et seq. (1995);
       Spano et al., Phys. Rev., 40:5783 et seq. (1989), which are hereby incorporated by
       reference) of the rod-like PPQ blocks. The 454-nm emission band with corresponding
       388-nm absorption band of the hollow PPQ$_{50}$PS$_{300}$ micelles were blue-shifted from those

5   of the isolated PPQ-PS chromophore, suggesting the occurrence of H-aggregation of the fluorescent PPQ blocks. The further blue shift and narrowing of the 430-nm emission band at 1 wt.% C_{60} loading suggested that the H-aggregates of PPQ blocks were modified compared to the empty PPQ_{50}-b-PS_{300} assemblies. The significantly red-shifted absorption (PLE) and emission bands at 506 and 600 nm, respectively, in the 5 wt.%

10   C_{60}/PPQ_{50}-b-PS_{300} assemblies compared to the isolated PPQ-PS chromophore were characteristic of J-aggregation of the conjugated PPQ blocks. The progressive evolution of the PLE and PL spectra with increasing amounts of fullerene molecules incorporated into the PPQ-PS assemblies could thus be understood as a consequence of the progressive transformation of the H-aggregates of PPQ blocks in the original empty hollow micelles

15   into all J-aggregates at 5 wt.% C_{60} loading which corresponds to 3.1 C_{60} molecules per PPQ_{50}-b-PS_{300} copolymer chain. Such a fullerene solubilization and encapsulation induced transformation of PPQ-PS rod-coil diblock copolymer chains in H-aggregates to J-aggregates is illustrated in Figure 45.

     These results further confirmed the profound effects of fullerene

20   solubilization and encapsulation on the aggregation behavior of the rod-coil diblock copolymers and their micellar assemblies. The strong interaction of the fullerenes with PS blocks and consequently on the molecular packing of the PPQ blocks also supported the micellar nature of the hollow spherical aggregates of PPQ-PS rod-coil block copolymers. Although the possible contribution of some vesicle-like trapping to the

25   fullerene solubilization in PPQ-PS assemblies could not be completely ruled out, all the present results supported micellar solubilization as the dominant mechanism. For example, trapped molecules in bilayer vesicles do not usually influence the molecular packing of the hollow spheres (Vesicles, Rosoff, Ed., Marcel Dekker, New York (1996), which is hereby incorporated by reference). The J-aggregation of conjugated PPQ blocks

30   in the spherical fullerene/PPQ-PS block copolymer assemblies confirmed that the fullerene molecules were excluded from the outer shell PPQ blocks (Figures 34 and 45).

     The observed J-aggregation of these self-organized fullerene-block copolymer micelles implied that they were highly ordered (Kasha, Radiation Research, 20:55 et seq. (1963); Czikkely et al., Chem. Phys., 6:11 et seq. (1970); Fidder et al., Phys.

35   Stat. Sol. B., 188:285 et seq. (1995); Hochstrasser et al., Photochem. Photobiology, 3:317 et seq. (1964); Chen et al., J. Am. Chem. Soc., 118:2584 et seq. (1996); Gratzel et al., Chem. Phys., 193:1 et seq. (1995); Spano et al., Phys. Rev., 40:5783 et seq. (1989), which are hereby incorporated by reference). This was in accord with the previously discussed

5   polarized optical microscopy observations (Figures 38-40). Together, these results

provided detailed knowledge of molecular packing and of the effects of solubilizates on

the molecular packing of block copolymer micelles, demonstrating the potential of optical

and photoelectronic techniques for characterizing micellar aggregates containing

electroactive and photoactive blocks. The fullerene-block copolymer assemblies *per se*

10   are also of potential broad interest as advanced mesoscopic materials with possible

cooperative electronic and optical properties similar to molecular aggregates of dyes

(Kasha, Radiation Research, 20:55 *et seq.* (1963); Czikkely et al., Chem. Phys., 6:11 *et*

seq. (1970); Fidder et al., Phys. Stat. Sol. B., 188:285 *et seq.* (1995); Hochstrasser et al.,

Photochem. Photobiology, 3:317 *et seq.* (1964); Chen et al., J. Am. Chem. Soc., 118:2584

15   *et seq.* (1996); Gratzel et al., Chem. Phys., 193:1 *et seq.* (1995); Spano et al., Phys. Rev.,

40:5783 *et seq.* (1989), which are hereby incorporated by reference) and composite

properties that combine the features of the fullerenes and conjugated polymers

(Dresselhaus et al., Science of Fullerenes and Carbon Nanotubes, Academic Press, San

Diego, CA (1996); Hirsch, The Chemistry of the Fullerenes, Georg Thieme Verlag,

20   Stuttgart (1994); The Chemical Physics of Fullerenes 10 (and 5) Years Later, Andreoni,

Ed., Kluwer Academic Publishers, Dordrecht, The Netherlands (1996); Hebard et al.,

Nature, 350:600-601 (1991); Zakhidov et al., Phys. Lett. A, 205:317-326 (1995); Kajii et

al., Synth. Met., 86:2351-2352 (1997); Sariciftci et al., Science, 258:1474-1476 (1992);

Sariciftci et al., Appl. Phys. Lett., 62:585-587 (1993); Wang et al., Nature, 356:585-587

25   (1992); Wang et al., J. Phys. Chem., 101:5627-5638 (1997), which are hereby

incorporated by reference). Development of methods to order or crystallize or dope the

encapsulated fullerenes inside the block copolymer micelles could open up many other

possible applications of these supramolecular materials.

30

Example 6 – Preparation of a Mesoporous Solid

    The self-organization of hollow spherical micelles from a rod-coil block

copolymer system in a selective solvent for the flexible-coil block and their long-range,

close-packed, self-ordering into iridescent, ordered mesoporous solids is reported. This

35   hierarchical self-assembly approach to mesoporous solids represents a non-template

strategy (Figure 12). The micellar structure, consisting of a hollow core, a rod-like inner

shell, and a flexible-coil outer corona, had a diffuse corona characteristic of coil-coil

block copolymer micelles (McConnell et al., Phys Rev. Lett., 71:2102-2105 (1993);

5   McConnell et al., Macromolecules, 28:6754-6764 (1995); McConnell et al., Macromolecules, 30:435-444 (1997); McConnell et al., Phys. Rev. E., 54:5447-5455 (1996); Halperin et al., Adv. Polym. Sci., 100:31-71 (1992); Förster et al., Adv. Mater., 10:195-217 (1998); Zhang et al., J. Am. Chem. Soc., 118:3168-3181 (1996); Zhang et al., Science, 268:1728-1731 (1995), which are hereby incorporated by reference). Steric

10   repulsion driven self-ordering and crystallization of coil-coil diblock micelles and their demonstrated control through the corona block length (McConnell et al., Phys Rev. Lett., 71:2102-2105 (1993); McConnell et al., Macromolecules. 28:6754-6764 (1995); McConnell et al., Macromolecules, 30:435-444 (1997); McConnell et al., Phys. Rev. E., 54:5447-5455 (1996)) are thus also viable options here.

15   The rod-coil block copolymer system investigated was poly(phenylquinoline)-block-polystyrene (PPQ$_m$PS$_n$, where m and n are the number of repeat units of the respective blocks) in carbon disulfide (CS$_2$), which is a selective solvent for PS block. The specific rod-coil block copolymer compositions studied were PPQ$_{10}$PS$_{300}$, PPQ$_{10}$PS$_{1000}$, and PPQ$_{50}$PS$_{2000}$ which were either identical to those

20   previously reported (Jenekhe et al., Science, 279:1903-1907 (1998), which is hereby incorporated by reference) or similarly made. The basic synthetic chemistry was that associated with the rigid, rod-like conjugated PPQ homopolymer (Agrawal et al., Macromolecules, 26:895-905 (1993); Agrawal et al., Chem. Mater., 8:579-589 (1996), which are hereby incorporated by reference), which is highly fluorescent and has

25   nonlinear optical properties (Agrawal et al., J. Phys. Chem., 96:2837-2843 (1992); Jenekhe et al., Chem. Mater., 9:409-412 (1997), which are hereby incorporated by reference).

        Solutions of the rod-coil block copolymers (0.005 to 1.0 wt.%) in CS$_2$ and monolayer and multilayer films cast from them at room temperature (25 °C) were

30   investigated. Direct optical, fluorescence, and scanning electron microscopy observations of discrete micellar aggregates and their higher order assembly into large-scale periodic microstructures were made. The possible effects of both the local structure of the micellar building block and the large-scale periodic microstructure on the spontaneous emission of the PPQ chromophores of the rod-coil blocks were probed by previously

35   described steady-state and time-resolved photoluminescence techniques (Osaheni et al., J. Am. Chem. Soc., 117:7389-7398 (1995); Jenekhe et al., Science, 265:765-768 (1994), which are hereby incorporated by reference).

From a small angle neutron scattering study of poly (p-phenylene)-*block*-polystyrene in a selective solvent for PS, spherical micelles of the conventional dense core-diffuse corona structure with a core diameter of 3 to 5 nm were observed. These rod-coil diblocks and star homopolymers formed ordered microporous films by an unclear phase separation mechanism.

The experimental results show that rod-coil block chains solved the steric problem associated with packing rod-like blocks radially into a sphere in a surprising way not anticipated by theory: a hollow sphere. Fluorescence photomicrographs of micelles formed by $PPQ_{10}PS_{300}$ in CS_2 provided evidence of hollow spheres (Figures 47A and 47B). The shape of the discrete micellar aggregates looked somewhat like red blood cells because of distortion and partial collapse of the hollow spheres due to drying. Additional microscopic observations under bright field and crossed polarizers confirmed that the micelles formed by all three copolymer samples had approximate diameters of 3 to 5 μm. Polarized optical microscopy indicated that the micelles were highly ordered. This ordering originated from orientationally ordered radial packing of the rigid, rod-like blocks; micellar aggregates of coil-coil block copolymers lack such order (Webber et al., Solvents and Self-Organization of Polymers, Kluwer Academic, Dordrecht (1996); Webber, J. Phys. Chem. B, 102:2618-2626 (1998); Tuzar et al., in Surface and Colloid Science, 15:1-83, Plenum, New York (1993); Halperin et al., Adv. Polym. Sci., 100:31-71 (1992); Förster et al., Adv. Mater., 10:195-217 (1998); Zhang et al., J. Am. Chem. Soc., 118:3168-3181 (1996); Zhang et al., Science, 268:1728-1731 (1995), which are hereby incorporated by reference). The hollow spherical structure of these rod-coil block micelles in CS_2 was, however, different from that formed by the same copolymers in trifluoroacetic acid/dichloromethane (a selective solvent for the rod-like blocks) (see Example 3; Jenekhe et al., Science, 279:1903-1907 (1998); Chen et al., Langmuir, 12:2995-3002 (1996), which are hereby incorporated by reference) in that here the solvated coil-like blocks were on the convex side. A profound consequence of the stiffness asymmetry of a rod-coil block copolymer was that the same macromolecule in two different selective solvents self-organized into two qualitatively different colloidal particles: hollow hard spheres and hollow soft spheres.

Self-ordering of these hollow soft spheres into two-(2-D) and three-dimensional (3-D) periodic structures was studied by optical and electron microscopy of micellar films cast from rod-coil block copolymer solutions of varying initial

5   concentrations in ways similar to prior studies of colloidal crystallization of polymer latex

spheres (Kose et al., Colloid Interface Sci., 46:460 (1974); Hachisu et al., Nature,

283:188-189 (1980); Clark et al., Nature, 281:57-60 (1979); Pieranski et al., Contemp.

Phys., 24:25-73 (1983); Pusey et al., Nature, 320:340-342 (1986); Bartlett et al., Phys.

Rev. Lett., 68:3801-3804 (1992); van Blaaderen et al., Nature, 385:321-324 (1997);

10   Weissman, et al., Science, 274:959-960 (1996), which are hereby incorporated by

reference). Only discrete, non-aggregated, micelles, were obtained from very dilute

solutions between 0.005 to 0.01 wt.% (Figures 47A and 47B). However, even at 0.01

wt.%, the particle number density was sufficiently high for the onset of 2-D micellar

ordering to be visible in regions of a monolayer film (Figure 47B, arrows). Micellar films

15   cast from 0.5 wt.% had a controllable thickness of about 4.5 to 35 μm and consisted of

stacks of one to eight layers of hexagonally close-packed (hcp) 2-D lattices of spherical

air holes in a polymeric matrix. An example is the ~27-μm thick micellar film of PPQ_{10}-

b-PS_{300} which revealed a 2-D hcp structure when viewed from the top (Figure 47C) and

was visually highly iridescent at various reflection angles akin to a credit card hologram.

20   The air holes revealed by carefully peeling off part of the top layer with an adhesive tape

largely reflected the original hollow spherical micelles. The moderate mechanical

properties of these self-ordered micellar films suggested that significant interdigitation of

the polystyrene coronal chains occurred between the micellar building blocks of the

microporous solid.

25   Defect-free microstructure of the periodic microporous films of all three

block copolymers covered areas as large as 1 cm^2 and varied with composition and

molecular weight. From the polarized optical and scanning electron (SEM) micrographs

of micellar films of PPQ_{50}-b-PS_{2000} (Figures 48A to C), 2-D hcp lattice of spherical air

holes having a diameter (D) of 3.4 ± 0.2 gm and a center-to-center hole periodicity (p) of

30   4.4 ± 0.2 gm were observed from the top layer. The ~31 μm film consisted of seven

layers of air hole lattices of which the top layer was clearly open (Figures 48B and C).

The progressive decreases of the hole diameter and periodicity of the microstructure with

the PS block length were approximately linear (Figure 48D), decreasing to 2.6 ± 0.2 and

2.8 ± 0.2 μm, respectively, for micellar films of PPQ_{10}-b-PS_{300}. The minimum wall

35   thickness h ($= p$-D), which was in the range of 0.2 to 1.0 μm for the three copolymer

compositions, also varied linearly with the PS coronal chain length. Evidence of the 3-D

order of these multilayer films included their colorful iridescence (Wijnhoven et al.,

5 <u>Science</u>, 281:802-804 (1998); Kose et al., <u>Colloid Interface Sci.</u>, 46:460-469 (1974); Hachisu et al., <u>Nature</u>, 283:188-189 (1980); Clark et al., <u>Nature</u>, 281:57-60 (1979); Pieranski et al., <u>Contemp. Phys.</u>, 24:25-73 (1983); Pusey et al., <u>Nature</u>, 320:340-342 (1986); Bartlett et al., <u>Phys. Rev. Lett.</u>, 68:3801-3804 (1992); van Blaaderen et al., <u>Nature</u>, 385:321-324 (1997); Weissman et al., <u>Science</u>, 274:959-960 (1996), which are

10 hereby incorporated by reference) and observation of ordered arrays of the air holes when multilayer films were viewed from the side or by sequential removal of layers from the top. Distinction between ABCABC- or ABABAB-type stacking of layers and hence whether the 3-D lattice was fcc or hcp could not be established.

15 **<u>Example 7</u> - Preparation of Microporous Films Containing Fullerenes**

Addition of small amounts (< 20 mg/g rod-coil block) of fullerene (C_{70} or C_{60}) into the solutions in CS_2 (see Example 6) significantly modified the microstructural parameters of the ordered microporous films (Figure 49). Although these fullerene-containing micellar films had superior iridescence colors compared to similar

20 microporous films without fullerene, they were more brittle with visible cracks. The hole diameter and periodicity decreased with the amount of fullerene loading, up to 29 and 25% reductions, respectively, at 10 mg C_{70}/g PPQ_{10}-b-PS_{300} (Figure 49B). The wall thickness increased slightly with fullerene loading. Similar effects of fullerene C_{70} or C_{60} on self-organized microporous films of PPQ_{10}-b-PS_{1000} and PPQ_{50}-b-PS_{2000} were

25 observed. Self-assembly of microporous films was no longer observed in any of the three rod-coil block copolymers at high fullerene loading (> 20 mg/g). These results suggested that the fullerene was incorporated within the PS corona of the micellar building blocks as expected from their mutual compatibility (Jenekhe et al., <u>Science</u>, 279:1903-1907 (1998), which is hereby incorporated by reference). These findings also suggested a simple way

30 of controlling the functional properties of the microporous materials independently of copolymer architecture and composition.

Because of their spatially periodic variation of refractive index, these self-organized ordered microporous materials with or without fullerenes are promising, easy to produce, photonic band gap structures (Wijnhoven et al., <u>Science</u>, 281:802-804 (1998);

35 Yablonovitch, <u>J. Opt. Soc. Am. B.</u>, 10:283-295 (1993); Joannopoulos et al., <u>Nature</u>, 386:143-145 (1997); Martorell et al., <u>Phys. Rev. Lett.</u>, 65:1877-1880 (1990); Miguez et al., <u>Appl. Phys. Lett.</u>, 71:1148-1150 (1997), which are hereby incorporated by reference). These periodic dielectric composites of air holes (refractive index $n_o = 1$) and rod-coil

5   block walls (n_o = 1.6 for PS, 1.8 for PPQ) have a high refractive index contrast. The

higher index contrast in fullerene-containing micellar films, C_{70} (n_o = 1.94) and C_{60}(n_o = .

2.00-2.12) (Dresselhaus et al., Science of Fullerenes and Carbon Nanotubes, Academic

Press, San Diego, CA (1996), which is hereby incorporated by reference), can explain

their superior optical properties. However, the present hole diameters and periodicities

10   were comparable to infrared (IR) wavelengths. Reductions in D and p to sizes

comparable to visible wavelengths are desirable for some photonic and optoelectronic

applications (Yablonovitch, J. Opt. Soc. Am. B., 10:283-295 (1993); Joannopoulos et al.,

Nature, 386:143-145 (1997); Martorell et al., Phys. Rev. Lett., 65:1877-1880 (1990);

Miguez et al., Appl. Phys. Lett., 71:1148-1150 (1997), which are hereby incorporated by

15   reference).

          Significant modification of the spontaneous emission of the PPQ blocks in

the self-assembled, periodic microporous films, compared to the isolated chromophores,

dispersed in a matrix of poly(ethylene oxide) (PEO), was observed by photoluminescence

emission (PL) and excitation (PLE) spectroscopies (Figure 50). Isolated PPQ

20   chromophores of PPQ_{10}-b-PS_{300} rod-coil block had emission and excitation bands at 466

and 393 nm, respectively. In contrast, the micellar films of PPQ_{10}-b-PS_{300} cast from a 0.5

wt.% solution had blue-shifted PL and PLE spectra with peaks at 437 and 388 nm,

respectively, (Figure 50A), and absorption band observed in the PLE was more narrow.

Time-resolved PL decay dynamics of the fluorescent PPQ blocks as isolated chains in

25   PEO revealed two lifetimes (1.1 ns (30%) and 4.7 ns (70%)) versus one lifetime (0.93ns)

(Figure 50B) in the micellar films. This represented a large reduction in the excited state

lifetime of PPQ chromophores in the microporous micellar films. Because the emission

band was far removed from photonic band gaps of these microporous films, which were

expected to be in the IR region, the large-scale periodic microstructure was ruled out as

30   the origin of the observed modification of photophysical properties. The decrease in

lifetime was also the opposite of the predicted effect of a photonic crystal on spontaneous

emission (Yablonovitch, J. Opt. Soc. Am. B., 10:283-295 (1993); Joannopoulos et al.,

Nature, 386:143-145 (1997); Martorell et al., Phys. Rev. Lett., 65:1877-1880 (1990);

Miguez, et al., Appl. Phys. Lett., 71:1148-1150 (1997), which are hereby incorporated by

35   reference). H-aggregation (Kasha, Radiation Research, 20:55 et seq. (1963);

Hochstrasser et al., Photochem. Photobiology, 3:317 et seq. (1964); Czikkely et al.,

Chem. Phys., 6:11-14 (1970); Chen et al., J. Am. Chem. Soc., 118:2584 et seq. (1996),

which are hereby incorporated by reference) of the PPQ blocks and hence the local

5   structure of the micellar building blocks best explained the observed photophysical properties. H-aggregation of the rigid rod-like blocks implied that they were orientationally aligned close to the radial direction in the spherical micellar assemblies (Figure 12). Such an H-aggregation of conjugated molecules can lead to novel cooperative optical and nonlinear optical properties (Kasha, Radiation Research, 20:55 *et*

10   *seq.* (1963); Hochstrasser et al., Photochem. Photobiology, 3:317 *et seq.* (1964); Czikkely et al., Chem. Phys., 6:11-14 (1970); Chen et al., J. Am. Chem. Soc., 118:2584 *et seq.* (1996), which are hereby incorporated by reference).

       Although the invention has been described in detail for the purpose of illustration, it is understood that such detail is solely for that purpose, and variations can

15   be made therein by those skilled in the art without departing from the spirit and scope of the invention which is defined by the following claims.

WHAT IS CLAIMED:

1. A method for producing microstructures, nanostructures, or objects comprising:

providing a rod-coil block copolymer comprising a rigid-rod block and a flexible-coil block;

mixing the rod-coil block copolymer and a selective solvent for one of the blocks which solubilizes that block; and

permitting the rod-coil block copolymer to self-assemble into organized mesostructures with a region of the unsolubilized block and a region of the solubilized block.

2. A method according to claim 1, wherein the rigid-rod block is selected from the group consisting of polyquinolines, polyquinoxalines, poly(p-phenylenes), poly(p-phenylene vinylenes), polypridines, poly(pyridine vinylenes), poly(naphthylene vinylenes), polythiophenes, poly(thiophene vinylenes), polypyrroles, polyanilines, polybenzimidazoles, polybenzothiazoles, polybenzoxazoles, polybenzobisazoles, aromatic polyamides, aromatic polyhydrazides, aromatic polyazomethines, aromatic polyesters, and aromatic polyimides.

3. A method according to claim 1, wherein the flexible-coil block is selected from the group consisting of polystyrene, poly(α-methyl styrene), poly(ethylene oxide, poly(propylene oxide), poly(acrylic acid), poly(methylacrylic acid), poly(2-vinylpyridine), poly(4-vinylpyridine), polyurethane, poly(vinyl pyrrolidone), poly(methyl methacrylate), poly(n-butyl methacrylate), polyisoprene, poly(butadiene), poly(dimethylsiloxane), poly(styrene sulfonic acid), and sodium poly(styrene sulfonate).

4. A method according to claim 1, wherein the rod-coil block copolymer is selected from the group consisting of a poly(phenylquinoline)-*block*-polystyrene and a poly(phenylquinoxaline)-*block*-polystyrene.

5. A method according to claim 4, wherein the selective solvent is selected from the group consisting of trifluoroacetic acid, mixtures of trifluoroacetic acid and dichloromethane, mixtures of trifluoroacetic acid and toluene, carbon disulfide, 1-nitropropane, ethylbenzene, cyclohexanone, water, dioxane/water, formamide, N,N-dimethyl-formamide, ethanol, methanol, and mixtures thereof.

6.   A method according to claim 1, wherein the rod-coil block copolymer is selected from the group consisting of a poly(phenylquinoline)-*block*-polystyrene-*block*-poly(phenylquinoline) and a poly(phenylquinoxaline)-*block*-polystyrene-*block*-poly(phenylquinoxaline).

7.   A method according to claim 6, wherein the selective solvent is selected from the group consisting of trifluoroacetic acid, mixtures of trifluoroacetic acid and dichloromethane, mixtures of trifluoroacetic acid and toluene, carbon disulfide, 1-nitropropane, ethylbenzene, cyclohexanone, water, dioxane/water, formamide, N,N-dimethyl-formamide, ethanol, methanol, and mixtures thereof.

8.   A method according to claim 1, wherein the selective solvent is for the rigid-rod block.

9.   A method according to claim 1, wherein the selective solvent is for the flexible-coil block.

10.   A method according to claim 1, wherein the microstructures, nanostructures, or objects are in a form selected from the group consisting of spheres, lamellae, cylinders, and vesicles.

11.   A method according to claim 1, wherein the rod-coil block copolymer has the structure:

rod block$_m$coil block$_n$

, wherein m=1 to 500 and n=10 to 5000.

12.   A method according to claim 1, wherein the rod-coil block copolymer has the structure:

rod block$_m$coil block$_n$rod block$_m$

, wherein m=1 to 500 and n=10 to 5000.

13.   A method according to claim 1 further comprising:

evaporating the solvent after said permitting.

14.   A microstructure, nanostructure, or object comprising:

a rod-coil block copolymer comprising a rigid-rod block and a flexible-coil block, wherein the rod-coil block copolymer forms an organized mesostructure with a region of one block and a region of the other block.

15.   A microstructure, nanostructure, or object according to claim 14, wherein the rigid-rod block is selected from the group consisting of polyquinolines, polyquinoxalines, poly(p-phenylenes), poly(p-phenylene vinylenes), polypridines, poly(pyridine vinylenes), poly(naphthylene vinylenes), polythiophenes, poly(thiophene vinylenes), polypyrroles, polyanilines, polybenzimidazoles, polybenzothiazoles, polybenzoxazoles, polybenzobisazoles, aromatic polyamides, aromatic polyhydrazides, aromatic polyazomethines, aromatic polyesters, and aromatic polyimides.

16.   A microstructure, nanostructure, or object according to claim 14, wherein the flexible-coil block is selected from the group consisting of polystyrene, poly(α-methyl styrene), poly(ethylene oxide, poly(propylene oxide), poly(acrylic acid), poly(methylacrylic acid), poly(2-vinylpyridine), poly(4-vinylpyridine), polyurethane, poly(vinyl pyrrolidone), poly(methyl methacrylate), poly(n-butyl methacrylate), polyisoprene, poly(butadiene), poly(dimethylsiloxane), poly(styrene sulfonic acid), and sodium poly(styrene sulfonate).

17.   A microstructure, nanostructure, or object according to claim 14, wherein the rod-coil block copolymer is selected from the group consisting of a poly(phenylquinoline)-*block*-polystyrene and a poly(phenylquinoxaline)-*block*-polystyrene.

18.   A microstructure, nanostructure, or object according to claim 14, wherein the rod-coil block copolymer is selected from the group consisting of a poly(phenylquinoline)-*block*-polystyrene-*block*-poly(phenylquinoline) and a poly(phenylquinoxaline)-*block*-polystyrene-*block*-poly(phenylquinoxaline).

19.   A microstructure, nanostructure, or object according to claim 14, wherein the microstructure, nanostructure, or object is in a form selected from the group consisting of spheres, lamellae, cylinders, and vesicles.

20.   An optical article comprising:

a microstructure, nanostructure or object according to claim 14 and

an optical component, wherein the microstructure, nanostructure or object is formed as a coating on the optical component.

21.   A method for producing a mesoporous solid comprising:

providing a rod-coil block copolymer comprising a rigid-rod block and a flexible-coil block;

mixing the rod-coil block copolymer and a selective solvent for the flexible-coil block which solubilizes that block;

permitting the rod-coil block copolymer to self-assemble into organized mesostructures with a region of the unsolubilized block and a region of the solubilized block;

evaporating the solvent; and

permitting the organized mesostructures to self-organize into a mesoporous solid.

22.   A method according to claim 21, wherein the rigid-rod block is selected from the group consisting of polyquinolines, polyquinoxalines, poly(p-phenylenes), poly(p-phenylene vinylenes), polypridines, poly(pyridine vinylenes), poly(naphthylene vinylenes), polythiophenes, poly(thiophene vinylenes), polypyrroles, polyanilines, polybenzimidazoles, polybenzothiazoles, polybenzoxazoles, polybenzobisazoles, aromatic polyamides, aromatic polyhydrazides, aromatic polyazomethines, aromatic polyesters, and aromatic polyimides.

23.   A method according to claim 21, wherein the flexible-coil block is selected from the group consisting of polystyrene, poly(α-methyl styrene), poly(ethylene oxide, poly(propylene oxide), poly(acrylic acid), poly(methylacrylic acid), poly(2-vinylpyridine), poly(4-vinylpyridine), polyurethane, poly(vinyl pyrrolidone), poly(methyl methacrylate), poly(n-butyl methacrylate), polyisoprene, poly(butadiene), poly(dimethylsiloxane), poly(styrene sulfonic acid), and sodium poly(styrene sulfonate).

24.   A method according to claim 21, wherein the rod-coil block copolymer is selected from the group consisting of a poly(phenylquinoline)-*block*-polystyrene and a poly(phenylquinoxaline)-*block*-polystyrene.

25.   A method according to claim 24, wherein the selective solvent is selected from the group consisting of carbon disulfide, 1-nitropropane, ethylbenzene, cyclohexanone, water, dioxane/water, formamide, N,N-dimethyl-formamide, ethanol, methanol, and mixtures thereof.

26.   A method according to claim 21, wherein the rod-coil block copolymer is selected from the group consisting of a poly(phenylquinoline)-*block*-polystyrene-*block*-poly(phenylquinoline) and a poly(phenylquinoxaline)-*block*-polystyrene-*block*-poly(phenylquinoxaline).

27.   A method according to claim 26, wherein the selective solvent is selected from the group consisting of carbon disulfide, 1-nitropropane, ethylbenzene, cyclohexanone, water, dioxane/water, formamide, N,N-dimethyl-formamide, ethanol, methanol, and mixtures thereof.

28.   A method according to claim 21, wherein the organized mesostructures are in a form selected from the group consisting of spheres, lamellae, cylinders, and vesicles.

29.   A method according to claim 21, wherein the rod-coil block copolymer has the structure:

rod block$_m$coil block$_n$

, wherein m=1 to 500 and n=10 to 5000.

30.   A method according to claim 21, wherein the rod-coil block copolymer has the structure:

rod block$_m$coil block$_n$rod block$_m$

, wherein m=1 to 500 and n=10 to 5000.

31.   A method for tissue engineering comprising:
providing a mesoporous solid according to claim 21;
adding a cell culture to the mesoporous solid; and
allowing the cells to grow on the mesoporous solid under conditions effective to produce an organized tissue layer.

32.   A method for producing a polymer adsorption layer on a substrate comprising:

providing a rod-coil block copolymer including a rigid-rod block and a flexible-coil block;

mixing the rod-coil block copolymer and a selective solvent for one of the blocks to form a solution of rod-coil block copolymer and solvent;

inserting a substrate into the solution;

permitting the rod-coil block copolymer to adsorb to the substrate; and

removing the substrate from the solution under conditions effective to form an adsorption layer of a polymer on the substrate.

33.   A method according to claim 32, wherein the rigid-rod block is selected from the group consisting of polyquinolines, polyquinoxalines, poly(p-phenylenes), poly(p-phenylene vinylenes), polypridines, poly(pyridine vinylenes), poly(naphthylene vinylenes), polythiophenes, poly(thiophene vinylenes), polypyrroles, polyanilines, polybenzimidazoles, polybenzothiazoles, polybenzoxazoles, polybenzobisazoles, aromatic polyamides, aromatic polyhydrazides, aromatic polyazomethines, aromatic polyesters, and aromatic polyimides.

34.   A method according to claim 32, wherein the flexible-coil block is selected from the group consisting of polystyrene, poly(α-methyl styrene), poly(ethylene oxide, poly(propylene oxide), poly(acrylic acid), poly(methylacrylic acid), poly(2-vinylpyridine), poly(4-vinylpyridine), polyurethane, poly(vinyl pyrrolidone), poly(methyl methacrylate), poly(n-butyl methacrylate), polyisoprene, poly(butadiene), poly(dimethylsiloxane), poly(styrene sulfonic acid), and sodium poly(styrene sulfonate).

35.   A method according to claim 32, wherein the rod-coil block copolymer is selected from the group consisting of a poly(phenylquinoline)-*block*-polystyrene and a poly(phenylquinoxaline)-*block*-polystyrene.

36.   A method according to claim 35, wherein the solvent is selected from the group consisting of trifluoroacetic acid, mixtures of trifluoroacetic acid and dichloromethane, mixtures of trifluoroacetic acid and toluene, carbon disulfide, 1-nitropropane, ethylbenzene, cyclohexanone, water, dioxane/water, formamide, N,N-dimethyl-formamide, ethanol, methanol, and mixtures thereof.

37.   A method according to claim 32, wherein the rod-coil block copolymer is selected from the group consisting of a poly(phenylquinoline)-*block*-polystyrene-*block*-poly(phenylquinoline) and a poly(phenylquinoxaline)-*block*-polystyrene-*block*-poly(phenylquinoxaline).

38.   A method according to claim 37, wherein the solvent is selected from the group consisting of trifluoroacetic acid, mixtures of trifluoroacetic acid and dichloromethane, mixtures of trifluoroacetic acid and toluene, carbon disulfide, 1-nitropropane, ethylbenzene, cyclohexanone, water, dioxane/water, formamide, N,N-dimethyl-formamide, ethanol, methanol, and mixtures thereof.

39.   A method according to claim 32, wherein the selective solvent is for the rigid-rod block.

40.   A method according to claim 32, wherein the selective solvent is for the flexible-coil block.

41.   A substrate with a polymeric adsorption layer comprising:

a substrate and

a rod-coil block copolymer comprising a rigid-rod block and a flexible-coil block, wherein one of the blocks of the rod-coil block copolymer is adsorbed to the substrate.

42.   A substrate with a polymeric adsorption layer according to claim 41, wherein the rigid-rod block is selected from the group consisting of polyquinolines, polyquinoxalines, poly(*p*-phenylenes), poly(*p*-phenylene vinylenes), polypridines, poly(pyridine vinylenes), poly(naphthylene vinylenes), polythiophenes, poly(thiophene vinylenes), polypyrroles, polyanilines, polybenzimidazoles, polybenzothiazoles, polybenzoxazoles, polybenzobisazoles, aromatic polyamides, aromatic polyhydrazides, aromatic polyazomethines, aromatic polyesters, and aromatic polyimides.

43.   A substrate with a polymeric adsorption layer according to claim 41, wherein the flexible-coil block is selected from the group consisting of polystyrene, poly(α-methyl styrene), poly(ethylene oxide, poly(propylene oxide), poly(acrylic acid), poly(methylacrylic acid), poly(2-vinylpyridine), poly(4-vinylpyridine), polyurethane, poly(vinyl pyrrolidone), poly(methyl methacrylate), poly(n-butyl methacrylate),

5 polyisoprene, poly(butadiene), poly(dimethylsiloxane), poly(styrene sulfonic acid), and

sodium poly(styrene sulfonate.

44.   A substrate with a polymeric adsorption layer according to claim

41, wherein the rod-coil block copolymer is selected from the group consisting of a

poly(phenylquinoline)-*block*-polystyrene and a poly(phenylquinoxaline)-*block*-

10 polystyrene.

45.   A substrate with a polymeric adsorption layer according to claim

41, wherein the rod-coil block copolymer is selected from the group consisting of a

poly(phenylquinoline)-*block*-polystyrene-*block*-poly(phenylquinoline) and a

poly(phenylquinoxaline)-*block*-polystyrene-*block*-poly(phenylquinoxaline).

15   46.   An optical article comprising:

a substrate;

a transparent conductor formed as a coating on the substrate;

a polymeric adsorption layer comprising a rod-coil block copolymer

comprising a rigid-rod block and a flexible-coil block, wherein one of the blocks of the

20 rod-coil block copolymer is adsorbed to the transparent conductor; and

a coating formed on the surface of the adsorption layer, wherein the

adsorption layer allows the emission of polarized light.

47.   A method for encapsulating guest molecules, macromolecules, or

nanoparticles comprising:

25   providing a rod-coil block copolymer comprising a rigid-rod block and a

flexible-coil block;

mixing the rod-coil block copolymer and a selective solvent for one of the

blocks which solubilizes that block to form a solution of rod-coil block copolymer and

solvent;

30   adding guest molecules, macromolecules, or nanoparticles to the solution;

and

permitting the rod-coil block copolymer to self-assemble into organized

mesostructures with a region of the unsolubilized block and a region of the solubilized

block under conditions effective to encapsulate the guest molecules, macromolecules, or

35 nanoparticles within the mesostructure.

48.   A method according to claim 47, wherein the rigid-rod block is selected from the group consisting of polyquinolines, polyquinoxalines, poly(*p*-phenylenes), poly(*p*-phenylene vinylenes), polypridines, poly(pyridine vinylenes), poly(naphthylene vinylenes), polythiophenes, poly(thiophene vinylenes), polypyrroles, polyanilines, polybenzimidazoles, polybenzothiazoles, polybenzoxazoles, polybenzobisazoles, aromatic polyamides, aromatic polyhydrazides, aromatic polyazomethines, aromatic polyesters, and aromatic polyimides.

49.   A method according to claim 47, wherein the flexible-coil block is selected from the group consisting of polystyrene, poly(α-methyl styrene), poly(ethylene oxide, poly(propylene oxide), poly(acrylic acid), poly(methylacrylic acid), poly(2-vinylpyridine), poly(4-vinylpyridine), polyurethane, poly(vinyl pyrrolidone), poly(methyl methacrylate), poly(n-butyl methacrylate), polyisoprene, poly(butadiene), poly(dimethylsiloxane), poly(styrene sulfonic acid), and sodium poly(styrene sulfonate).

50.   A method according to claim 47, wherein the rod-coil block copolymer is selected from the group consisting of a poly(phenylquinoline)-*block*-polystyrene and a poly(phenylquinoxaline)-*block*-polystyrene.

51.   A method according to claim 40, wherein the solvent is selected from the group consisting of trifluoroacetic acid, mixtures of trifluoroacetic acid and dichloromethane, mixtures of trifluoroacetic acid and toluene, carbon disulfide, 1-nitropropane, ethylbenzene, cyclohexanone, water, dioxane/water, formamide, N,N-dimethyl-formamide, ethanol, methanol, and mixtures thereof.

52.   A method according to claim 47, wherein the rod-coil block copolymer is selected from the group consisting of a poly(phenylquinoline)-*block*-polystyrene-*block*-poly(phenylquinoline) and a poly(phenylquinoxaline)-*block*-polystyrene-*block*-poly(phenylquinoxaline).

53.   A method according to claim 52, wherein the solvent is selected from the group consisting of trifluoroacetic acid, mixtures of trifluoroacetic acid and dichloromethane, mixtures of trifluoroacetic acid and toluene, carbon disulfide, 1-nitropropane, ethylbenzene, cyclohexanone, water, dioxane/water, formamide, N,N-dimethyl-formamide, ethanol, methanol, and mixtures thereof.

54. A method according to claim 47, wherein the guest molecule is selected from the group consisting of fullerenes, carbon nanotubes, drug formulations, cosmetic formulations, metal particles, semiconductor particles, and magnetic particles.

55. A method according to claim 47, wherein the mesostructure is in a form selected from the group consisting of spheres, lamellae, cylinders, and vesicles.

56. A method according to claim 47, wherein the rod-coil block copolymer has the structure:

rod block$_m$coil block$_n$

, wherein m=1 to 500 and n=10 to 5000.

57. A method according to claim 47, wherein the rod-coil block copolymer has the structure:

rod block$_m$coil block$_n$rod block$_m$

, wherein m=1 to 500 and n=10 to 5000.

58. An organized mesostructure with an encapsulated guest molecule, macromolecule, or nanoparticle comprising:

a rod-coil block copolymer comprising a rigid-rod block and a flexible-coil block, wherein the rod-coil block copolymer forms an organized mesostructure with a region of one block and a region the other block and

a guest molecule, macromolecule, or nanoparticle, wherein the guest molecule, macromolecule, or nanoparticle is encapsulated within the mesostructure.

59. An organized mesostructure with an encapsulated guest molecule, macromolecule, or nanoparticle according to claim 58, wherein the rigid-rod block is selected from the group consisting of polyquinolines, polyquinoxalines, poly(p-phenylenes), poly(p-phenylene vinylenes), polypridines, poly(pyridine vinylenes), poly(naphthylene vinylenes), polythiophenes, poly(thiophene vinylenes), polypyrroles, polyanilines, polybenzimidazoles, polybenzothiazoles, polybenzoxazoles, polybenzobisazoles, aromatic polyamides, aromatic polyhydrazides, aromatic polyazomethines, aromatic polyesters, and aromatic polyimides.

60.   An organized mesostructure with an encapsulated guest molecule, macromolecule, or nanoparticle according to claim 58, wherein the flexible-coil block is selected from the group consisting of polystyrene, poly(α-methyl styrene), poly(ethylene oxide, poly(propylene oxide), poly(acrylic acid), poly(methylacrylic acid), poly(2-vinylpyridine), poly(4-vinylpyridine), polyurethane, poly(vinyl pyrrolidone), poly(methyl methacrylate), poly(n-butyl methacrylate), polyisoprene, poly(butadiene), poly(dimethylsiloxane), poly(styrene sulfonic acid), and sodium poly(styrene sulfonate).

61.   An organized mesostructure with an encapsulated guest molecule, macromolecule, or nanoparticle according to claim 58, wherein the rod-coil block copolymer is selected from the group consisting of a poly(phenylquinoline)-*block*-polystyrene and a poly(phenylquinoxaline)-*block*-polystyrene.

62.   An organized mesostructure with an encapsulated guest molecule, macromolecule, or nanoparticle according to claim 58, wherein the rod-coil block copolymer is selected from the group consisting of a poly(phenylquinoline)-*block*-polystyrene-*block*-poly(phenylquinoline) and a poly(phenylquinoxaline)-*block*-polystyrene-*block*-poly(phenylquinoxaline).

63.   An organized mesostructure with an encapsulated guest molecule, macromolecule, or nanoparticle according to claim 58, wherein the guest molecule is selected from the group consisting of fullerenes, carbon nanotubes, drug formulations, cosmetic formulations, metal particles, semiconductor particles, and magnetic particles.

64.   An organized mesostructure with an encapsulated guest molecule, macromolecule, or nanoparticle according to claim 58, wherein the mesostructure is in a form selected from the group consisting of spheres, lamellae, cylinders, and vesicles.

65.   An organized mesostructure with an encapsulated guest molecule, macromolecule, or nanoparticle according to claim 58, wherein the rod-coil block copolymer has the structure:

rod block$_m$coil block$_n$

, wherein m=1 to 500 and n=10 to 5000.

66.   An organized mesostructure with an encapsulated guest molecule, macromolecule, or nanoparticle according to claim 58, wherein the rod-coil block copolymer has the structure:

rod block$_m$coil block$_n$rod block$_m$

, wherein m=1 to 500 and n=10 to 5000.

67.   A method for solubilizing guest molecules, macromolecules, or nanoparticles comprising:

providing a rod-coil block copolymer comprising a rigid-rod block and a flexible-coil block;

mixing the rod-coil block copolymer and a selective solvent for one of the blocks which solubilizes that block to form a solution of rod-coil block copolymer and solvent;

adding guest molecules, macromolecules, or nanoparticles to the solution; and

permitting the rod-coil block copolymer to self-assemble into organized mesostructures with a region of the unsolubilized block and a region of the solubilized block under conditions effective to solubilize the guest molecules, macromolecules, or nanoparticles.

68.   A method according to claim 67, wherein the rigid-rod block is selected from the group consisting of polyquinolines, polyquinoxalines, poly(p-phenylenes), poly(p-phenylene vinylenes), polypridines, poly(pyridine vinylenes), poly(naphthylene vinylenes), polythiophenes, poly(thiophene vinylenes), polypyrroles, polyanilines, polybenzimidazoles, polybenzothiazoles, polybenzoxazoles, polybenzobisazoles, aromatic polyamides, aromatic polyhydrazides, aromatic polyazomethines, aromatic polyesters, and aromatic polyimides.

69.   A method according to claim 67, wherein the flexible-coil block is selected from the group consisting of polystyrene, poly(α-methyl styrene), poly(ethylene oxide, poly(propylene oxide), poly(acrylic acid), poly(methylacrylic acid), poly(2-vinylpyridine), poly(4-vinylpyridine), polyurethane, poly(vinyl pyrrolidone), poly(methyl methacrylate), poly(n-butyl methacrylate), polyisoprene, poly(butadiene), poly(dimethylsiloxane), poly(styrene sulfonic acid), and sodium poly(styrene sulfonate).

70.   A method according to claim 67, wherein the rod-coil block copolymer is selected from the group consisting of a poly(phenylquinoline)-*block*-polystyrene and a poly(phenylquinoxaline)-*block*-polystyrene.

71.   A method according to claim 70, wherein the solvent is selected from the group consisting of trifluoroacetic acid, mixtures of trifluoroacetic acid and dichloromethane, mixtures of trifluoroacetic acid and toluene, carbon disulfide, 1-nitropropane, ethylbenzene, cyclohexanone, water, dioxane/water, formamide, N,N-dimethyl-formamide, ethanol, methanol, and mixtures thereof.

72.   A method according to claim 67, wherein the rod-coil block copolymer is selected from the group consisting of a poly(phenylquinoline)-*block*-polystyrene-*block*-poly(phenylquinoline) and a poly(phenylquinoxaline)-*block*-polystyrene-*block*-poly(phenylquinoxaline).

73.   A method according to claim 72, wherein the solvent is selected from the group consisting of trifluoroacetic acid, mixtures of trifluoroacetic acid and dichloromethane, mixtures of trifluoroacetic acid and toluene, carbon disulfide, 1-nitropropane, ethylbenzene, cyclohexanone, water, dioxane/water, formamide, N,N-dimethyl-formamide, ethanol, methanol, and mixtures thereof.

74.   A method according to claim 67, wherein the guest molecule is selected from the group consisting of fullerenes, carbon nanotubes, drug formulations, cosmetic formulations, metal particles, semiconductor particles, and magnetic particles.

75.   A method according to claim 67, wherein the mesostructure is in a form selected from the group consisting of spheres, lamellae, cylinders, and vesicles.

76.   A method according to claim 67, wherein the rod-coil block copolymer has the structure:

rod block$_m$coil block$_n$

, wherein m=1 to 500 and n=10 to 5000.

77.   A method according to claim 67, wherein the rod-coil block copolymer has the structure:

rod block_mcoil block_nrod block_m

, wherein m=1 to 500 and n=10 to 5000.

78.   A method of making molecular composites and nanocomposites of flexible-coil polymers and rigid-rod polymers comprising:

providing a solution of flexible-coil polymer and rigid-rod polymer and adding a rod-coil block copolymer comprising a rigid-rod block and a flexible-coil block to the solution under conditions effective to form a substantially fine dispersion of the flexible-coil polymer and rigid-rod polymer.

79.   A method according to claim 78, wherein the rigid-rod block is selected from the group consisting of polyquinolines, polyquinoxalines, poly(p-phenylenes), poly(p-phenylene vinylenes), polypridines, poly(pyridine vinylenes), poly(naphthylene vinylenes), polythiophenes, poly(thiophene vinylenes), polypyrroles, polyanilines, polybenzimidazoles, polybenzothiazoles, polybenzoxazoles, polybenzobisazoles, aromatic polyamides, aromatic polyhydrazides, aromatic polyazomethines, aromatic polyesters, and aromatic polyimides.

80.   A method according to claim 78, wherein the flexible-coil block is selected from the group consisting of polystyrene, poly(α-methyl styrene), poly(ethylene oxide, poly(propylene oxide), poly(acrylic acid), poly(methylacrylic acid), poly(2-vinylpyridine), poly(4-vinylpyridine), polyurethane, poly(vinyl pyrrolidone), poly(methyl methacrylate), poly(n-butyl methacrylate), polyisoprene, poly(butadiene), poly(dimethylsiloxane), poly(styrene sulfonic acid), and sodium poly(styrene sulfonate).

81.   A method according to claim 78, wherein the rod-coil block copolymer is selected from the group consisting of a poly(phenylquinoline)-*block*-polystyrene and a poly(phenylquinoxaline)-*block*-polystyrene.

82.   A method according to claim 81, wherein the selective solvent is selected from the group consisting of trifluoroacetic acid, mixtures of trifluoroacetic acid and dichloromethane, mixtures of trifluoroacetic acid and toluene, carbon disulfide, 1-nitropropane, ethylbenzene, cyclohexanone, water, dioxane/water, formamide, N,N-dimethyl-formamide, ethanol, methanol, and mixtures thereof.

83.   A method according to claim 78, wherein the rod-coil block copolymer is selected from the group consisting of a poly(phenylquinoline)-*block*-polystyrene-*block*-poly(phenylquinoline) and a poly(phenylquinoxaline)-*block*-polystyrene-*block*-poly(phenylquinoxaline).

84.   A method according to claim 83, wherein the selective solvent is selected from the group consisting of trifluoroacetic acid, mixtures of trifluoroacetic acid and dichloromethane, mixtures of trifluoroacetic acid and toluene, carbon disulfide, 1-nitropropane, ethylbenzene, cyclohexanone, water, dioxane/water, formamide, N,N-dimethyl-formamide, ethanol, methanol, and mixtures thereof.

85.   A method according to claim 78, wherein the rod-coil block copolymer has the structure:

rod block$_m$coil block$_n$

, wherein m=1 to 500 and n=10 to 5000.

86.   A method according to claim 78, wherein the rod-coil block copolymer has the structure:

rod block$_m$coil block$_n$rod block$_m$

, wherein m=1 to 500 and n=10 to 5000.

I   Rod   Coil

II   —NHCO

     Rod   Coil

III   —NHCONH

     Rod   Coil

IV   Rod   Coil   Rod

V   —NHCO   OCNH—

     Rod   Coil   Rod

VI   —NHCONH   NHCONH—

     Rod   Coil   Rod
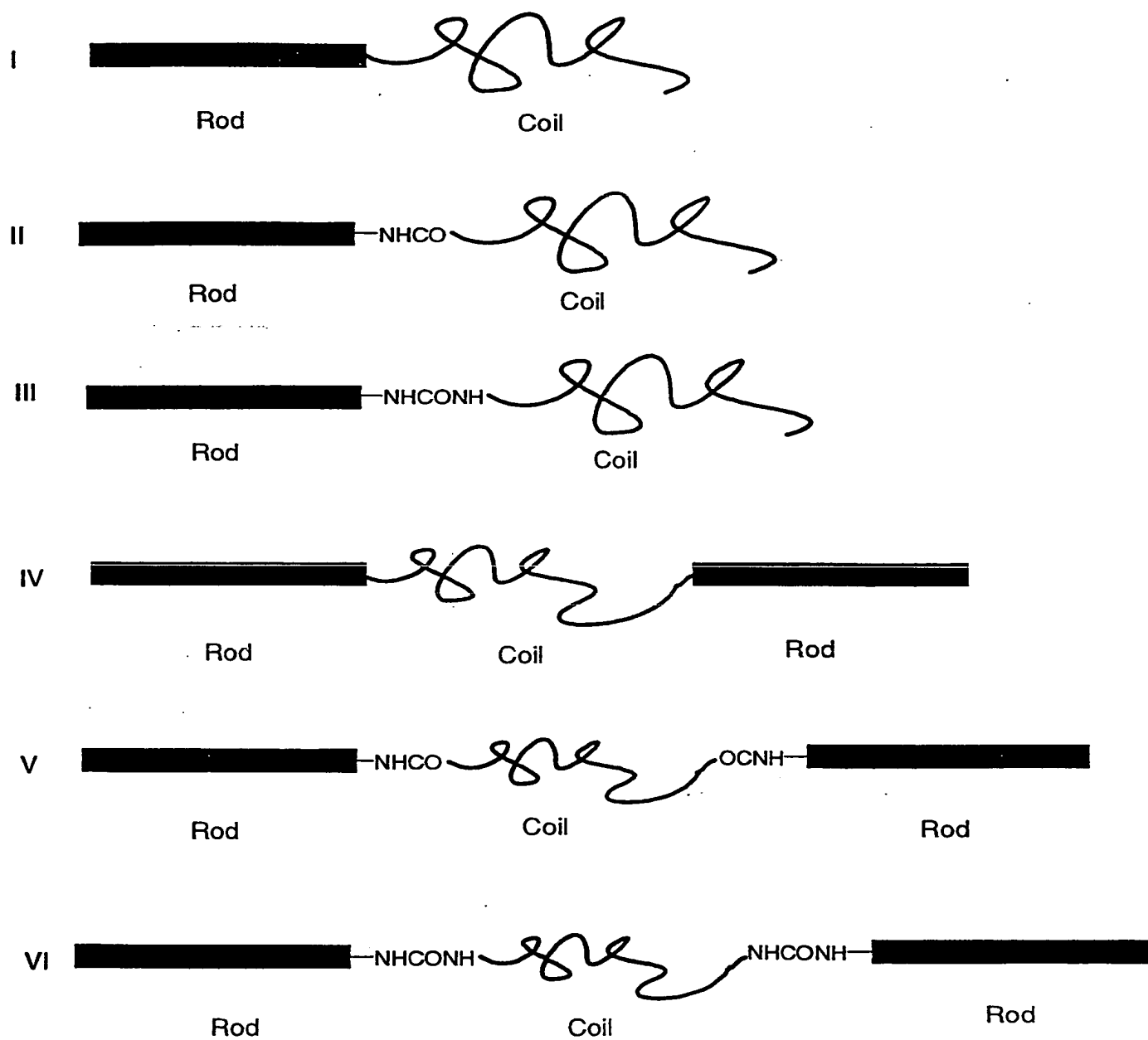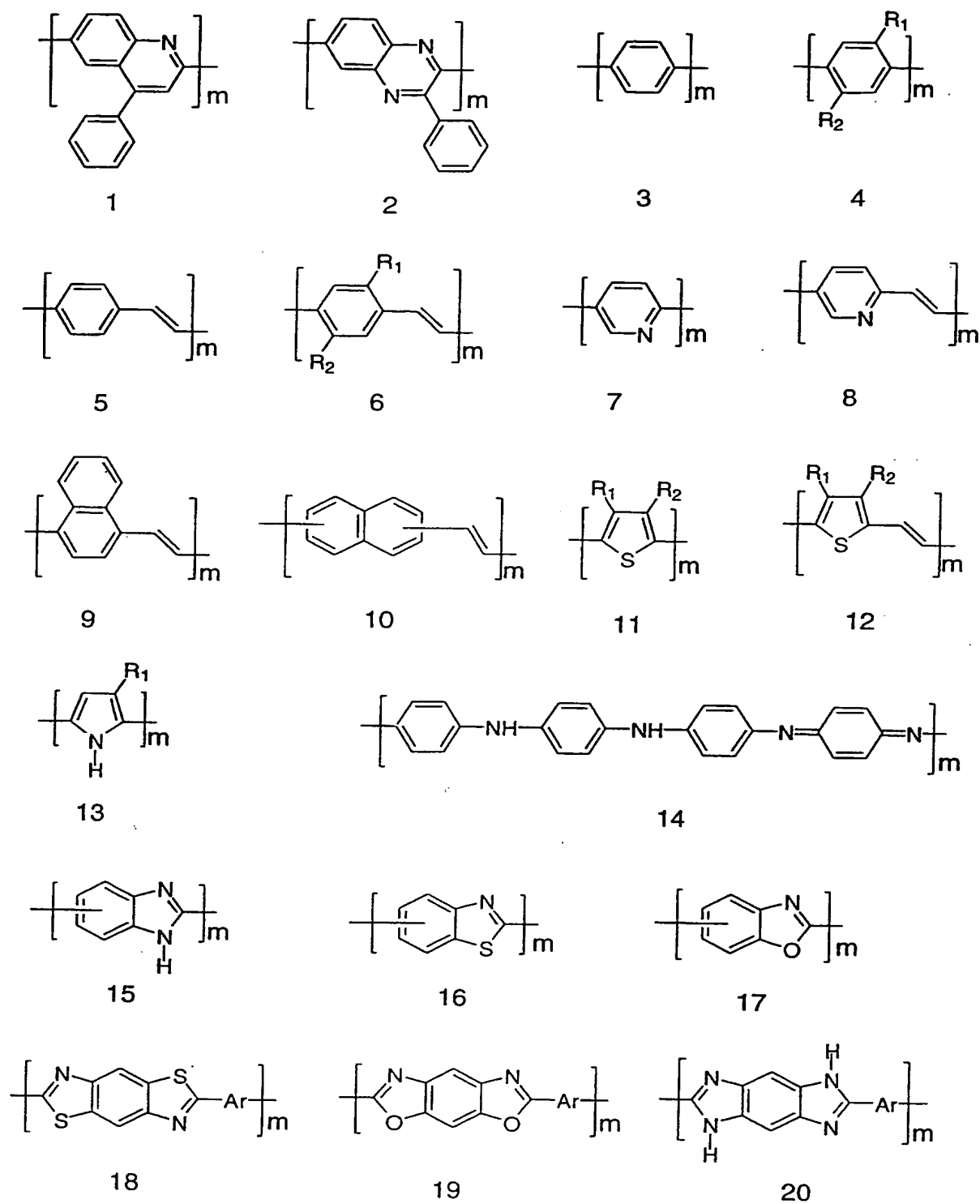
FIGURE 1
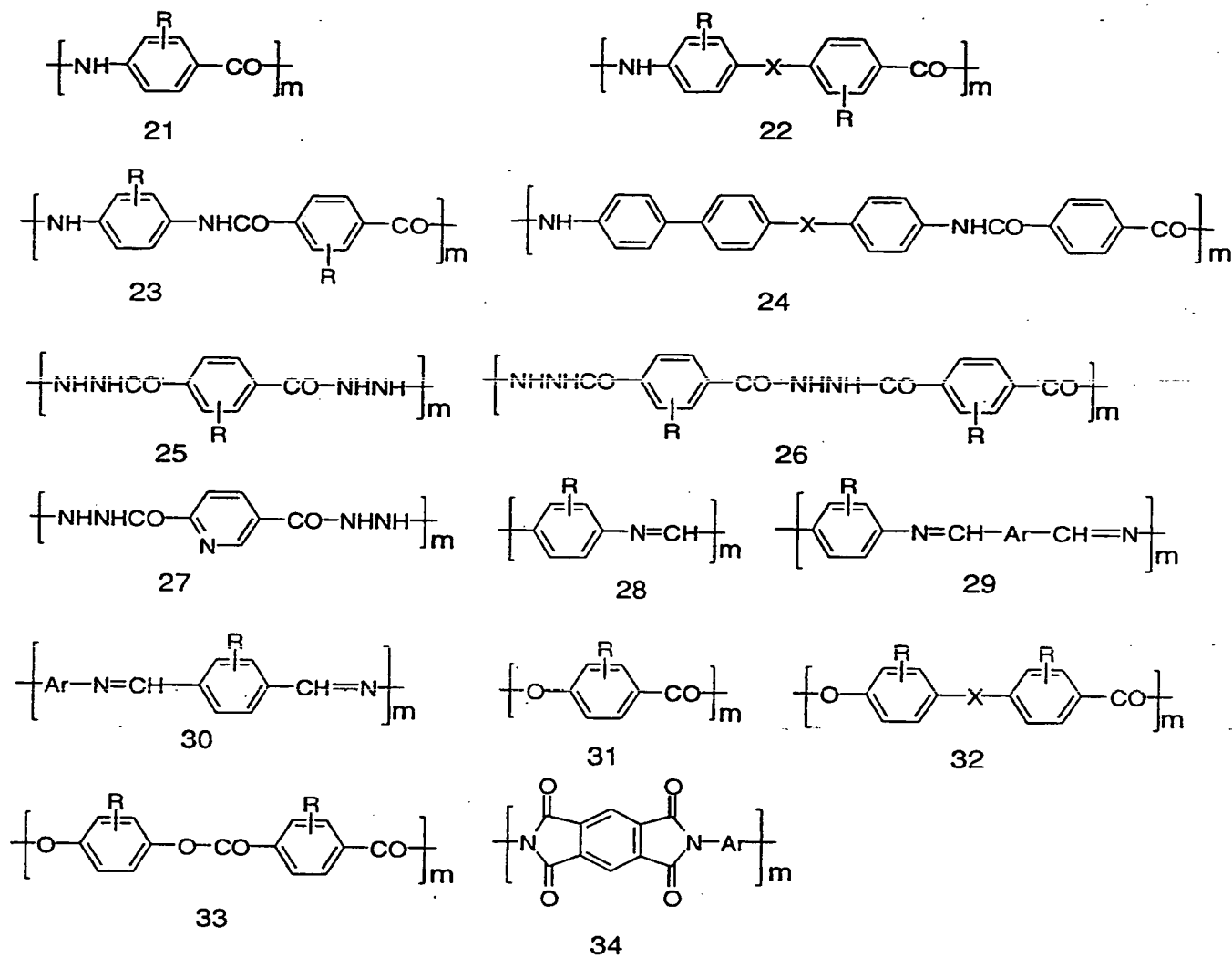
FIGURE 2

R = H, C_nH_{2n+1}, CF_3, ⟨benzene⟩ , OH, Cl, F, SO_3H, SO_3Na

X = ⎯ (nil)

= ⎯O⎯

= ⎯S⎯, ⎯SO_2⎯, ⎯N=N⎯, ⎯$C(CH_3)_2$⎯

= ⎯CH_2⎯, ⎯CH=CH⎯, ⎯CH=N⎯

Ar = , ,
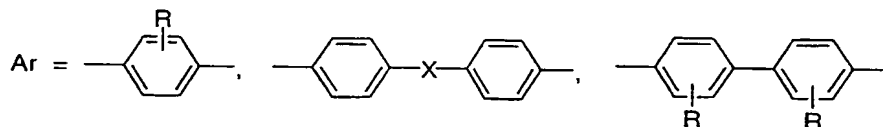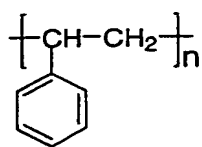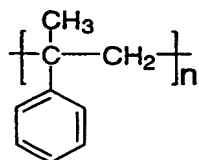
FIGURE 3

35   36   37   38
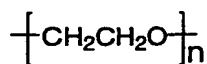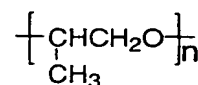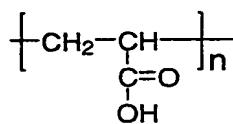
39   40   41   42
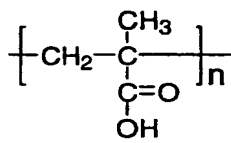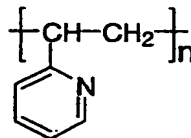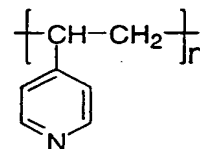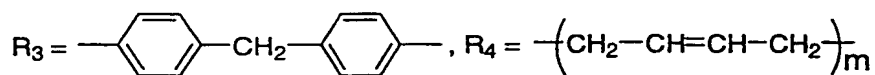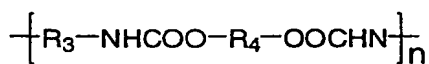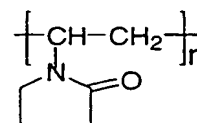
$R_3 =$, $R_4 =$ 43   44
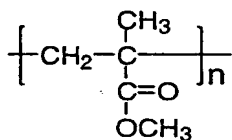
45   46   47   48

49   50   51

FIGURE 4

FIGURE 5

FIGURE 6

PPQ-b-PS

PPQ   PS

Solvent for PPQ

Solvent
Evaporation
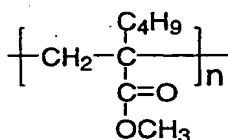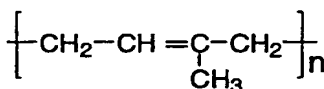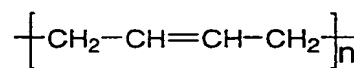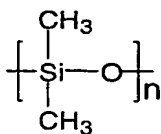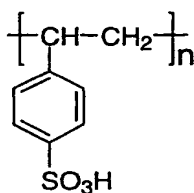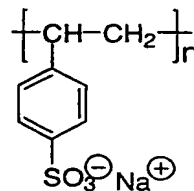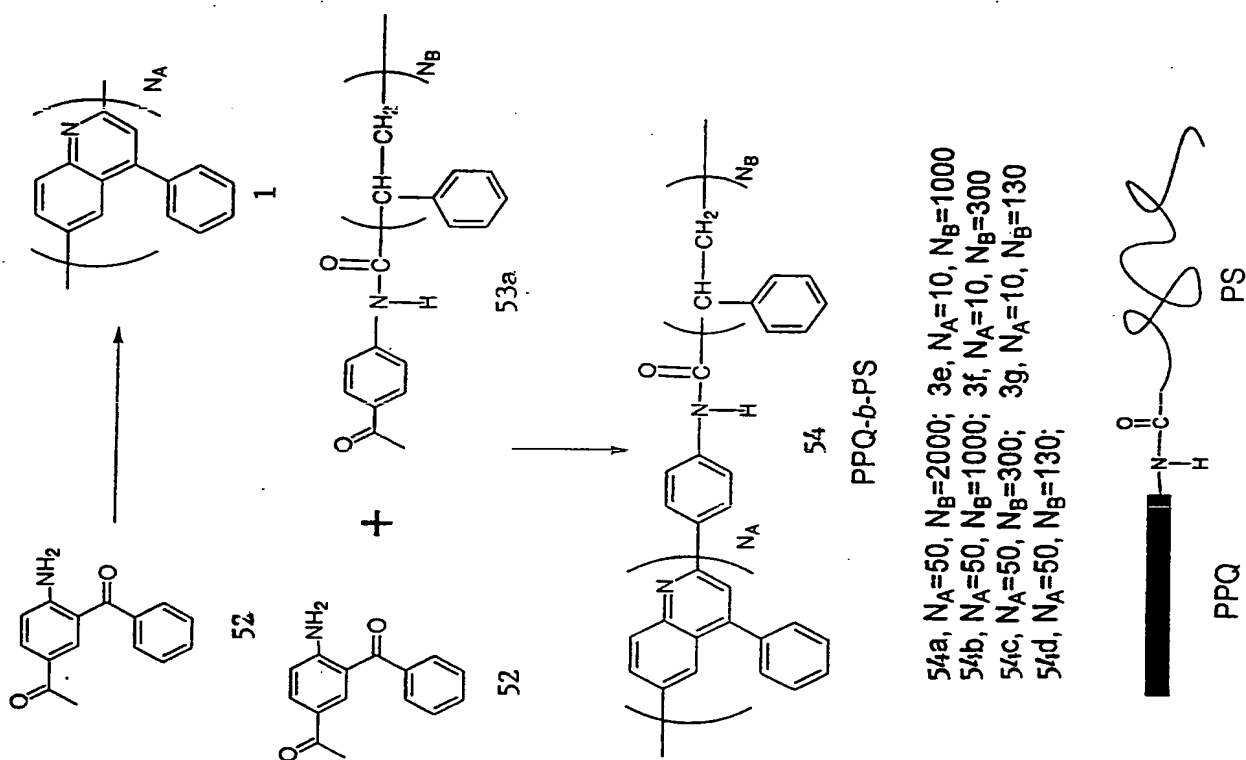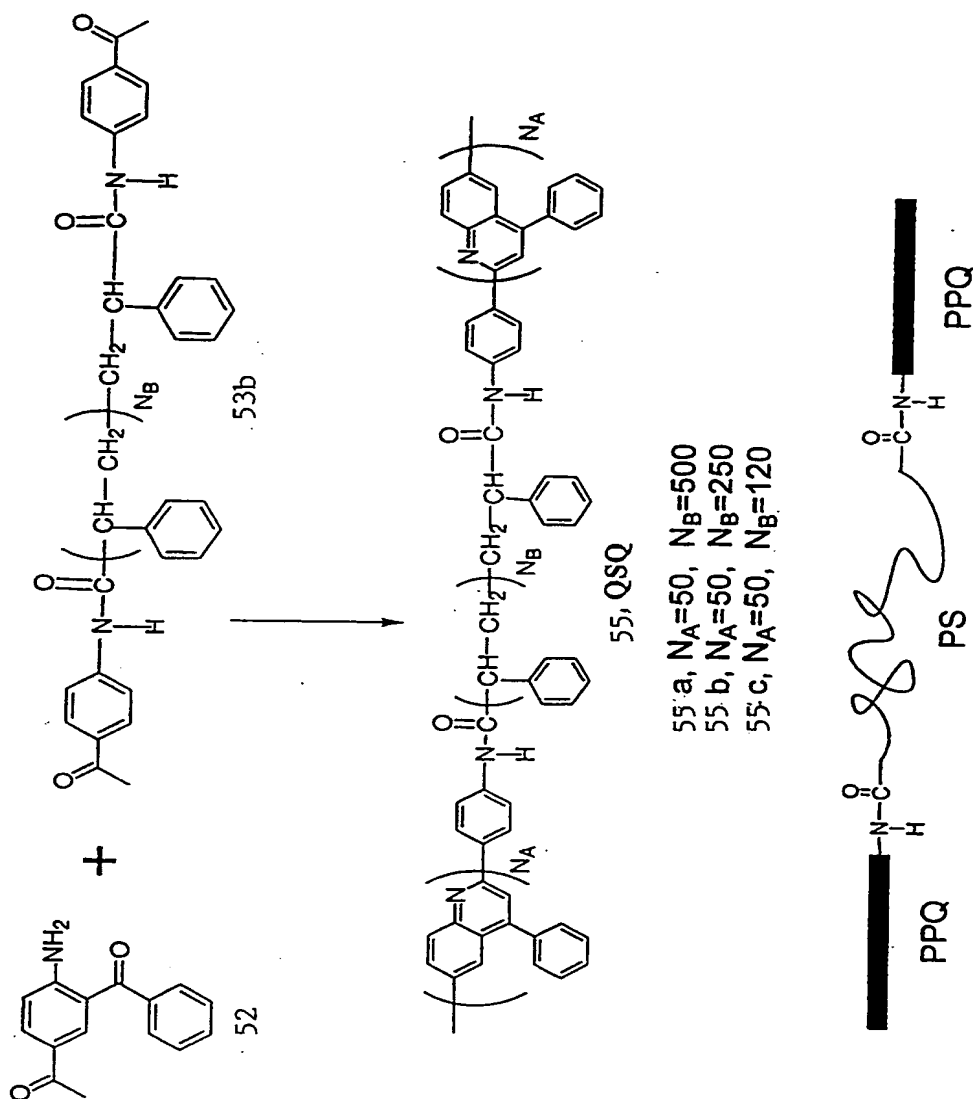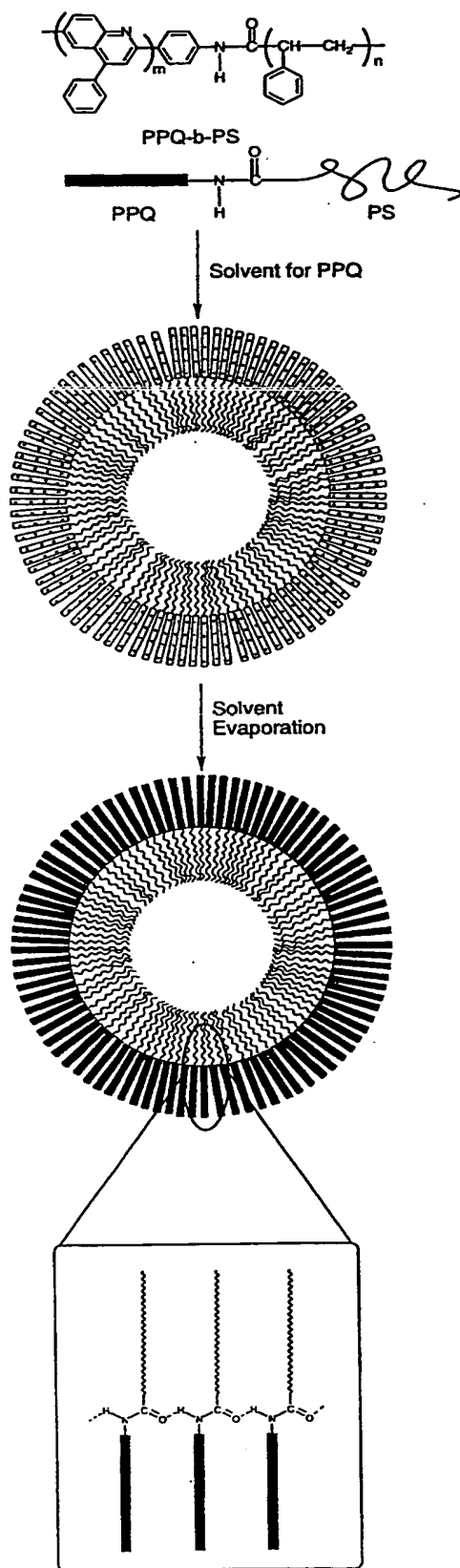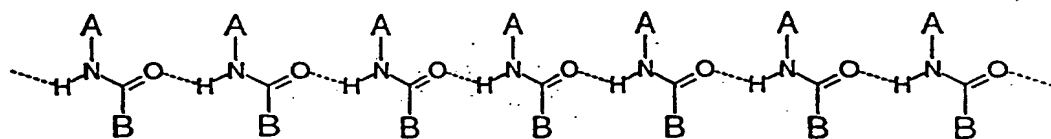
FIGURE 7

(a) Hydrogen-Bonded Chain
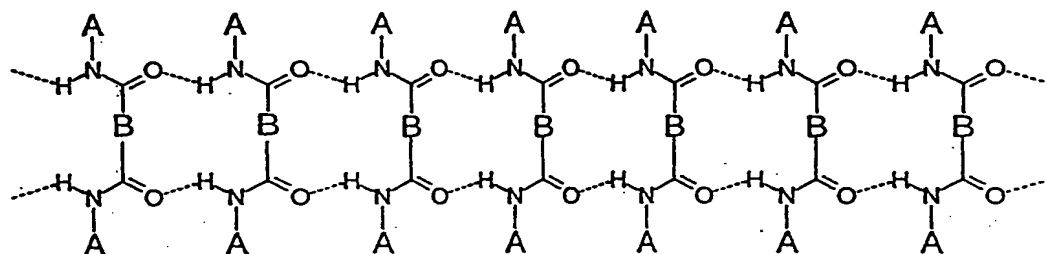
(b) Hydrogen-Bonded Tape
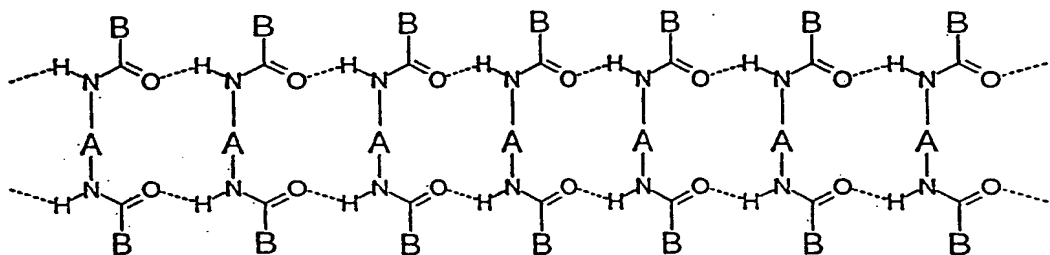
(c) Hydrogen-Bonded Tape

FIGURE 8
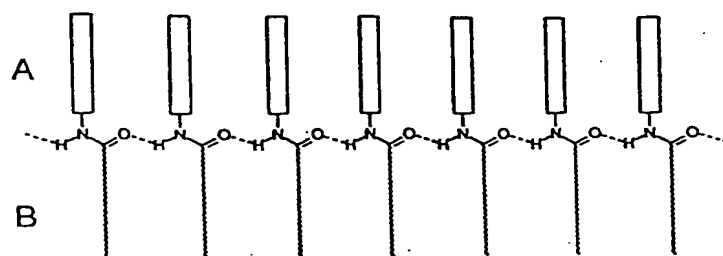
(a) Hydrogen-Bonded Single Layer
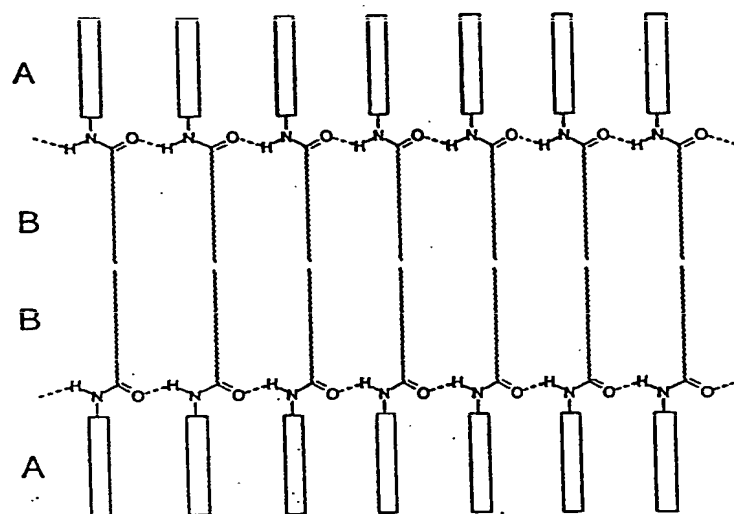
(b) Hydrogen-Bonded Bilayer
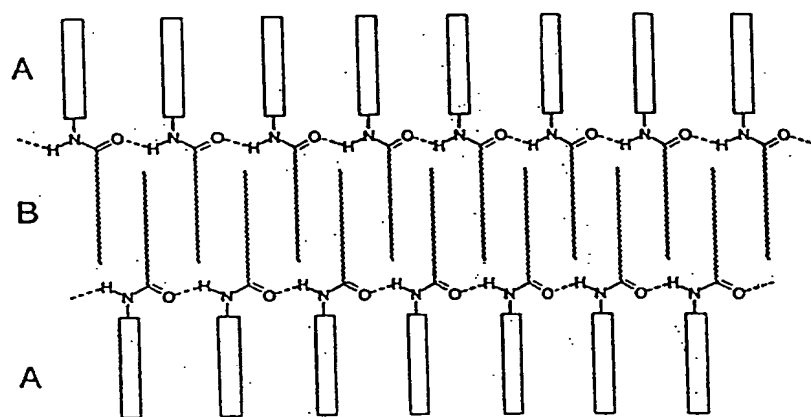
(c) Interdigitated Hydrogen-Bonded Bilayer

FIGURE 9
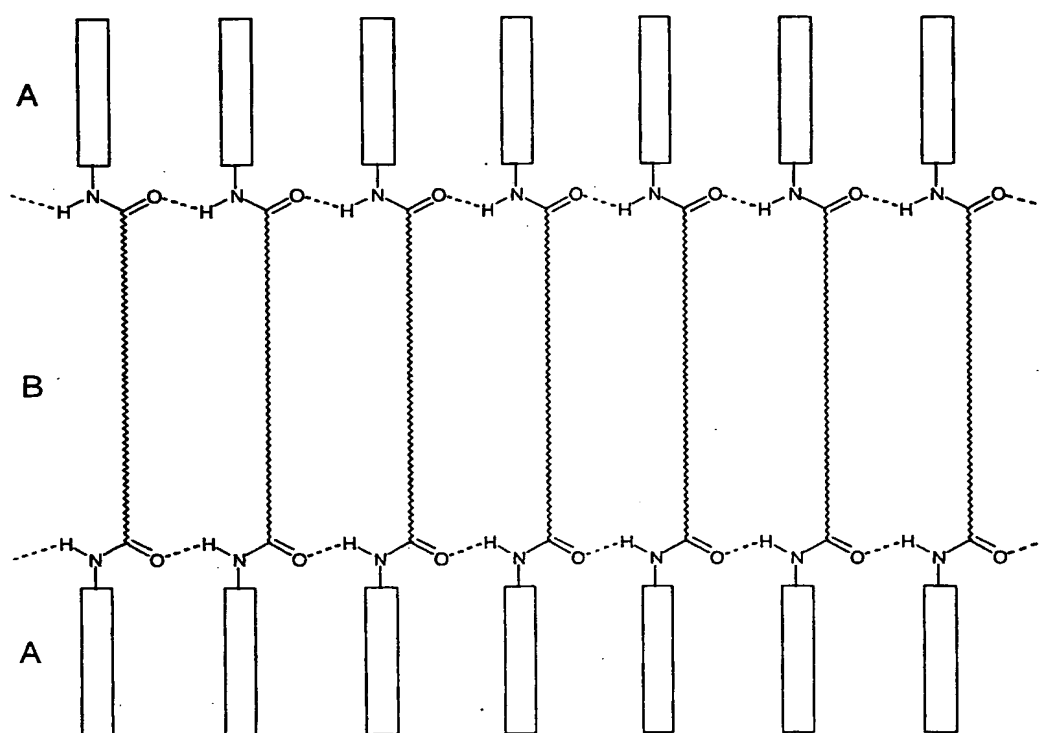
Hygrogen-Bonded Tapes in Rod-Coil-Rod Triblock Copolymers

FIGURE 10

AB Rod-Coil Diblocks

56 57 58

59 60 61

62 63

64 65
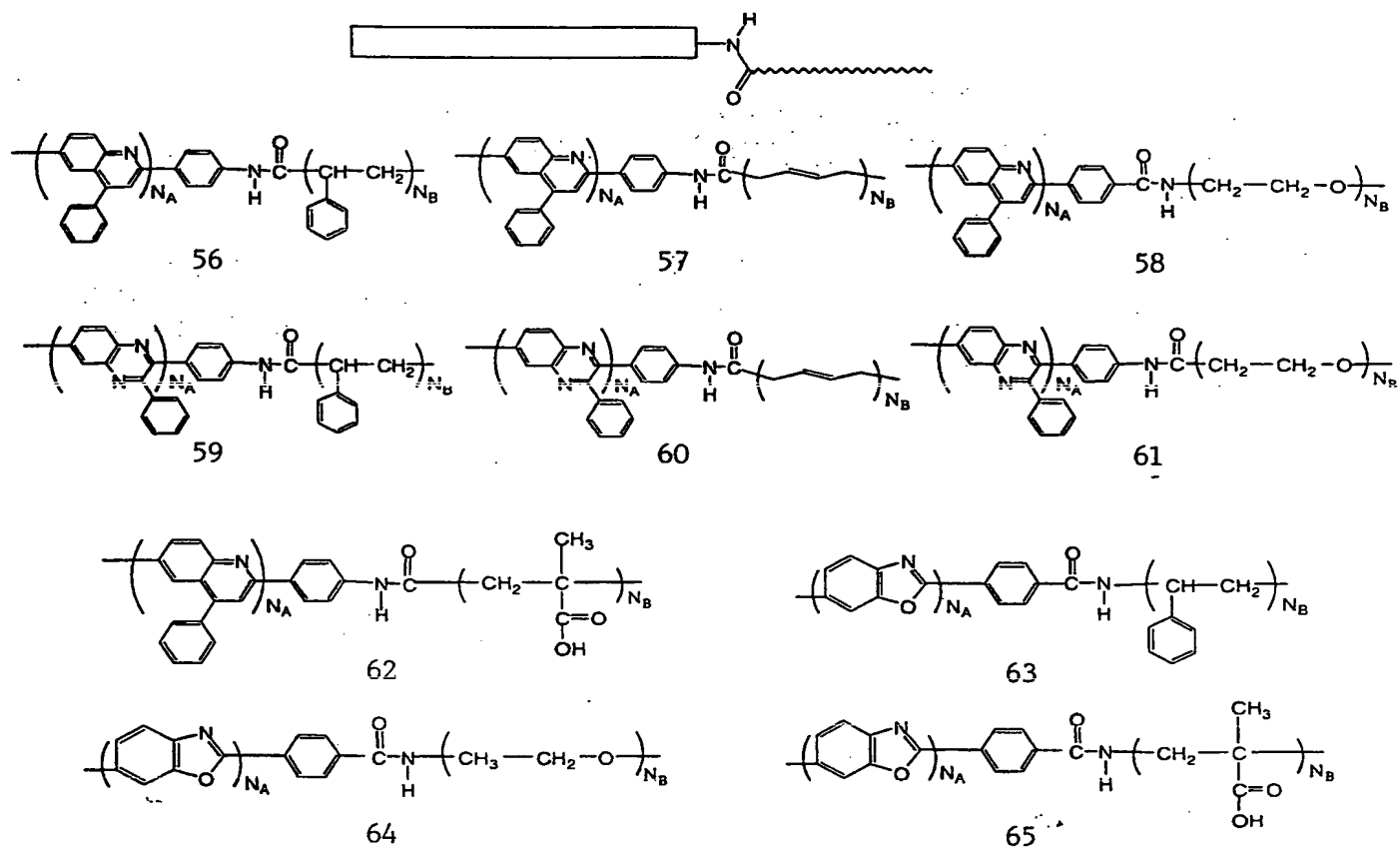
ABA Rod-Coil-Rod Triblocks

A   B   A

$$B= -\left(CH-CH_2\right)_{N_B} ; \left(\right)_{N_B} ; -\left(CH_2-CH_2-O\right)_{N_B} ; -\left(CH_2-C\right)_{N_B}$$

FIGURE 11

$$PPQ_mPS_n$$

Rod   Coil

Good solvent for coil

Solvent evaporation
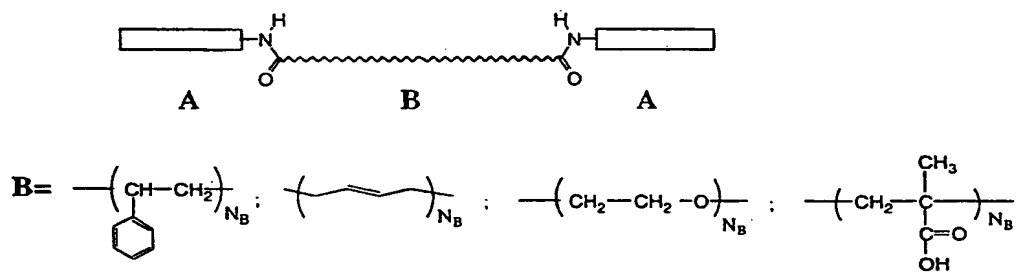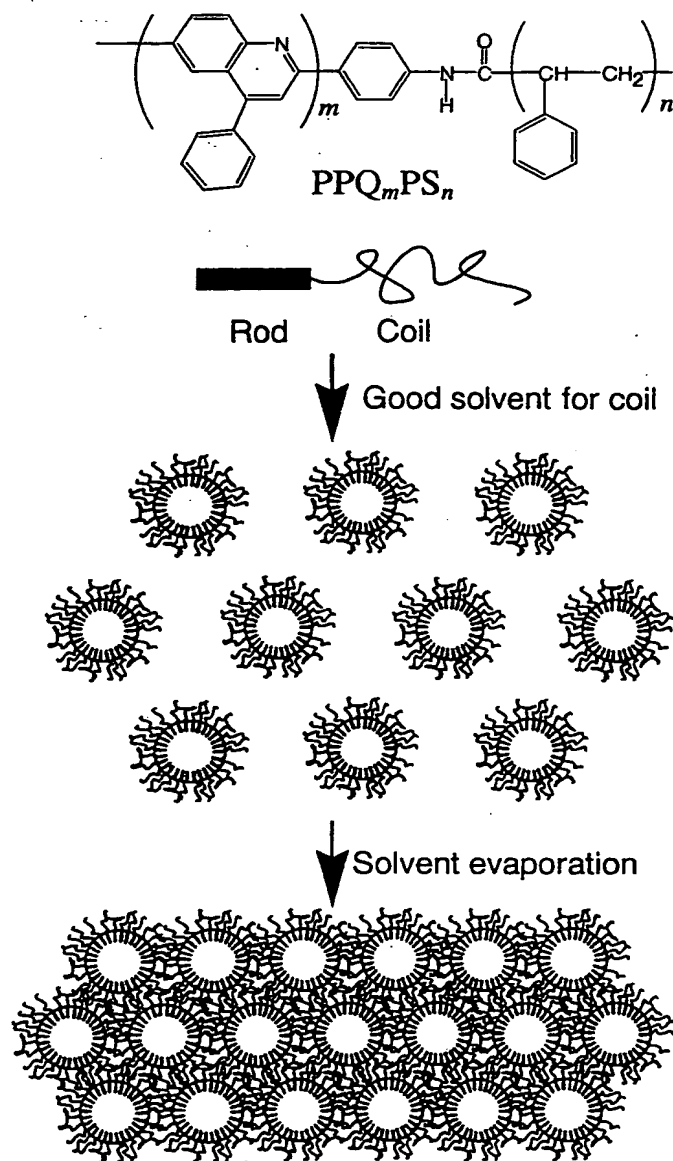
FIGURE 12

FIGURE 13

FIGURE 14

10 μm

10 μm

10 μm
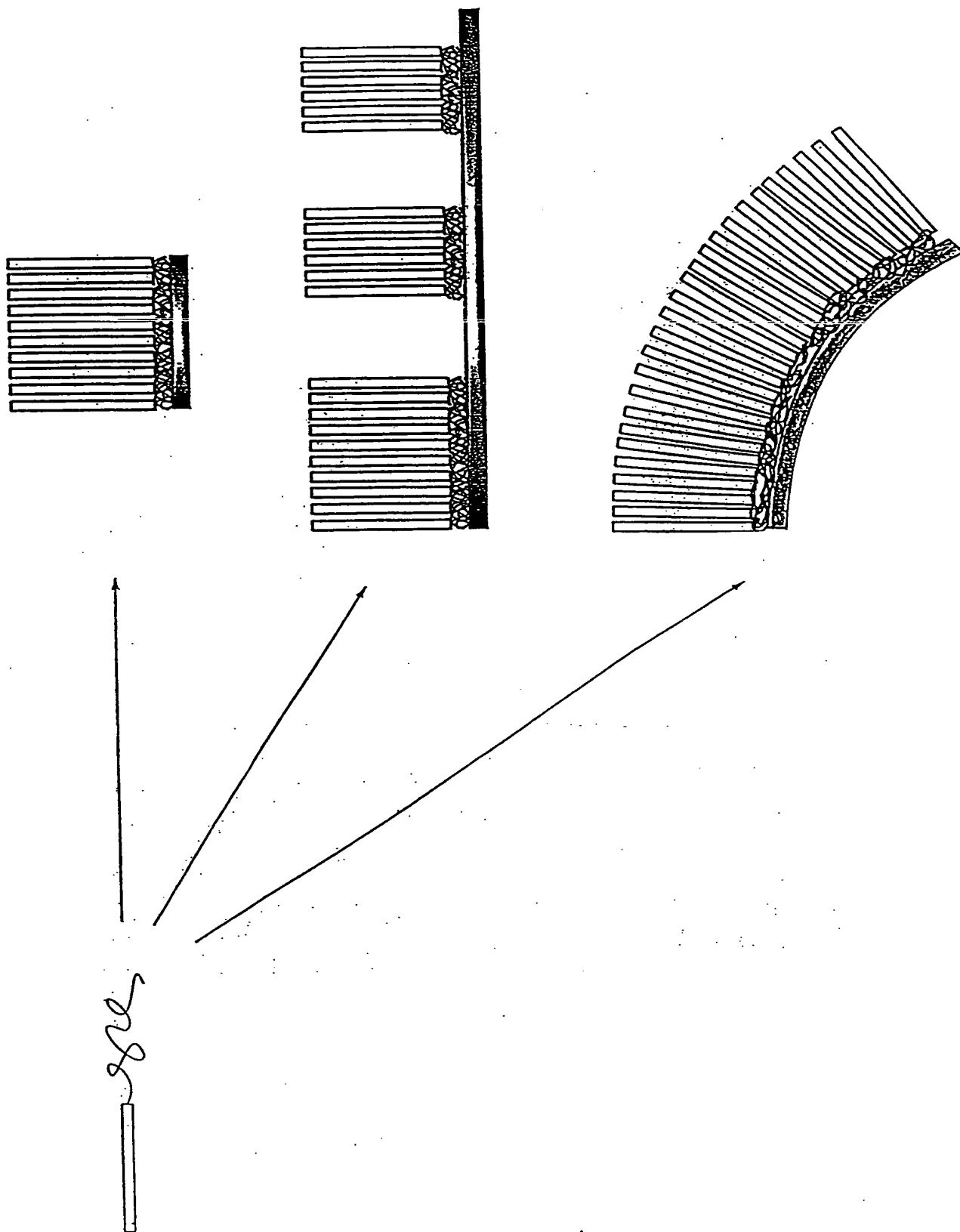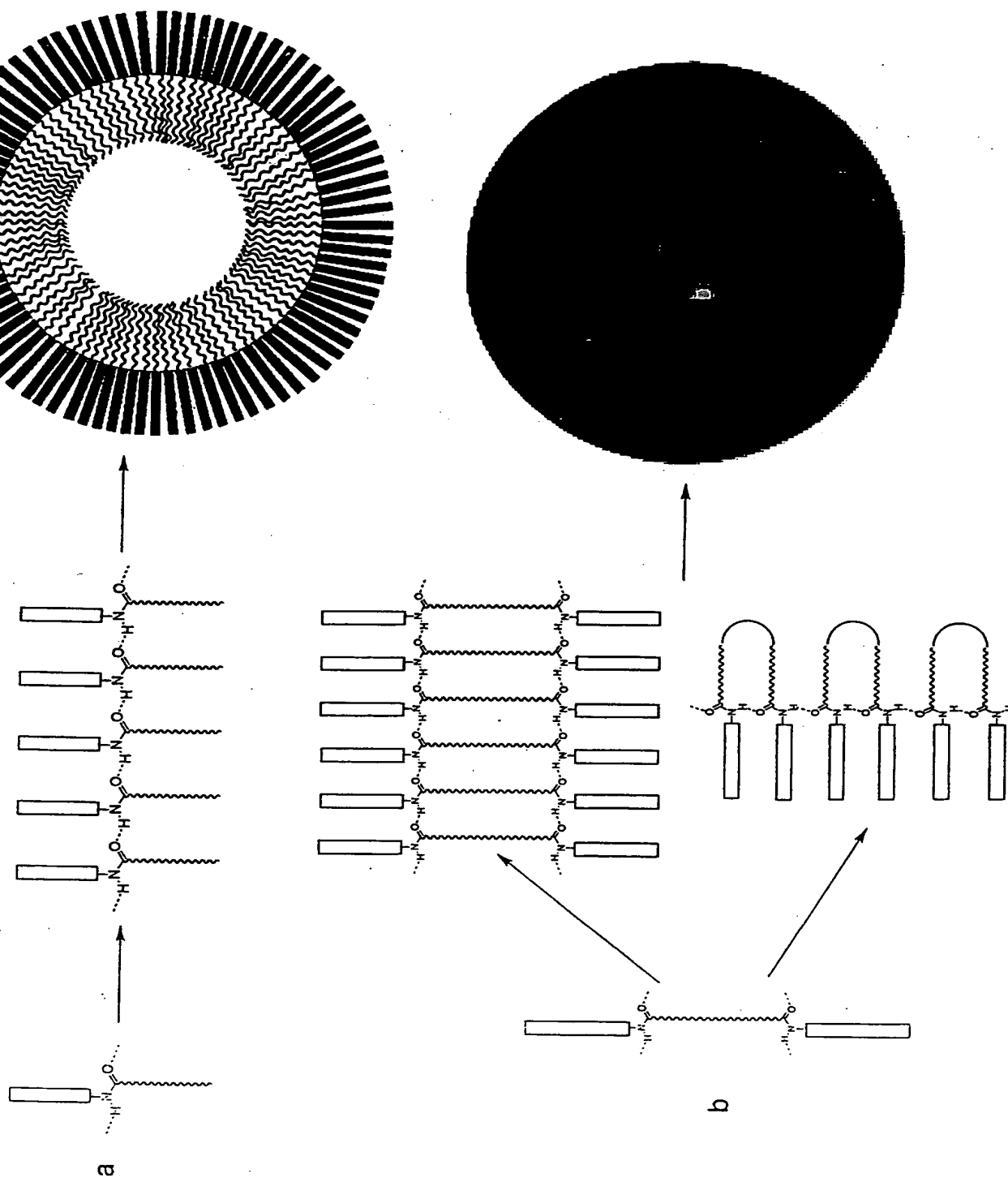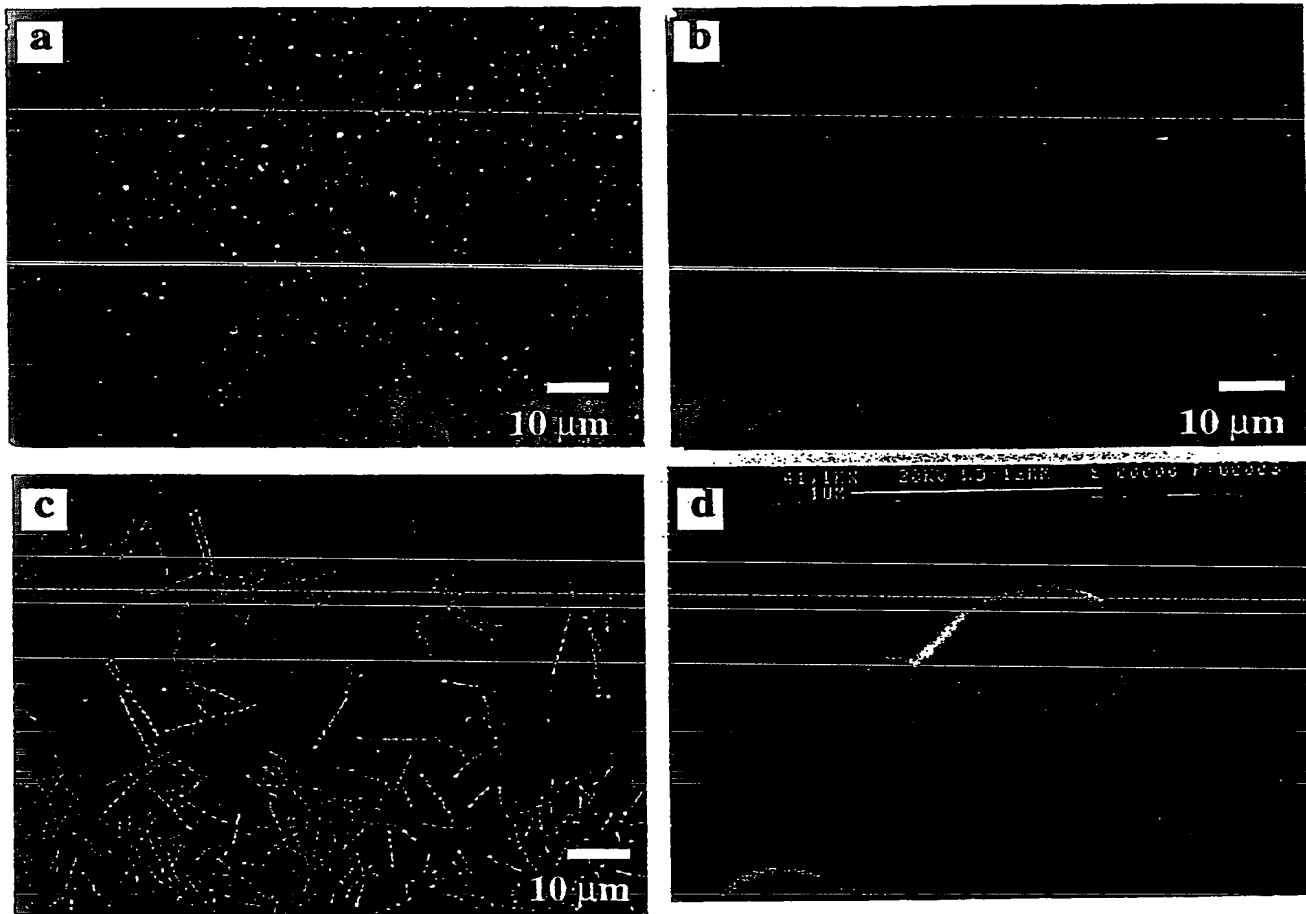
BEST AVAILABLE COPY

BEST AVAILABLE COPY

FIGURE 15
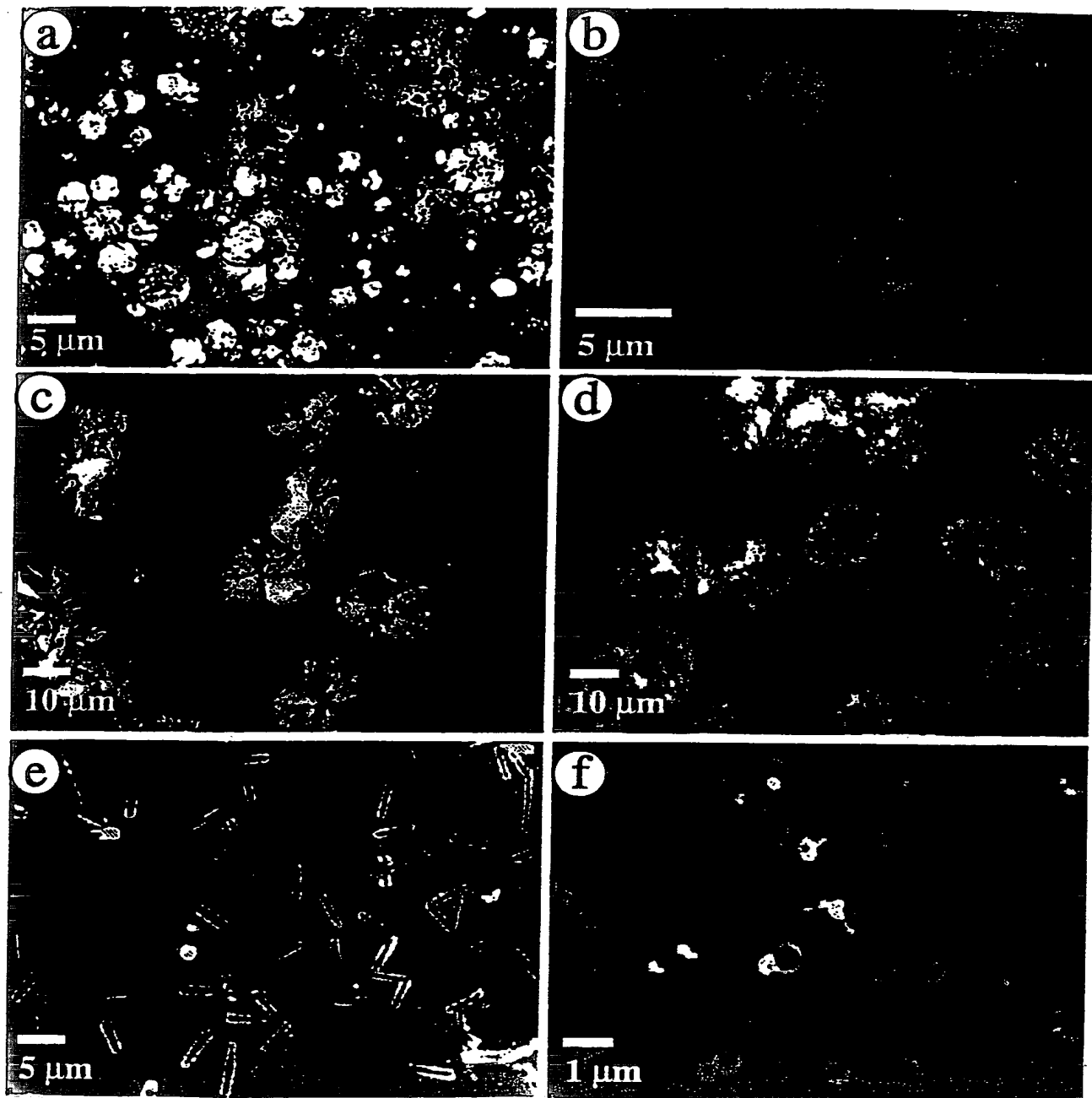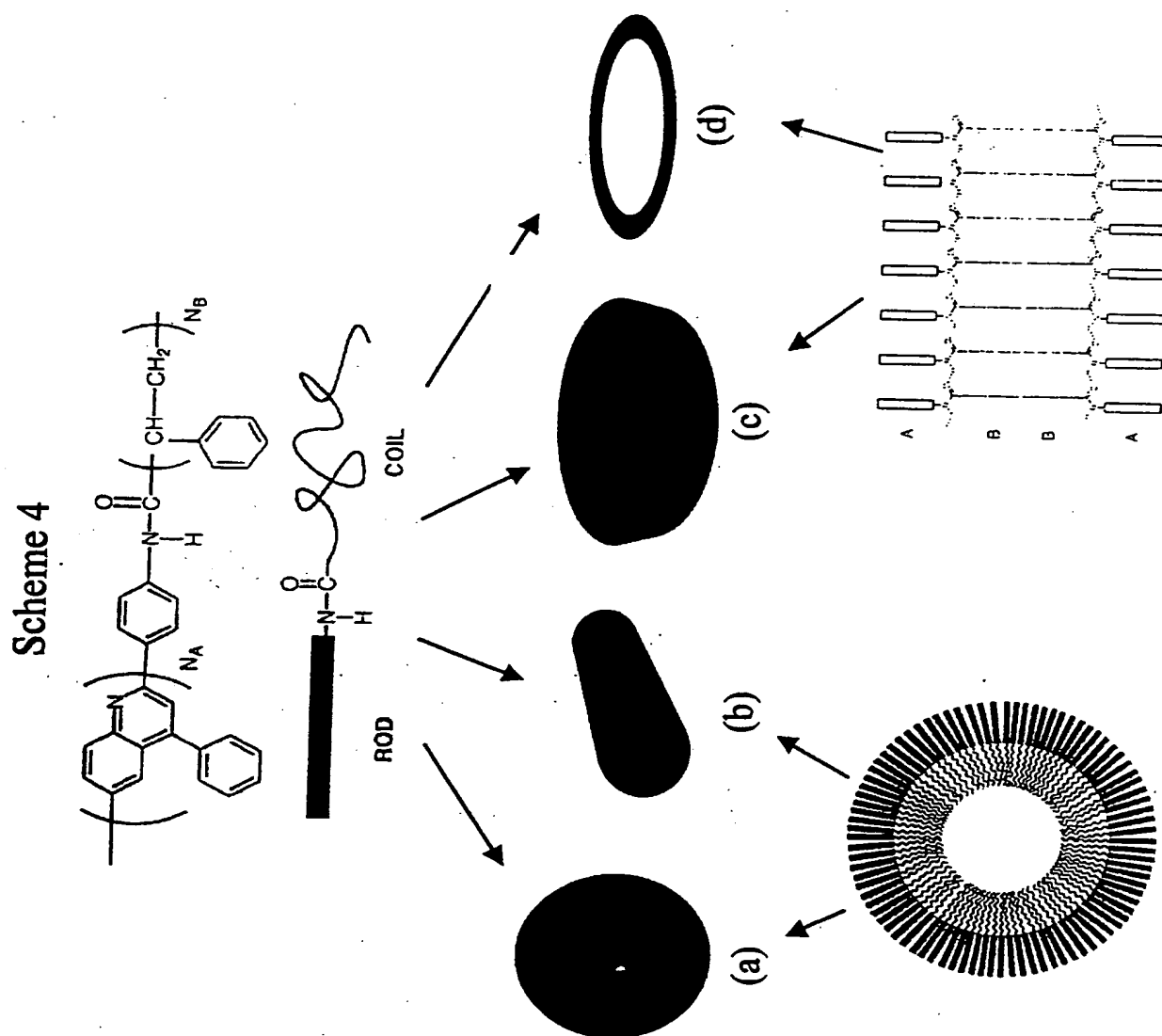
FIGURE 16

FIGURE 17

BEST AVAILABLE COPY
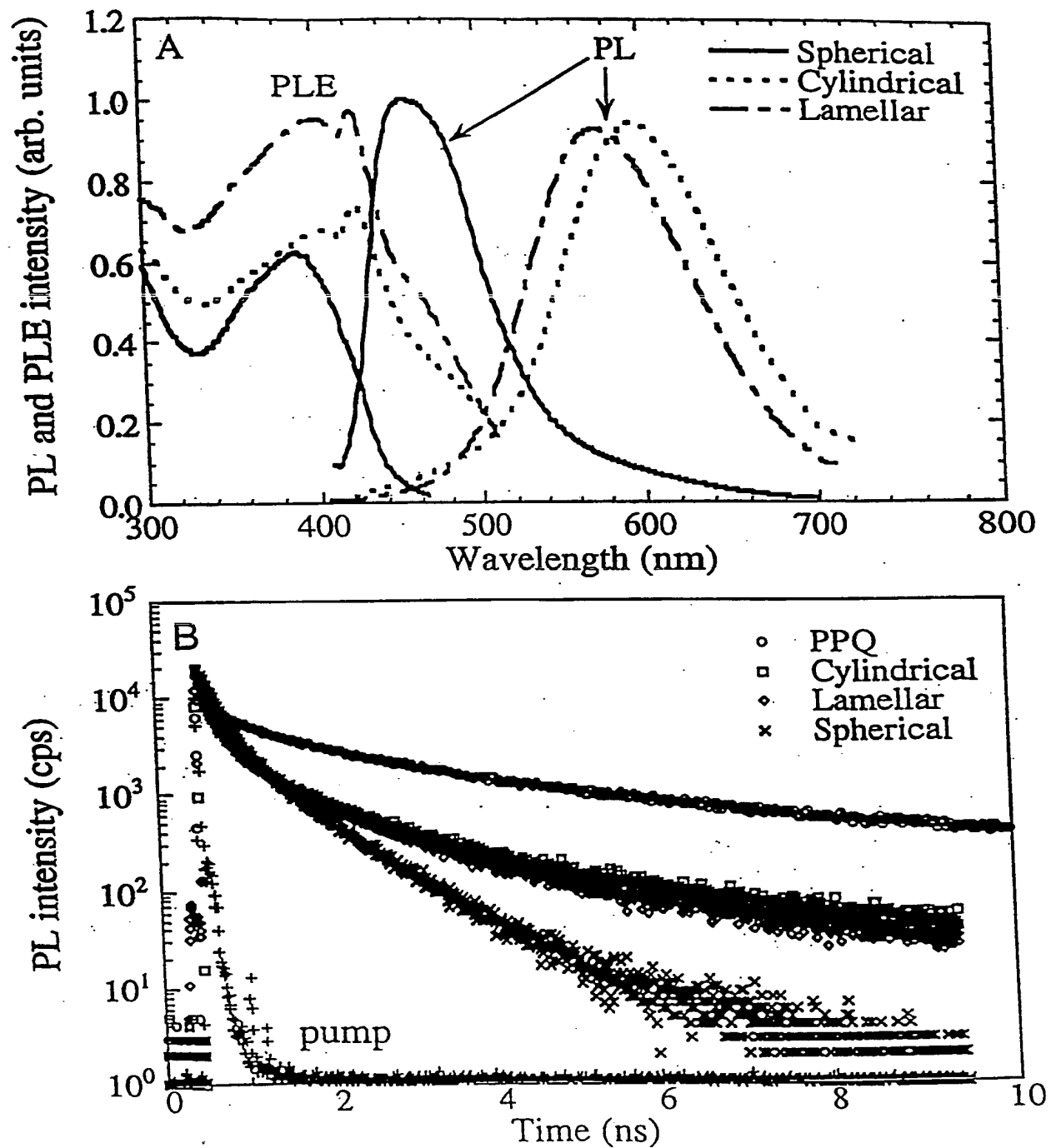
FIGURE 18

FIGURE 19

BEST AVAILABLE COPY
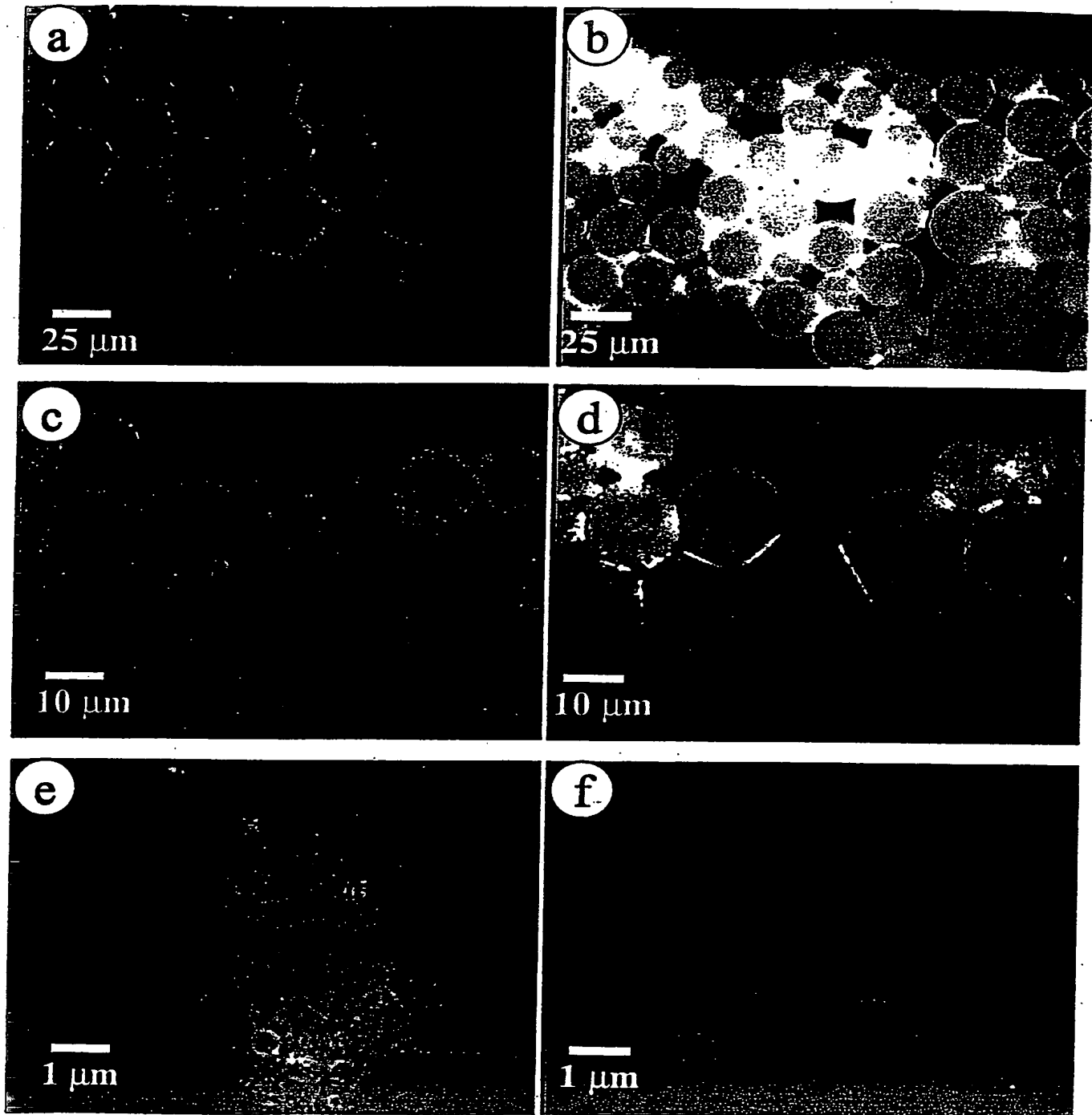
FIGURE 20

FIGURE 21

Scheme 5

(a)

(b)
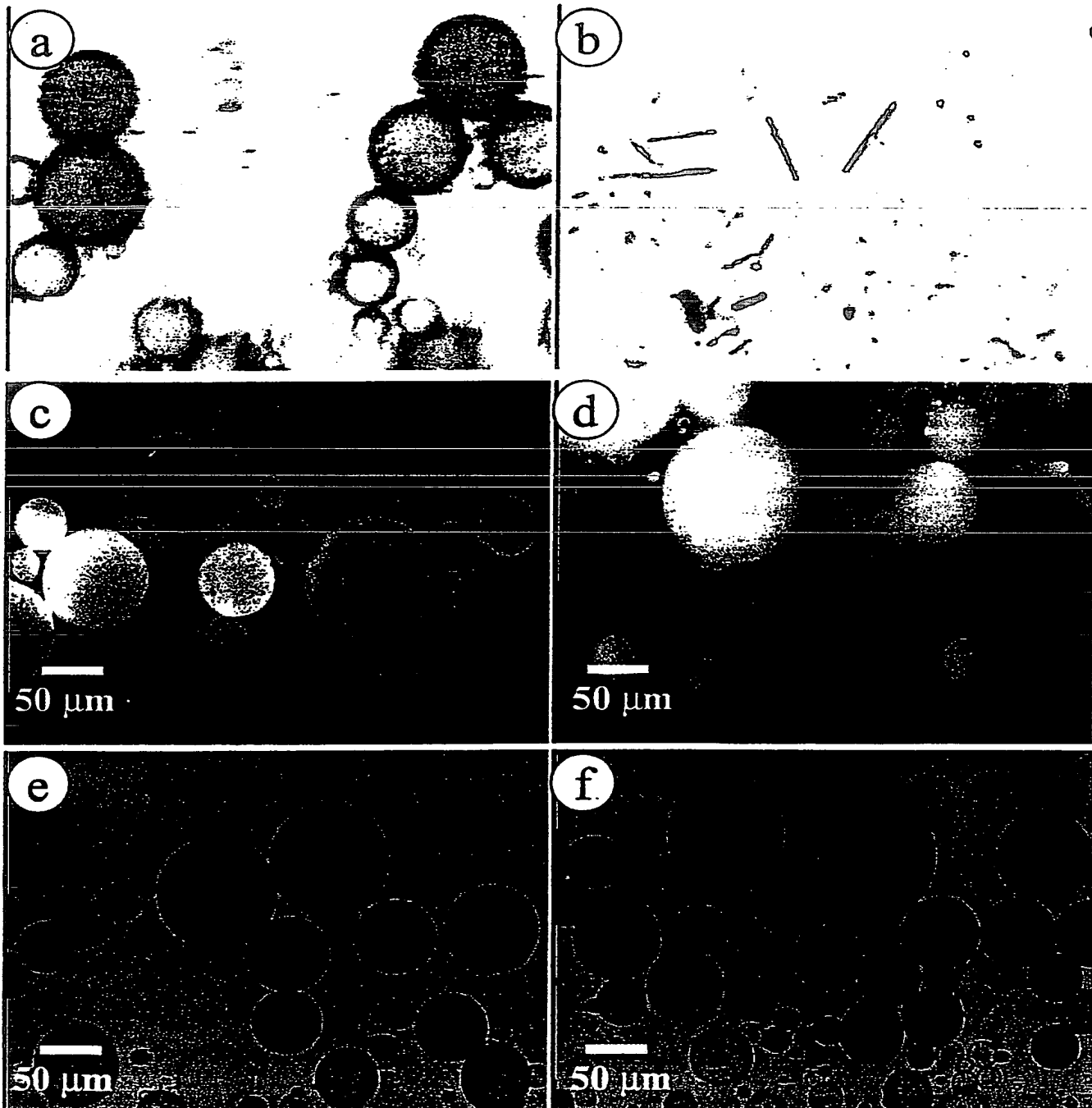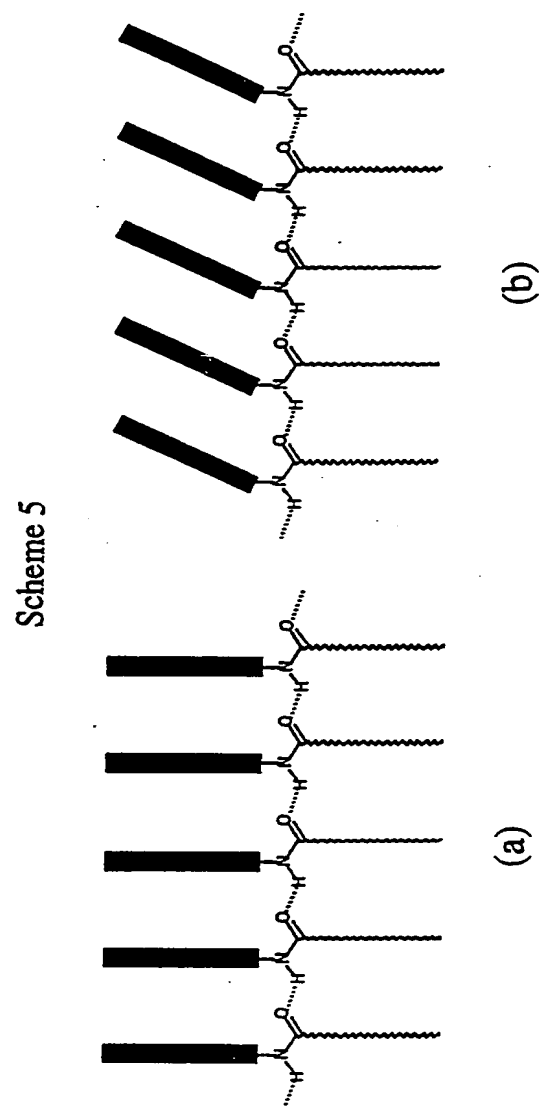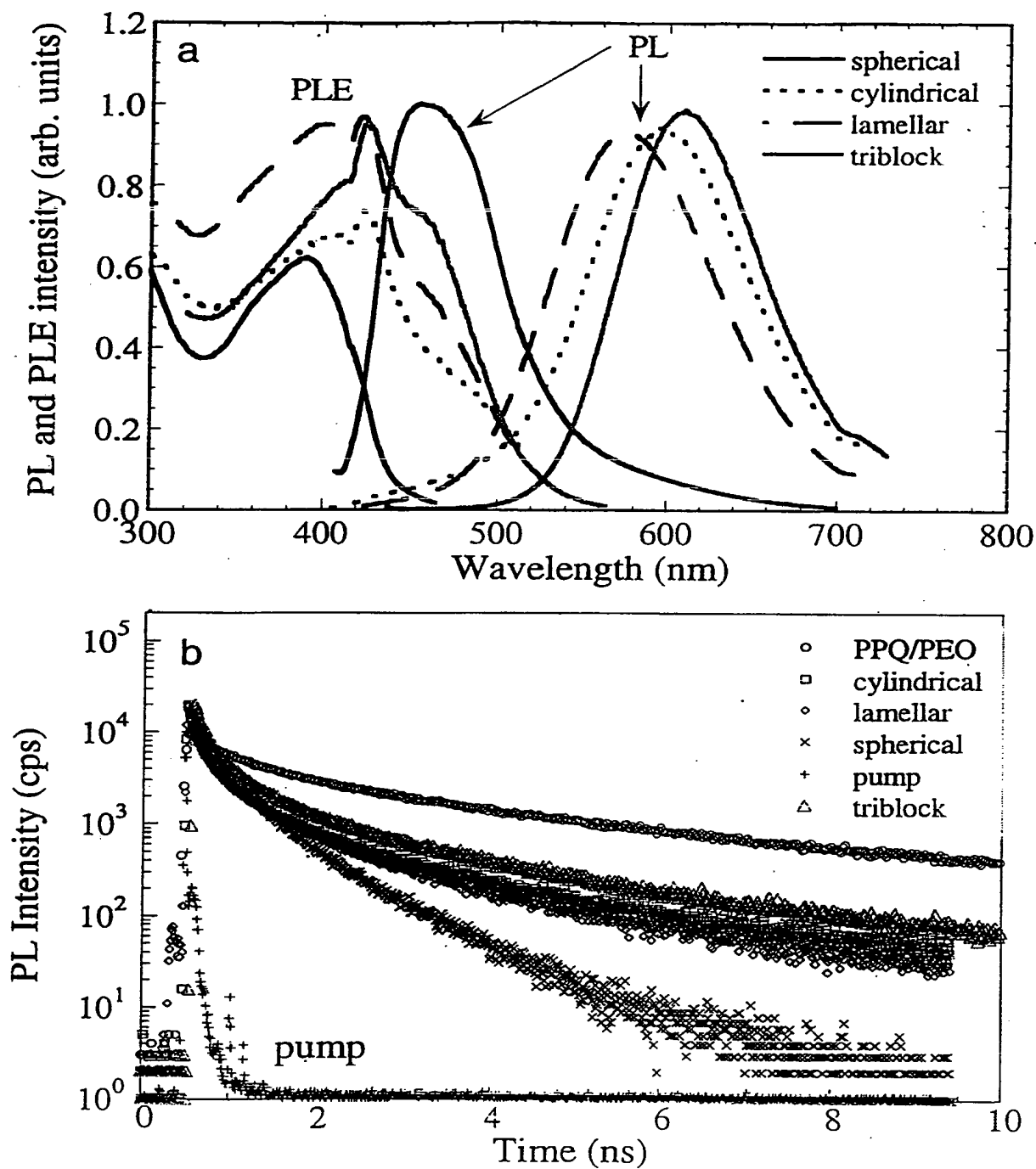
FIGURE 22

FIGURE 23
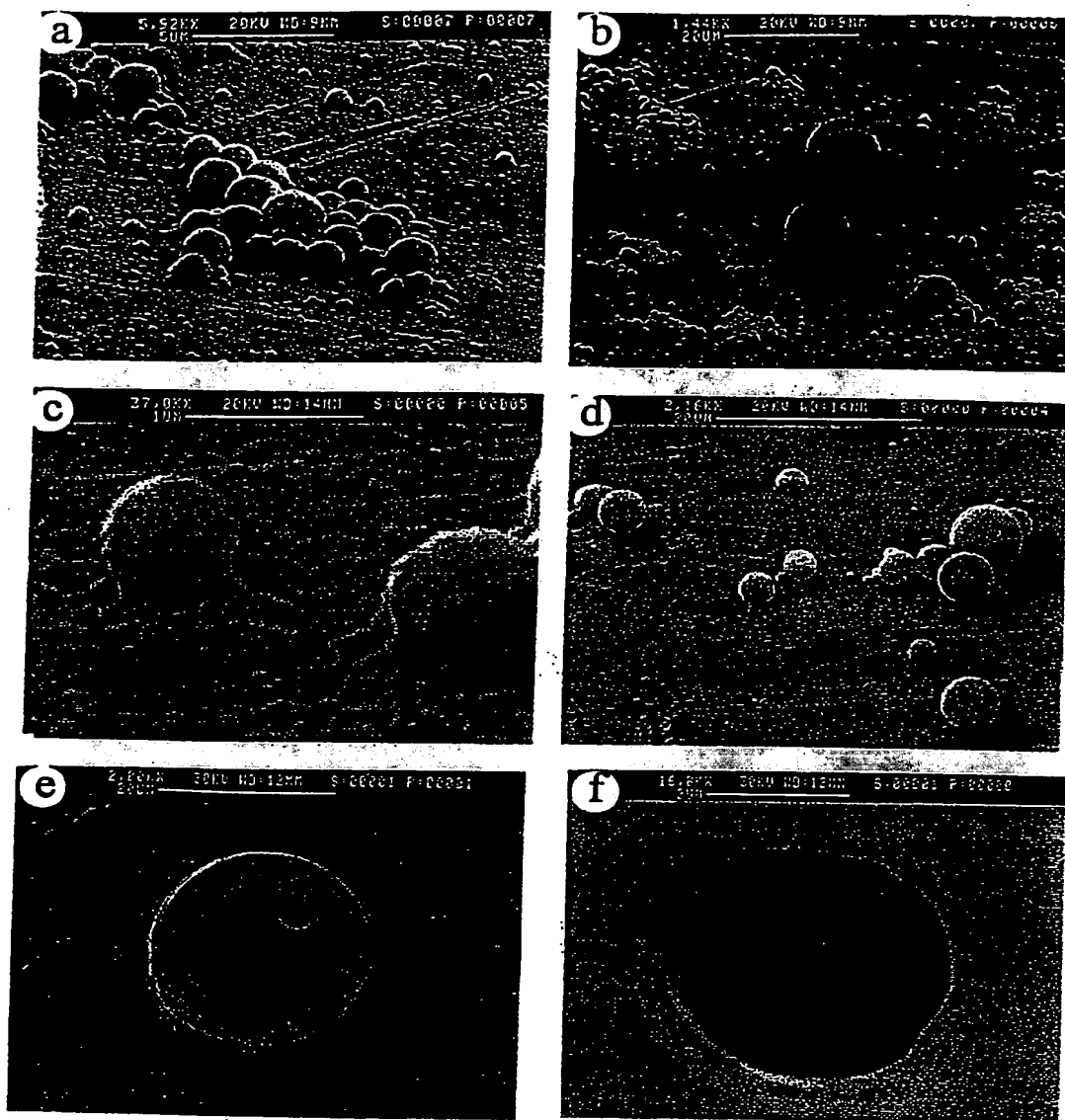
FIGURE 24

FIGURE 25

A

5 μm

B

5 μm

C

5 μm
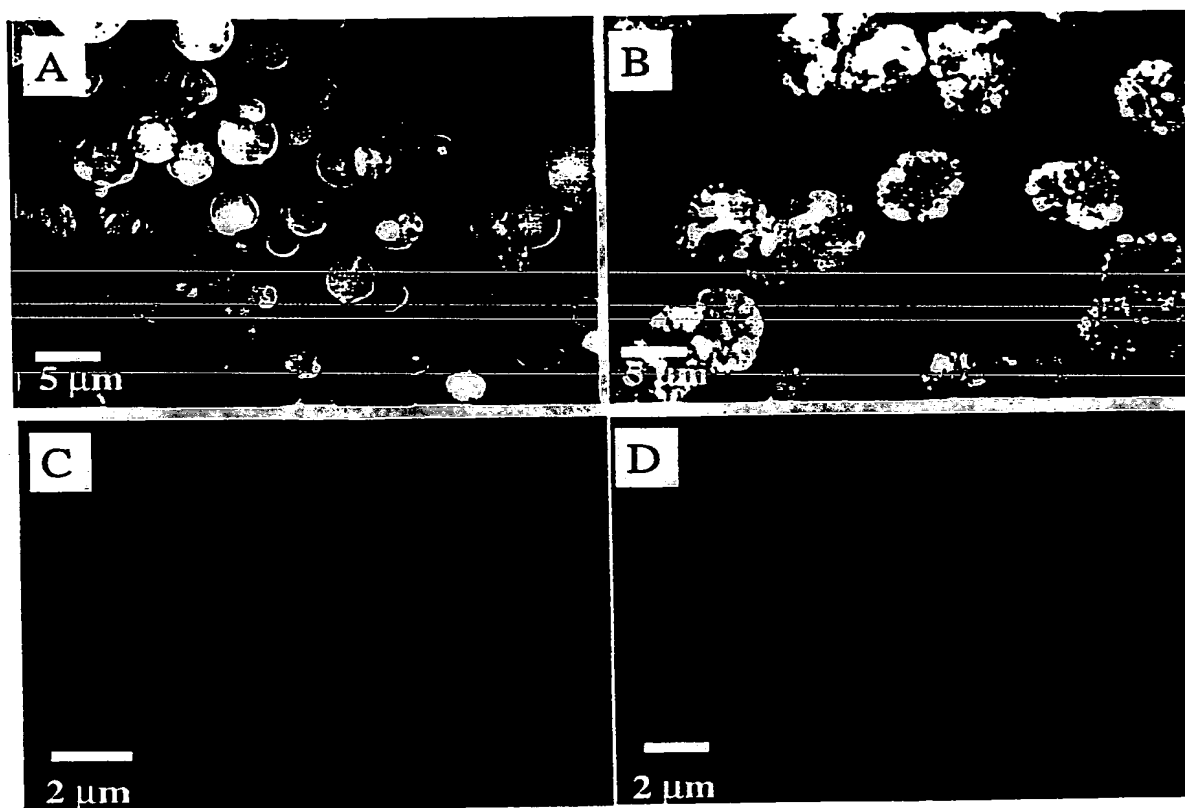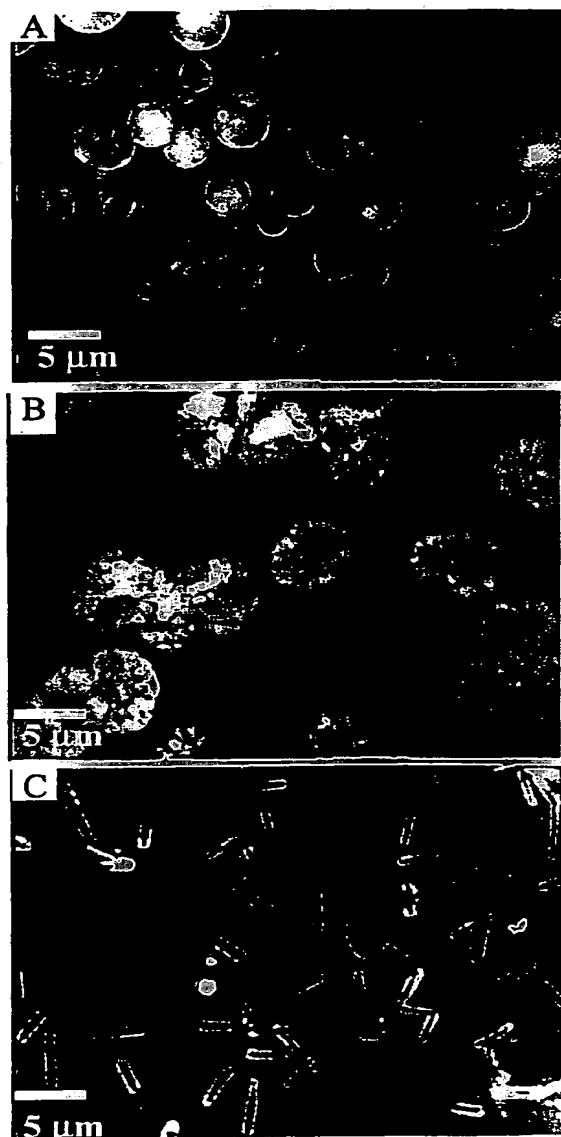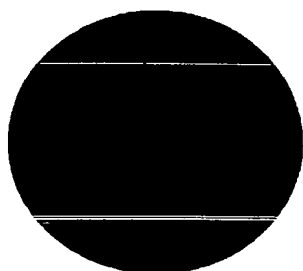
FIGURE 26

(a)
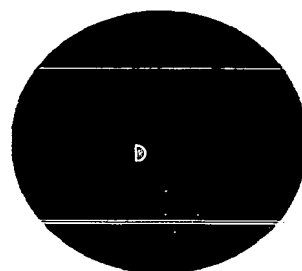
(b)
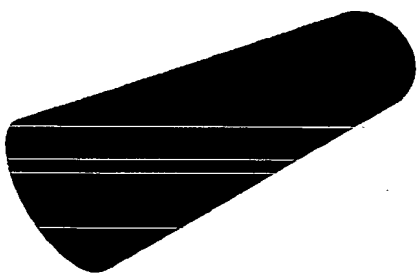
(c)
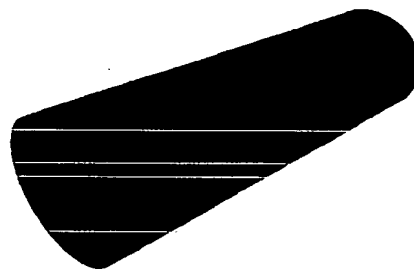
(d)
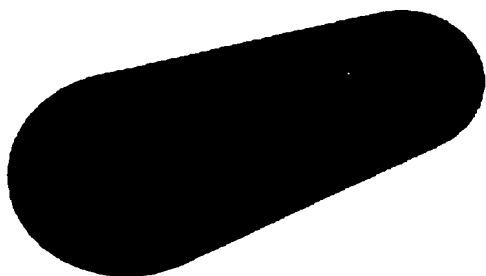
(e)
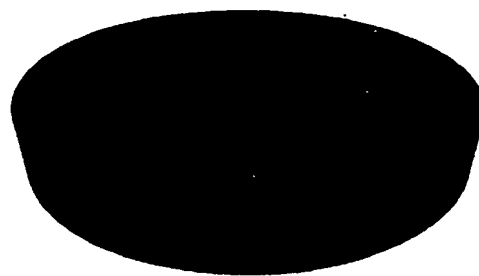
(f)
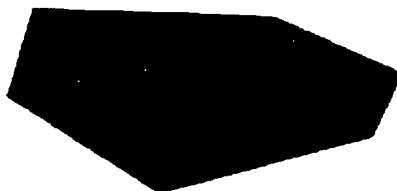
(g)

FIGURE 27
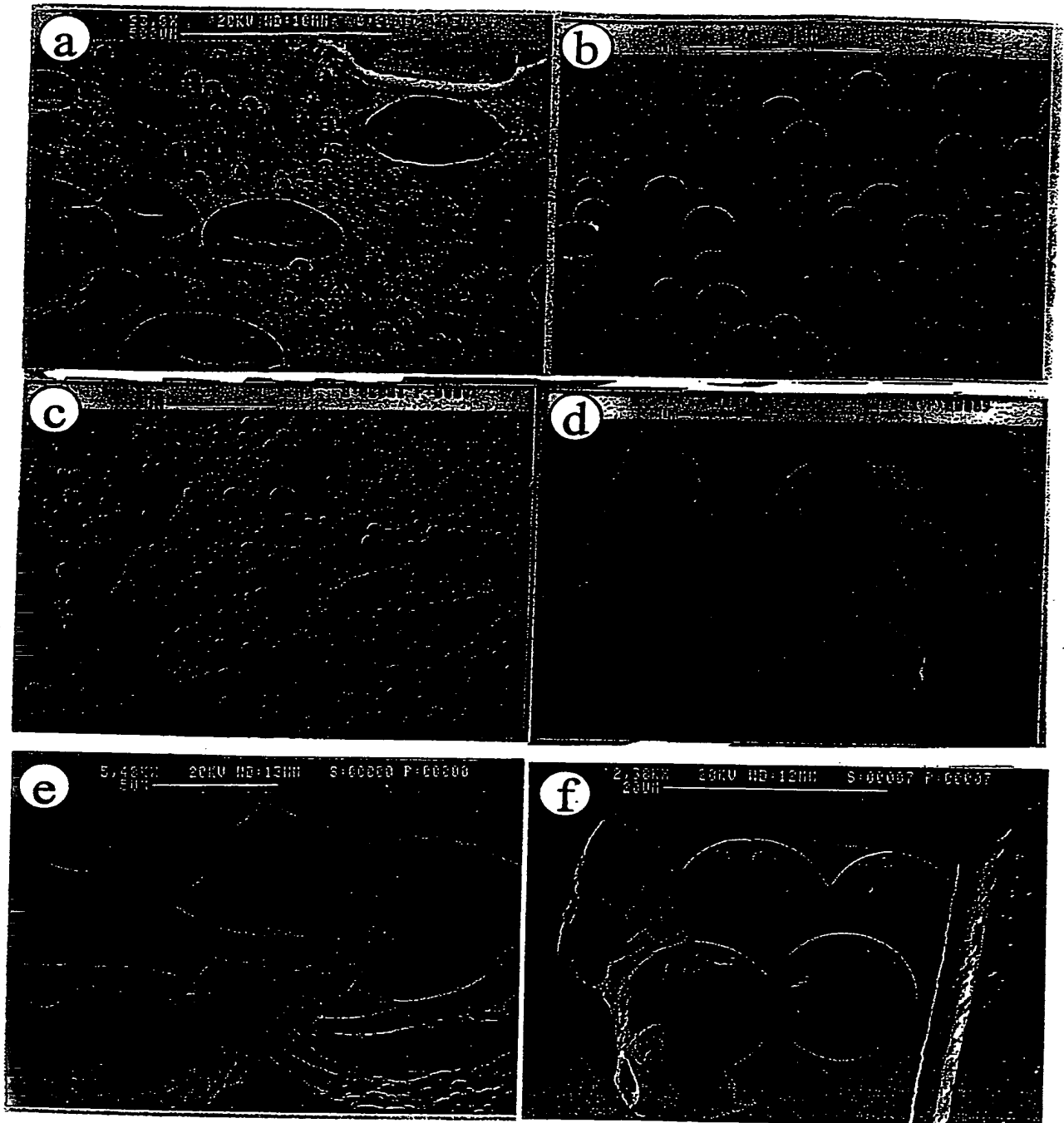
FIGURE 28
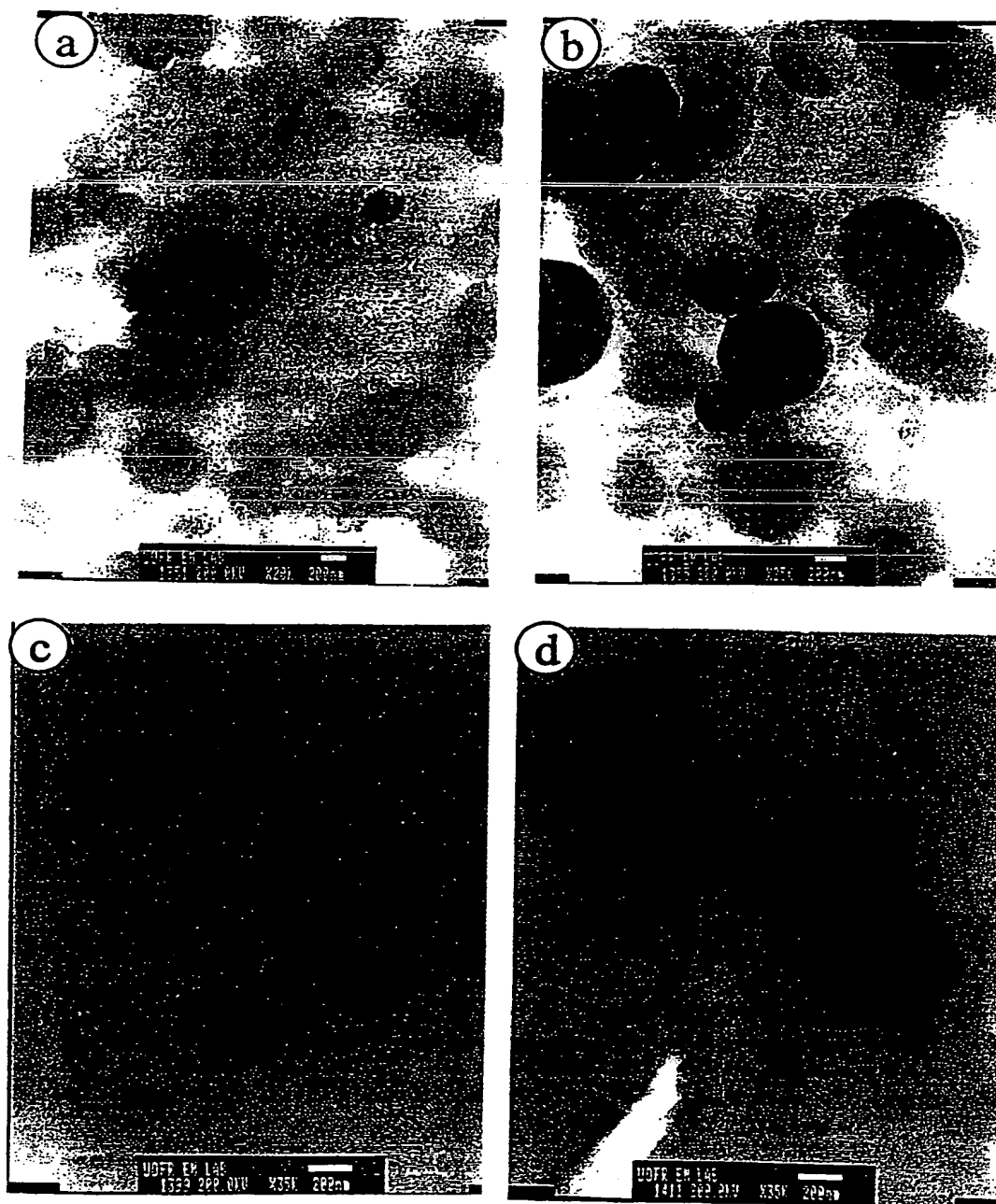
FIGURE 29
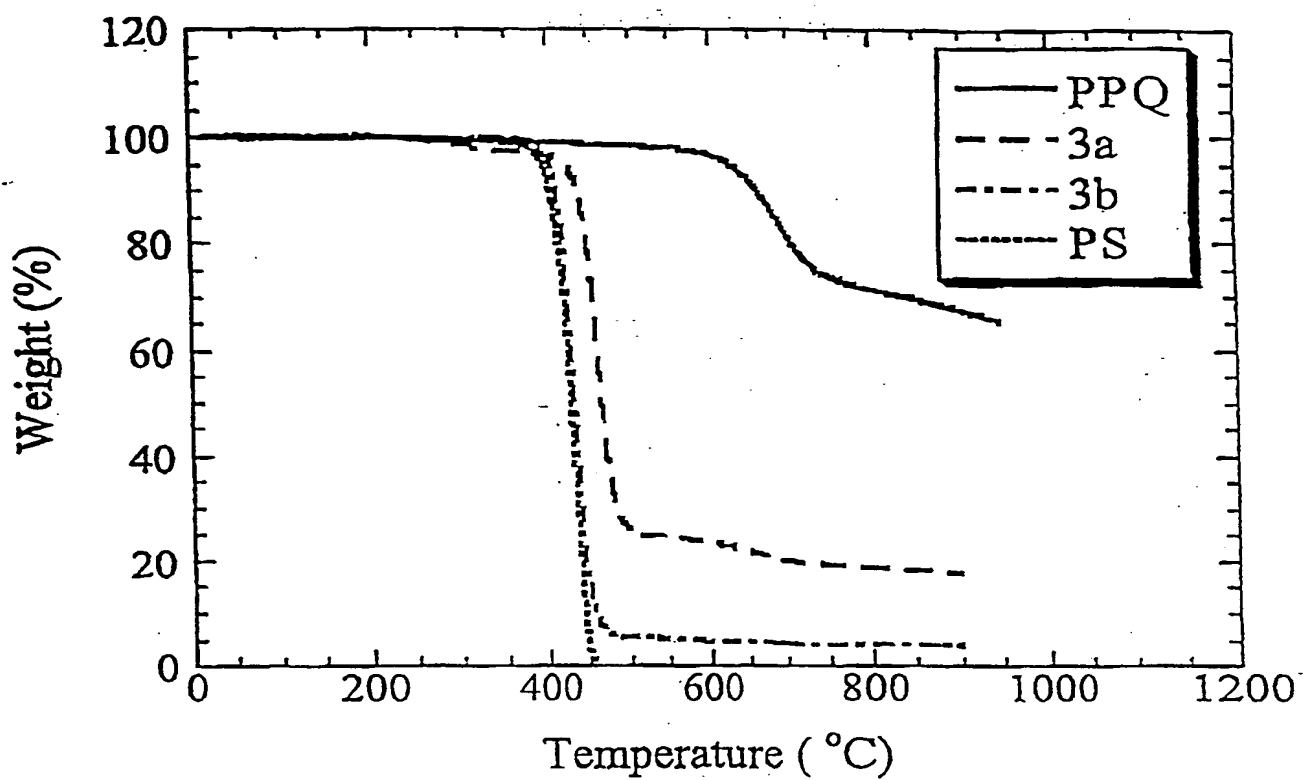
FIGURE 30
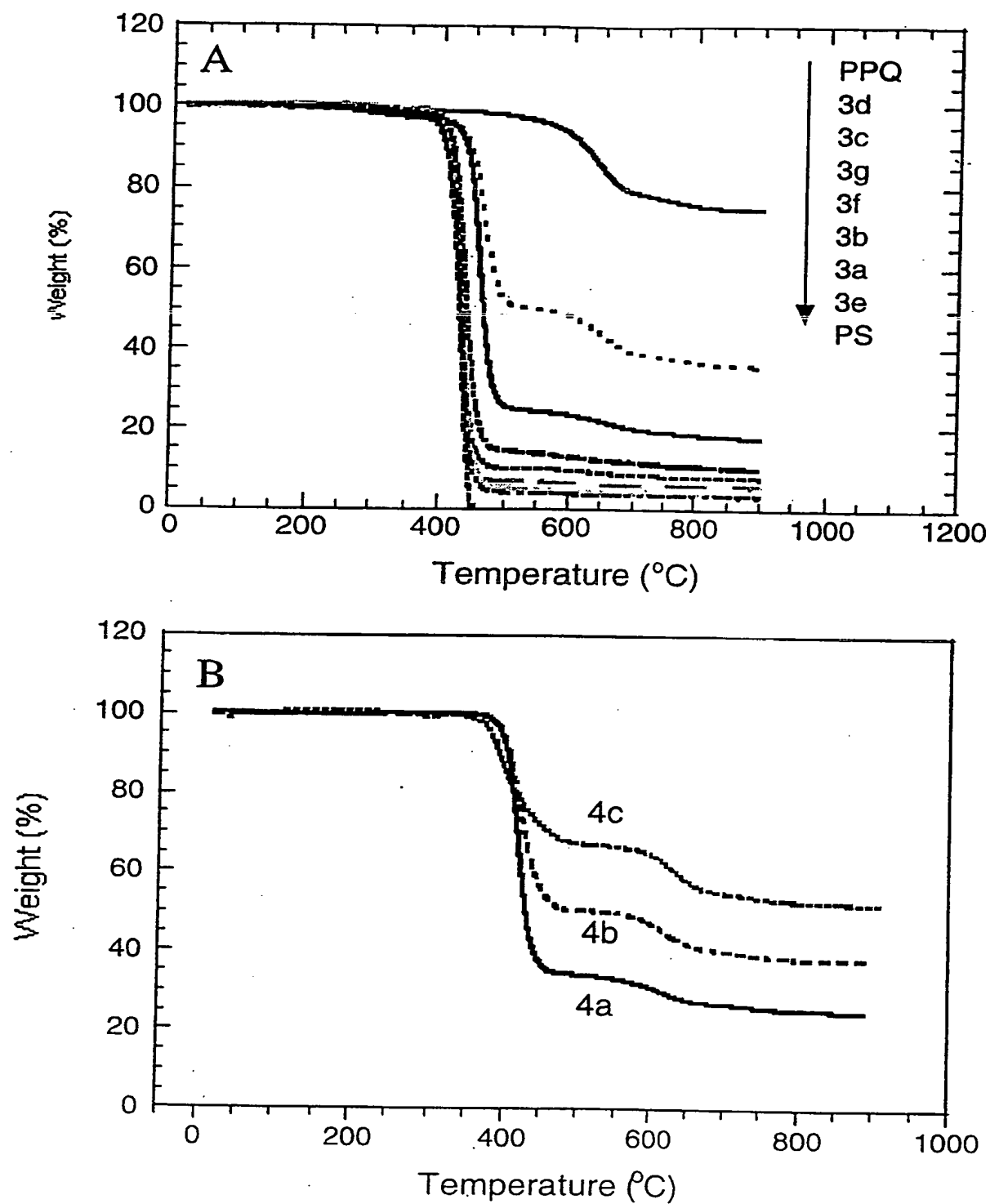
FIGURE 31
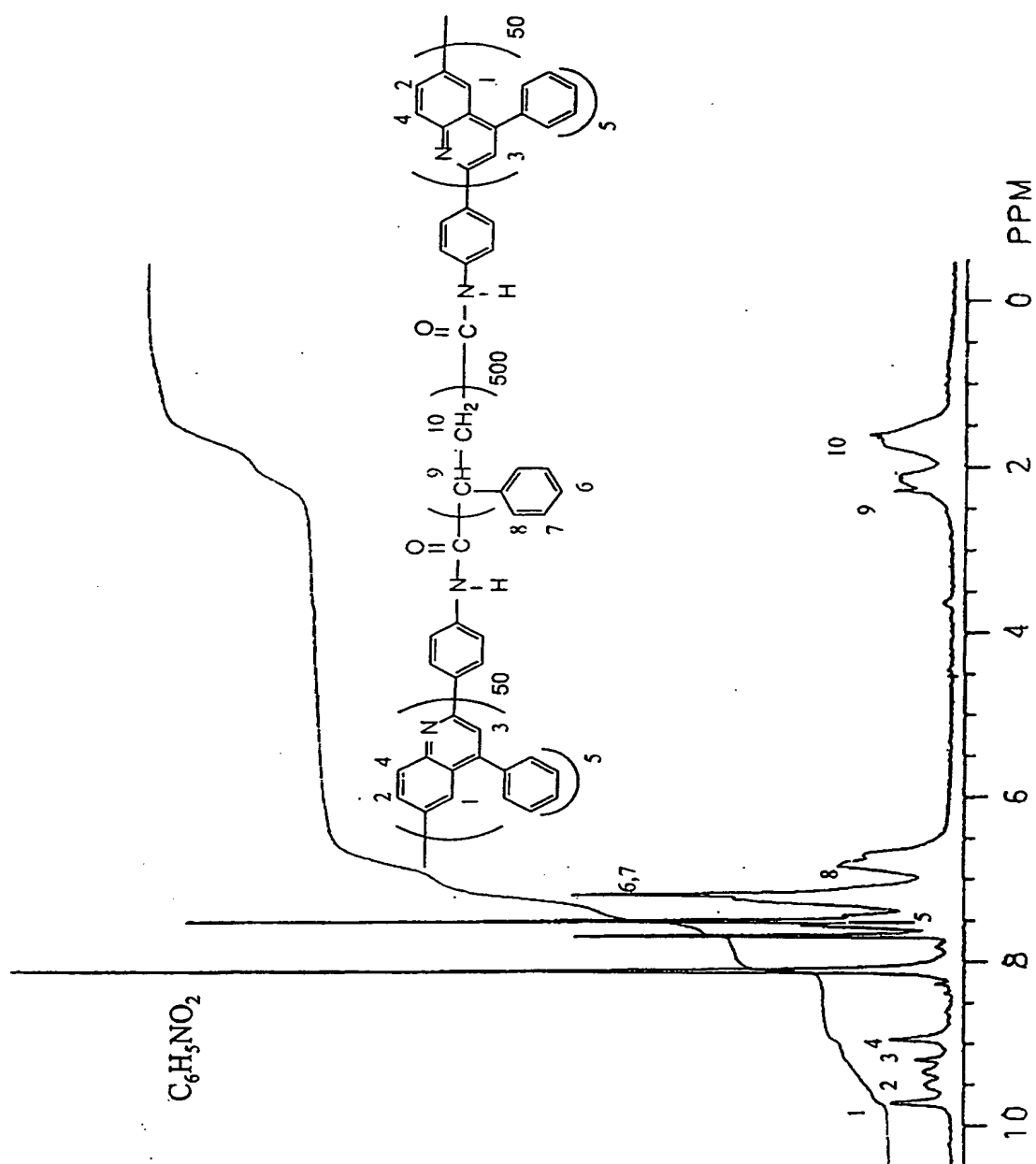
FIGURE 32

FIGURE 33

Scheme 1

C₆₀ or C₇₀

C₆₀ or C₇₀

PPQ-b-PS

PS

PPQ
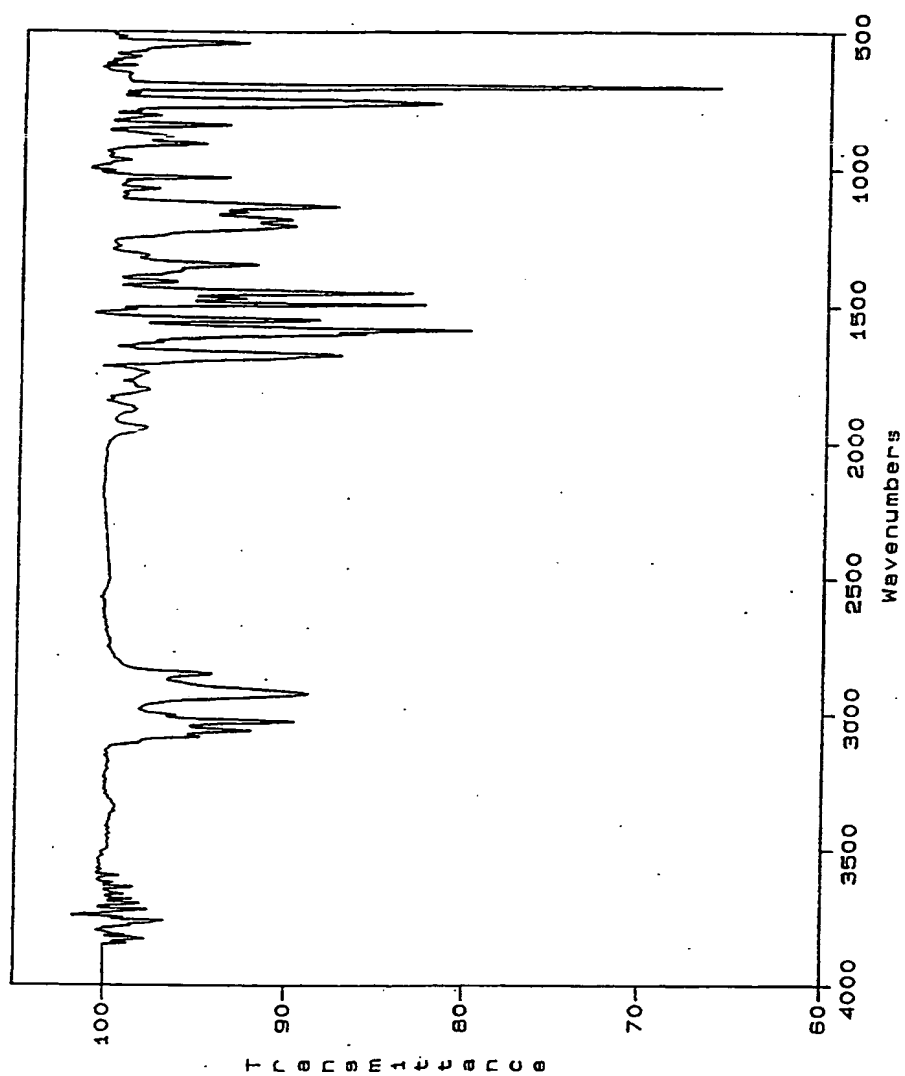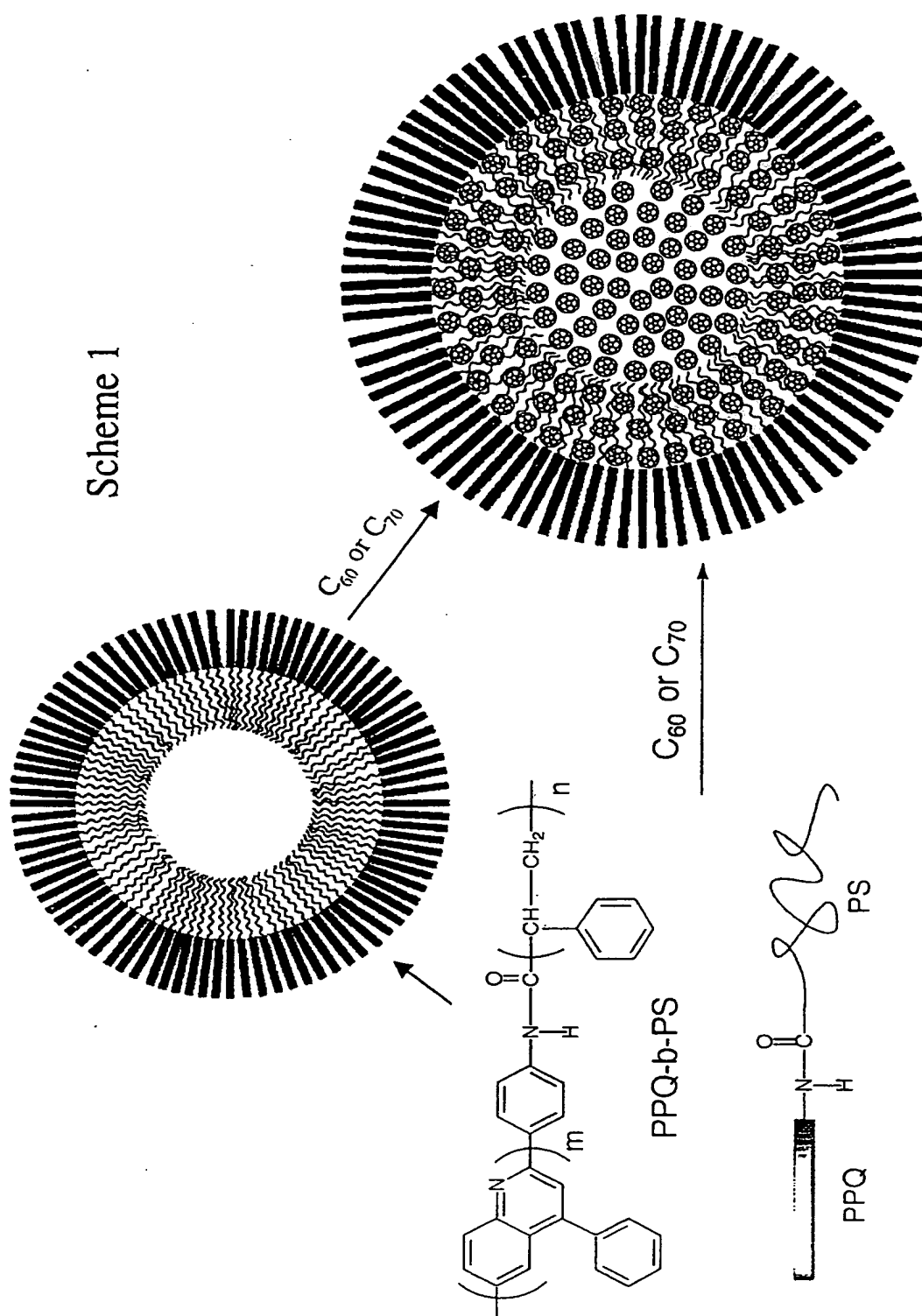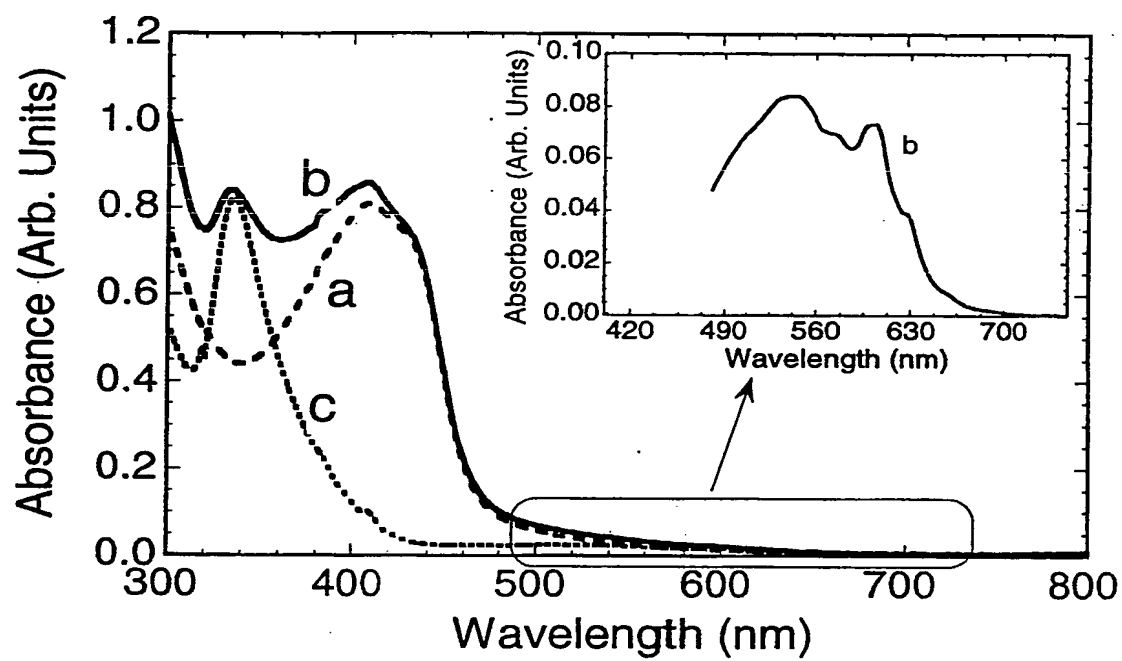
FIGURE 34

FIGURE 35
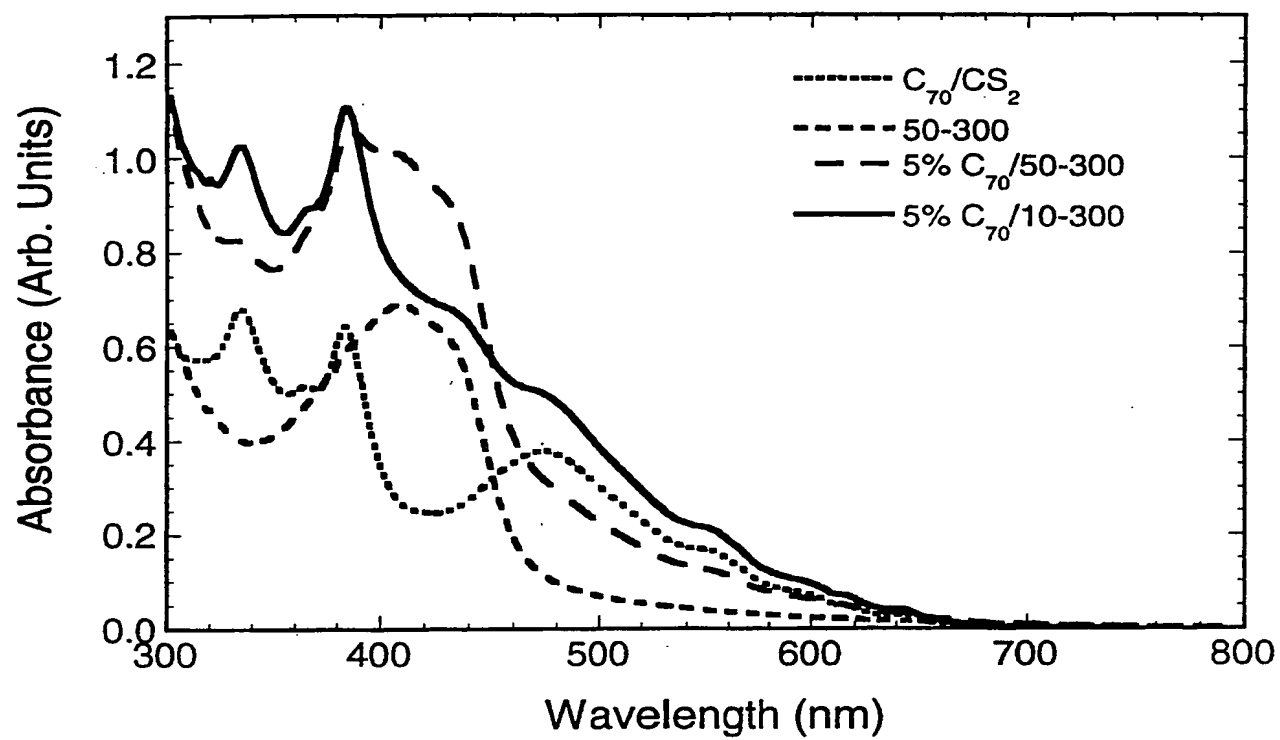
FIGURE 36
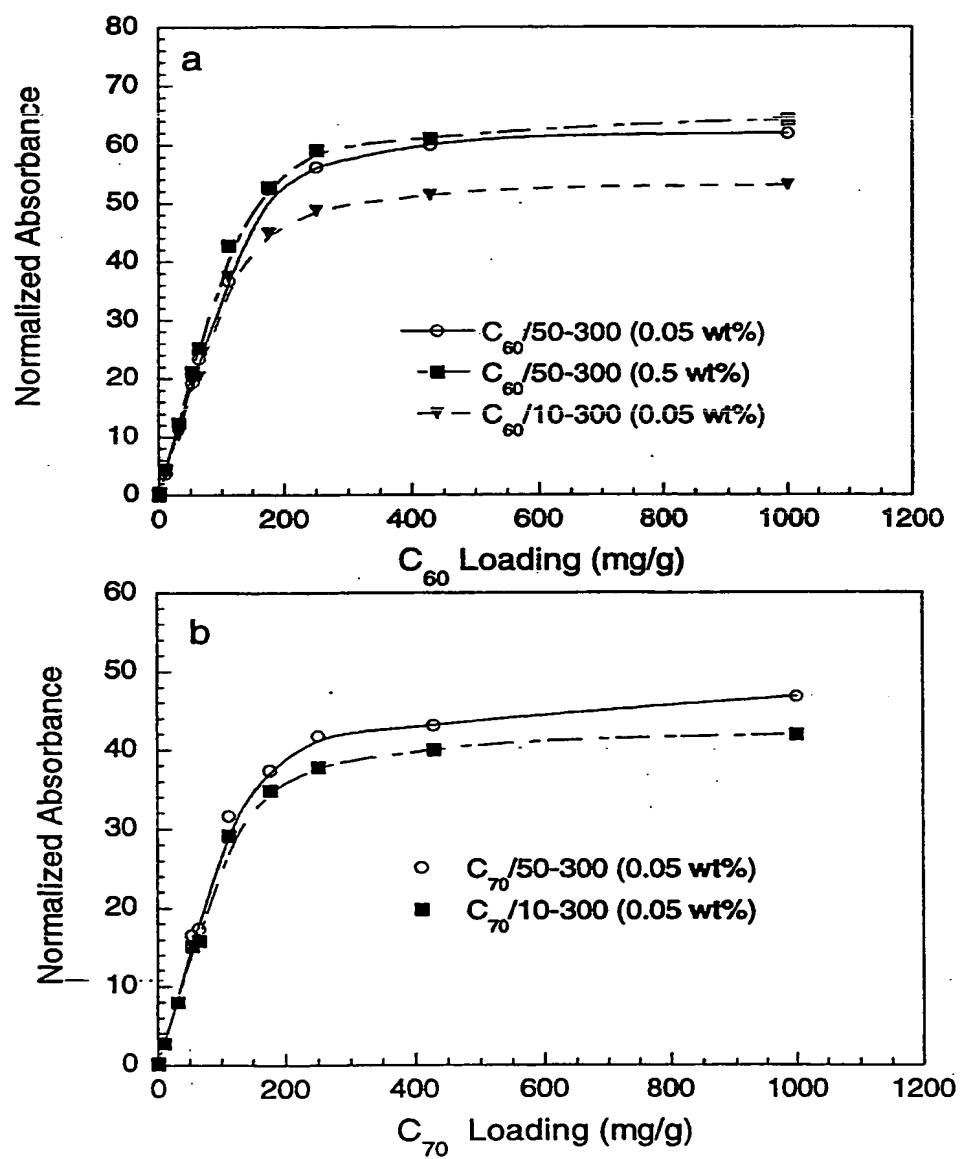
FIGURE 37
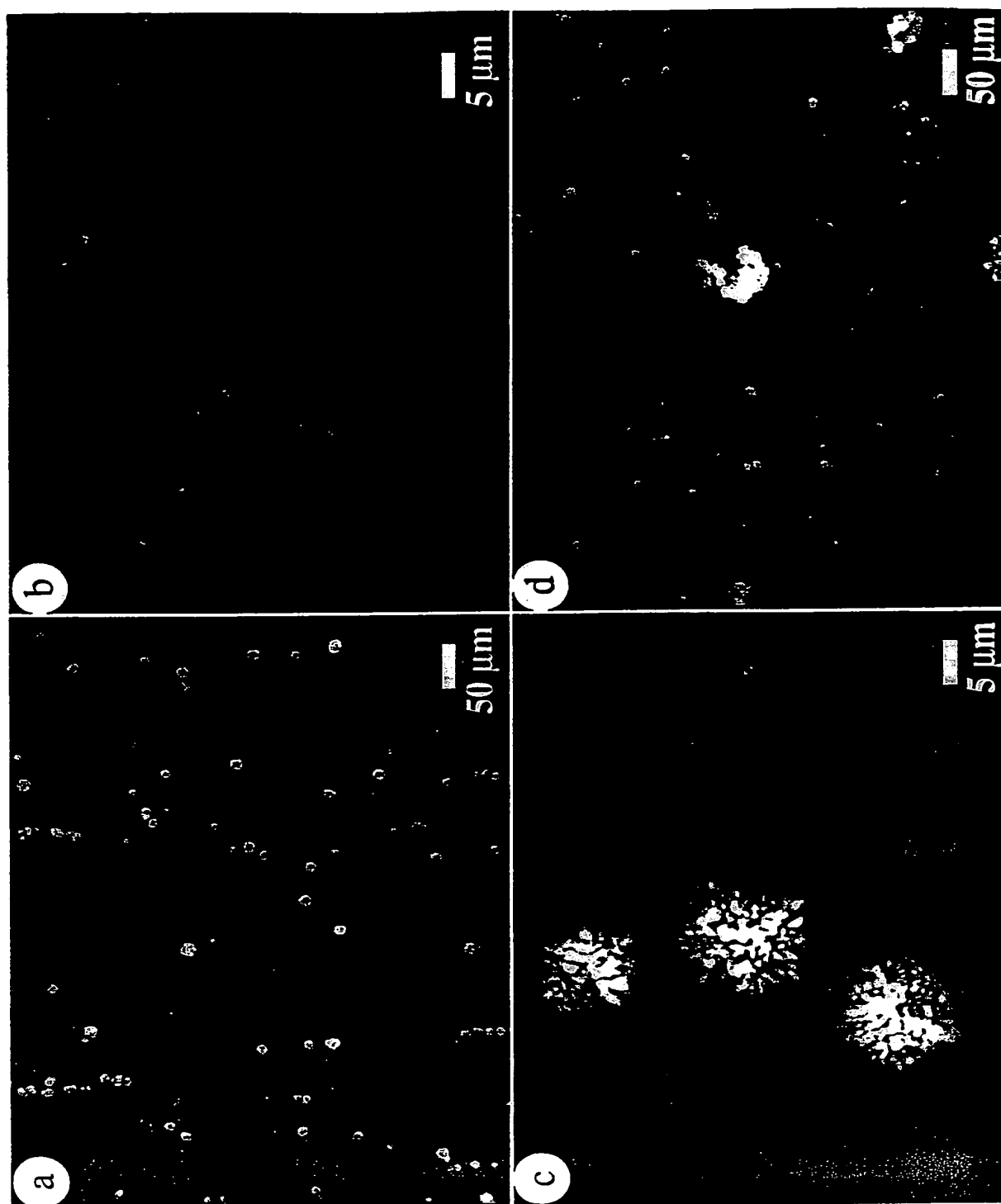
FIGURE 38
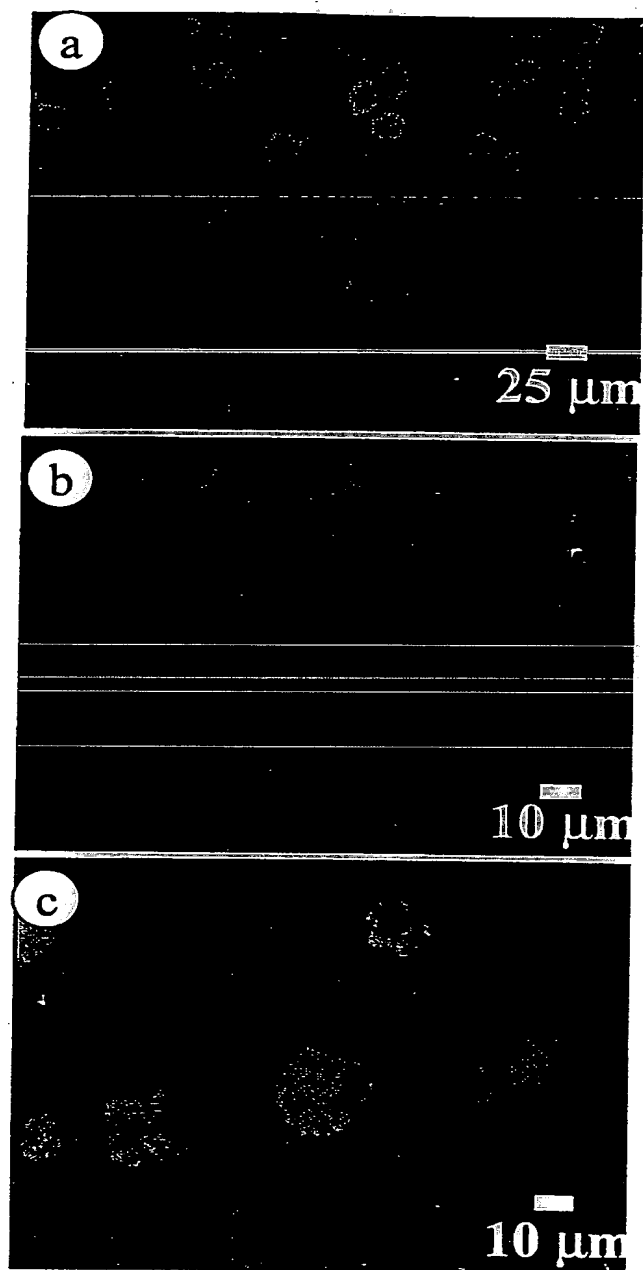
FIGURE 39
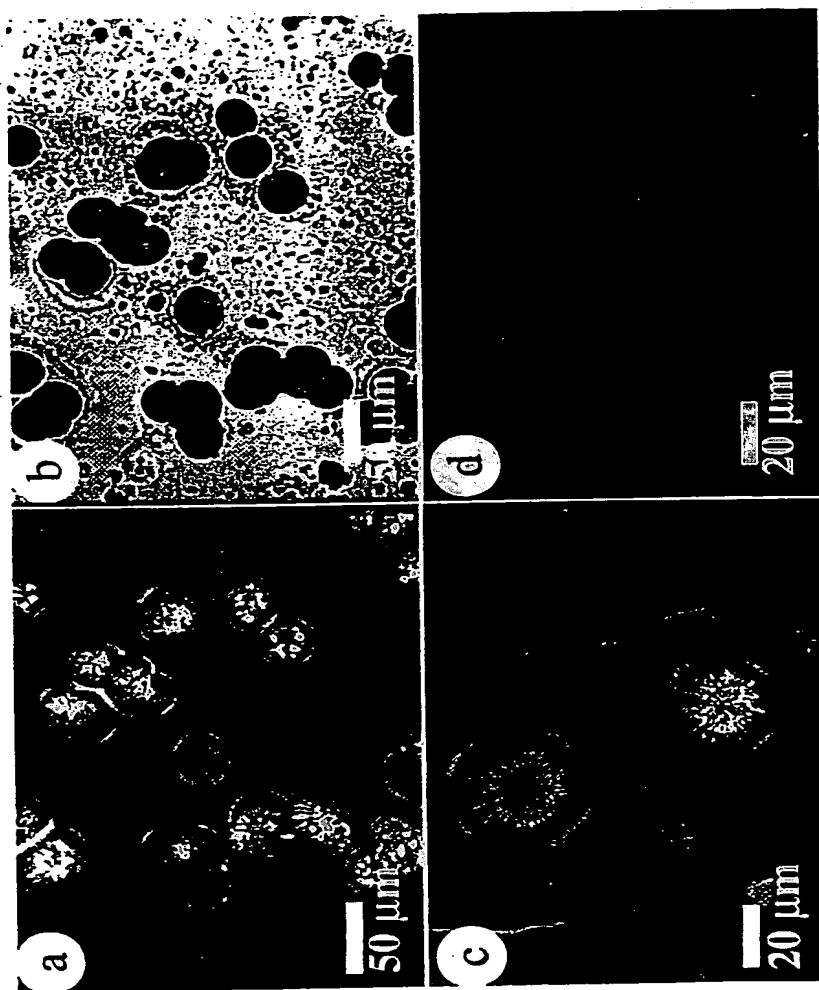
FIGURE 40
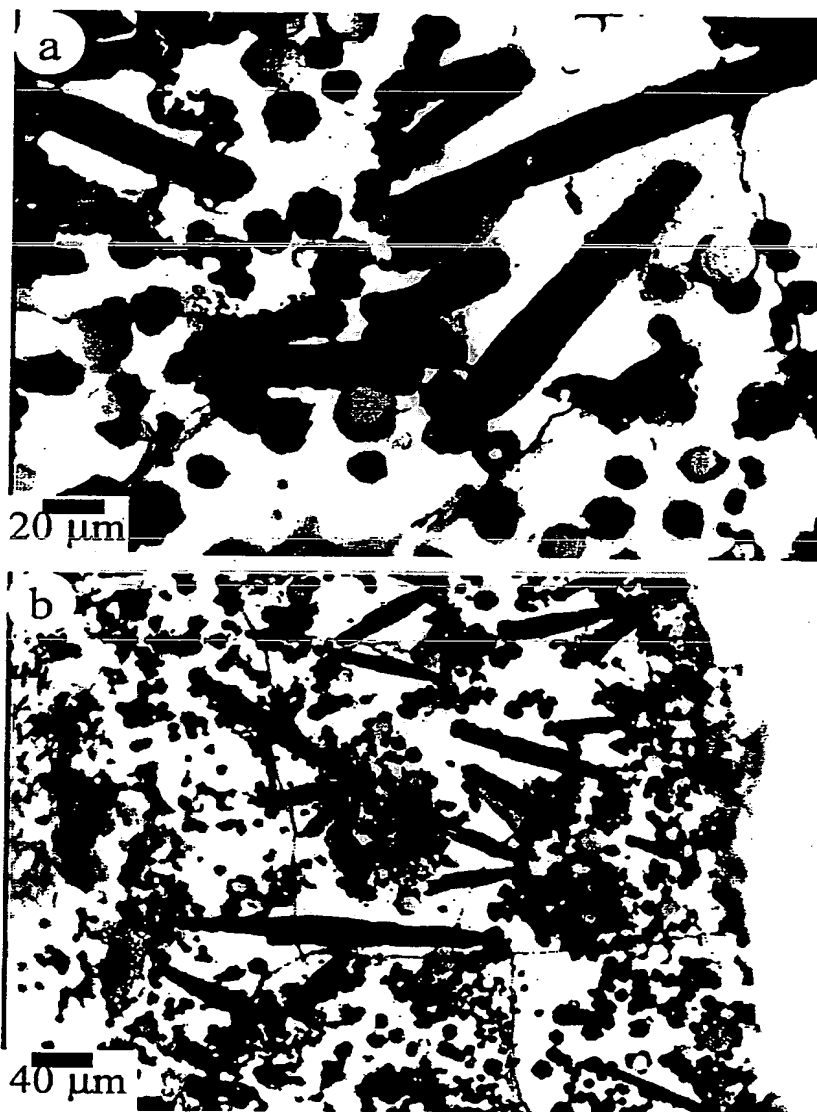
FIGURE 41
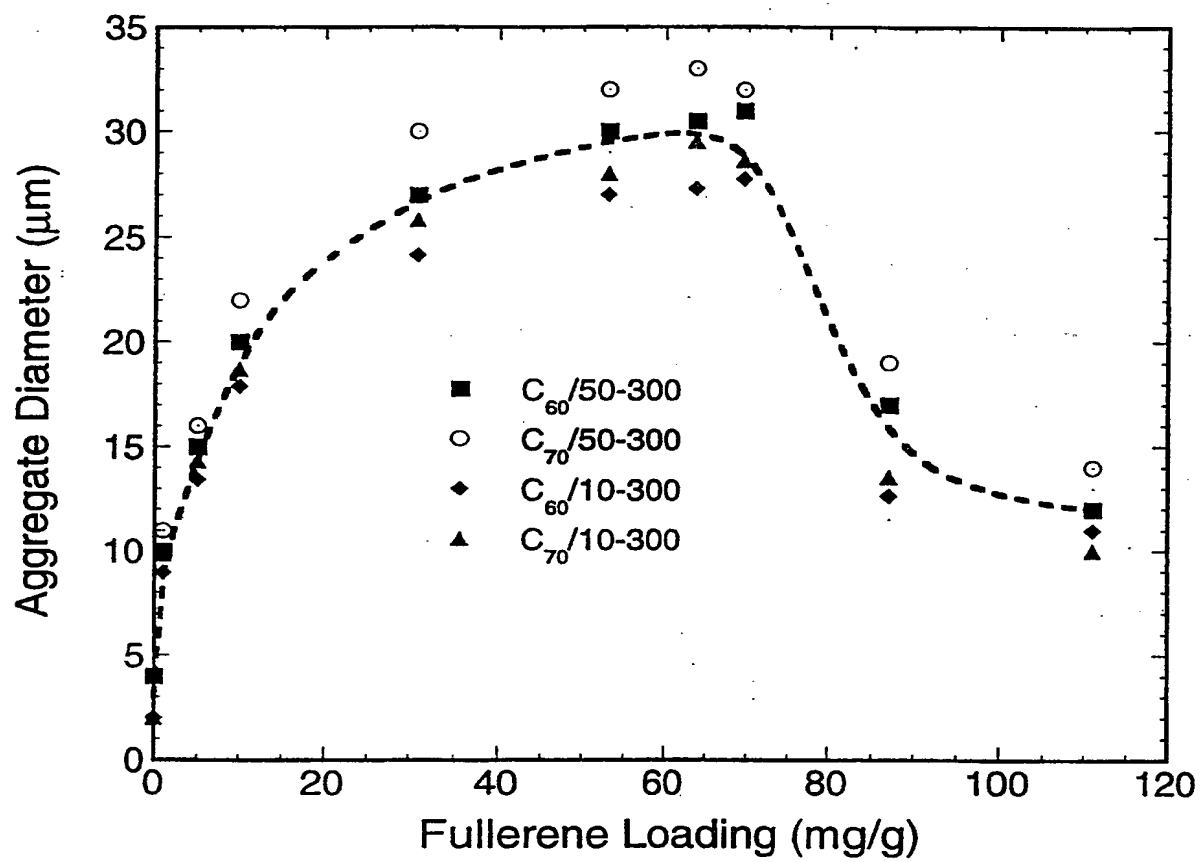
FIGURE 42
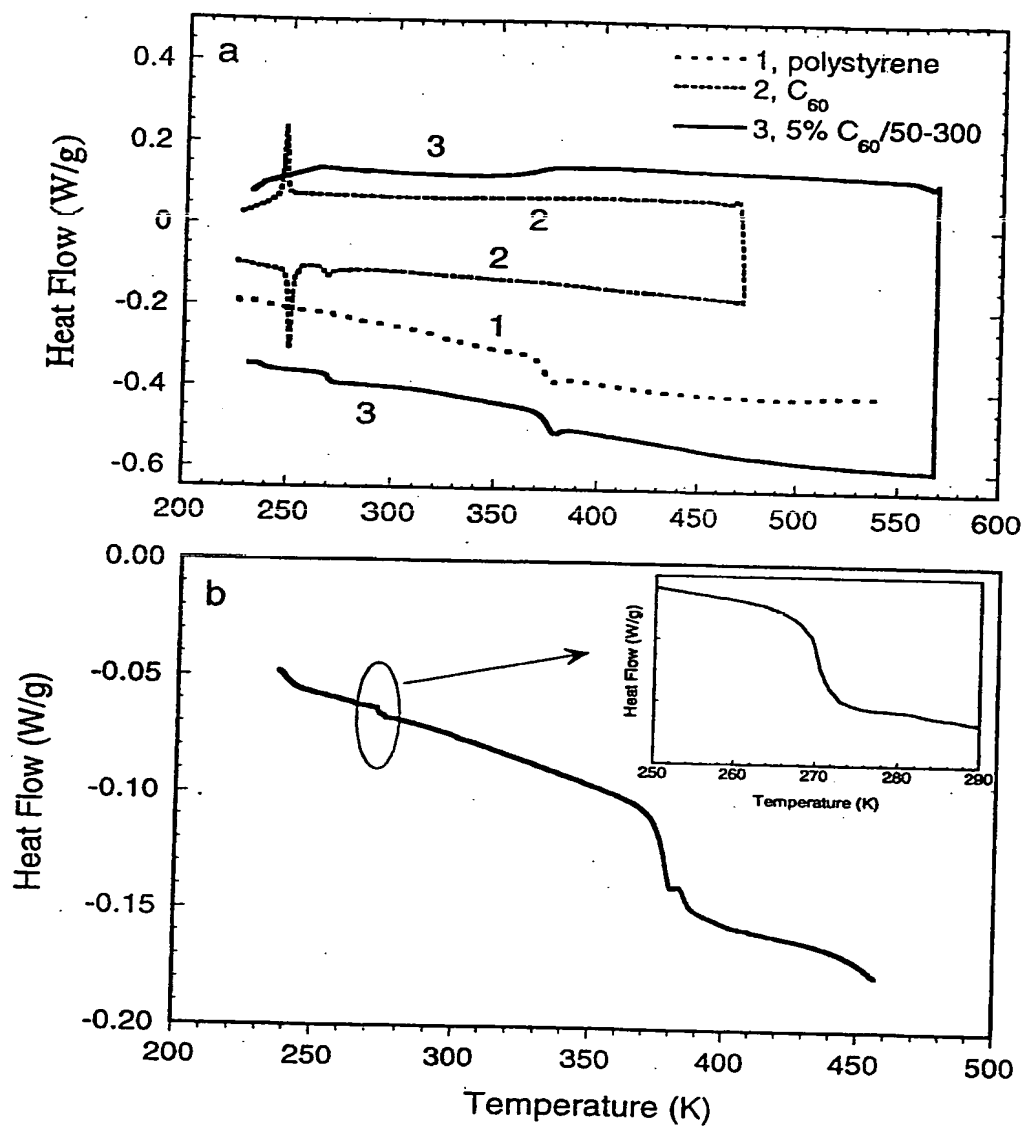
FIGURE 43

FIGURE 44

Scheme 2

(a)

(b)
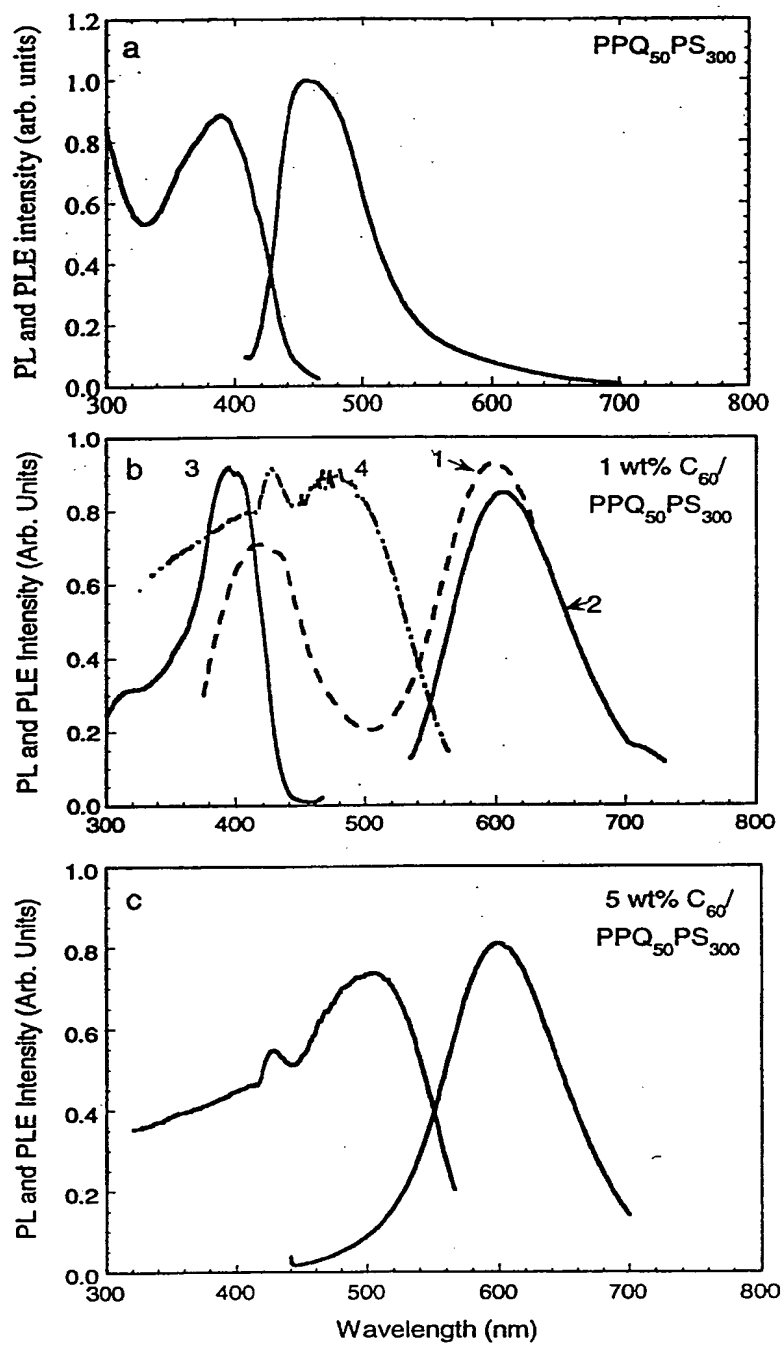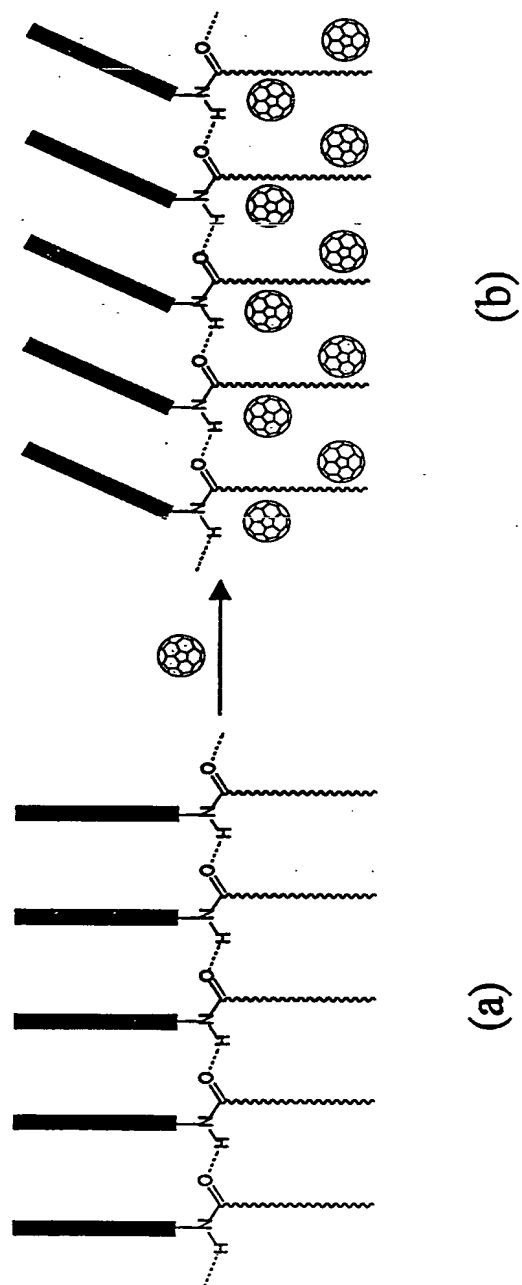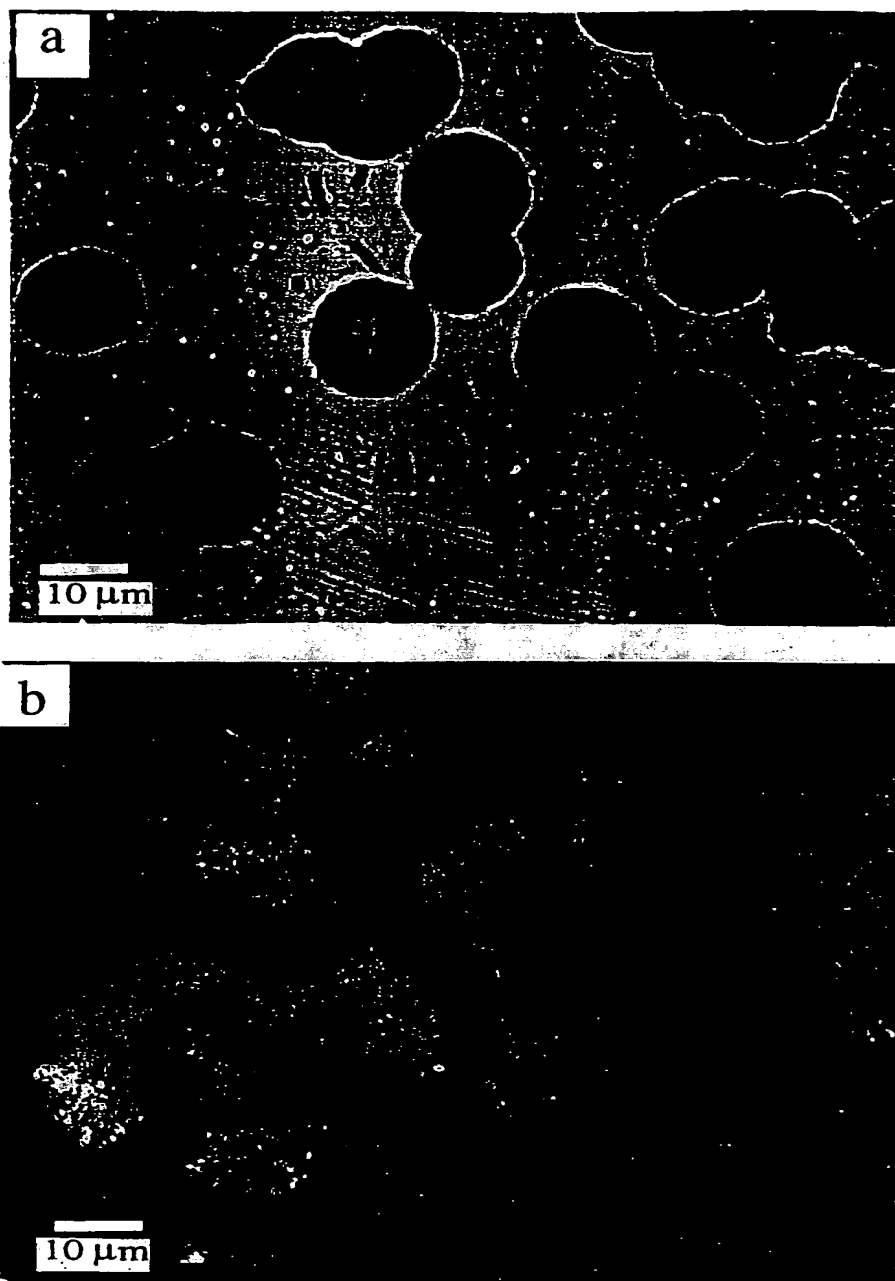
FIGURE 45

FIGURE 46
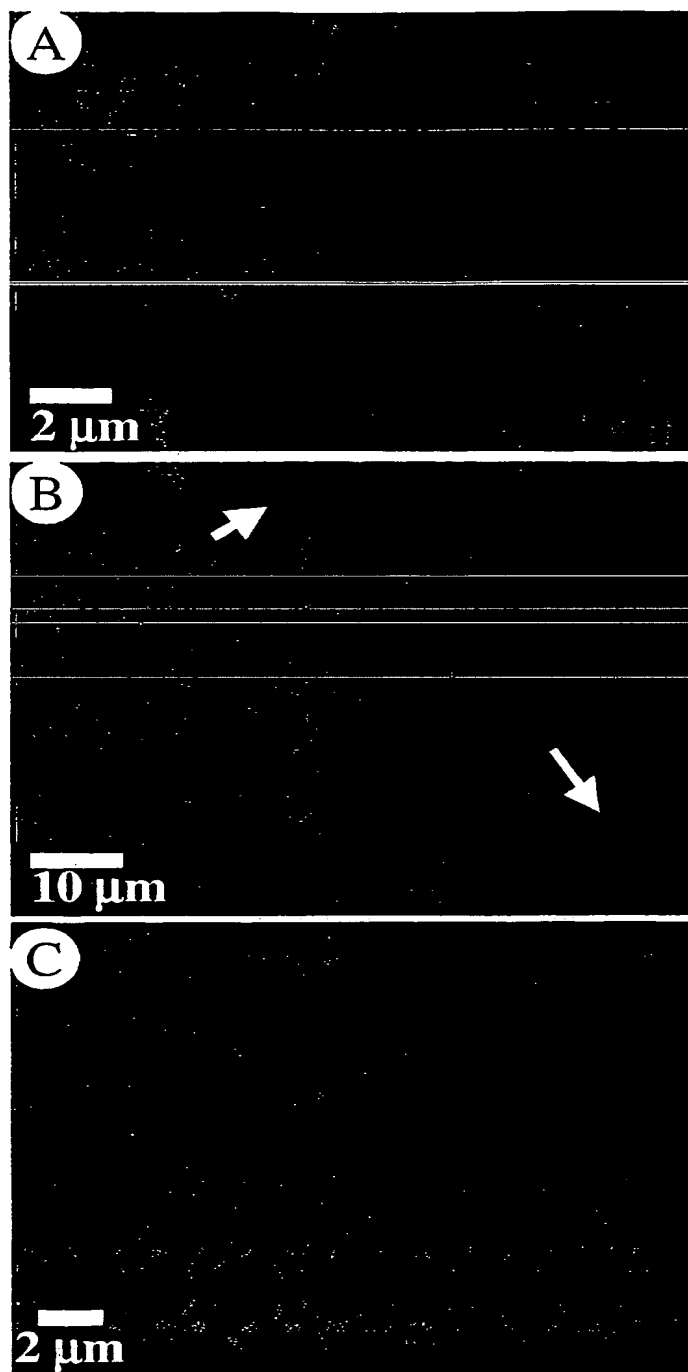
FIGURE 47
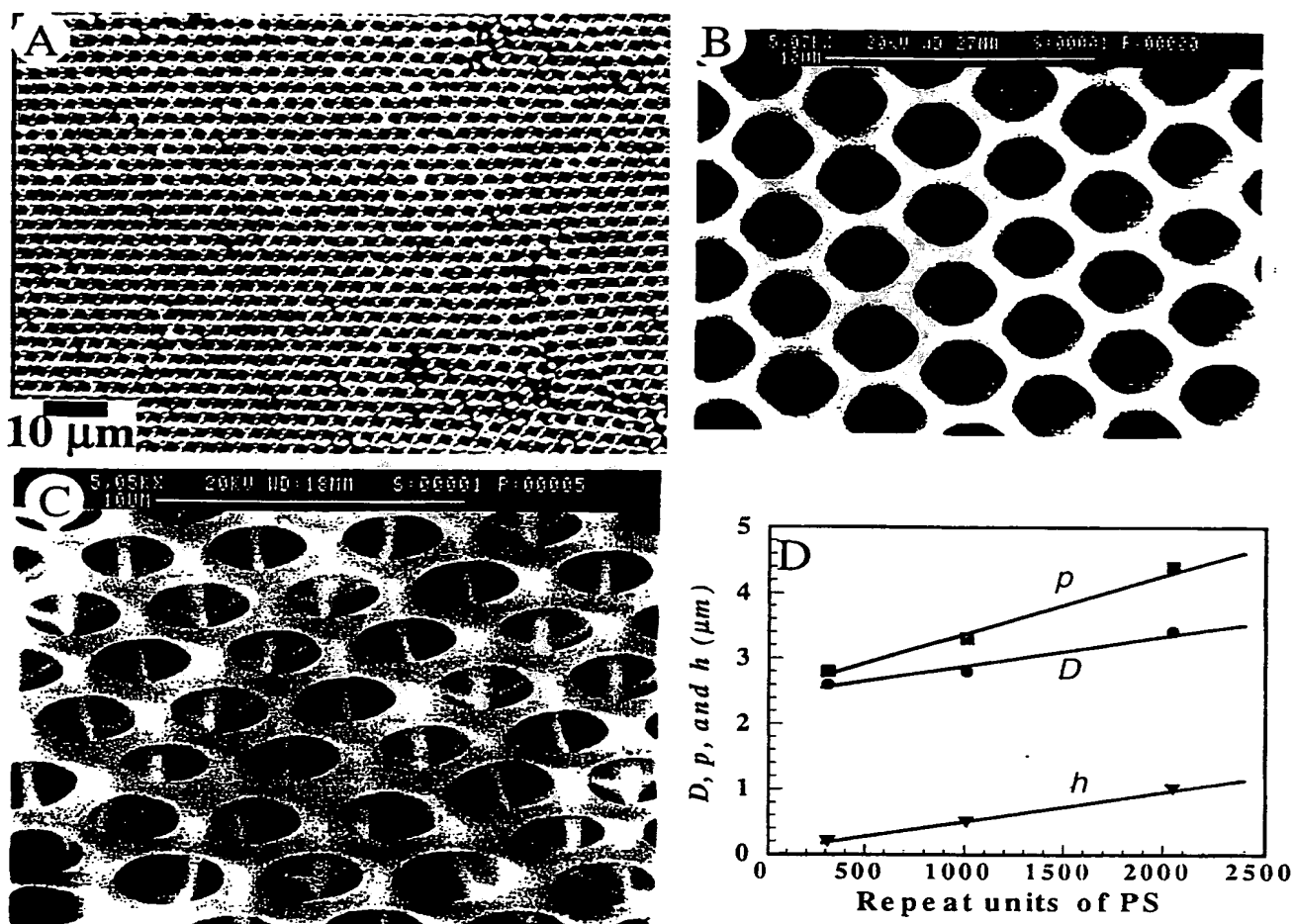
FIGURE 48
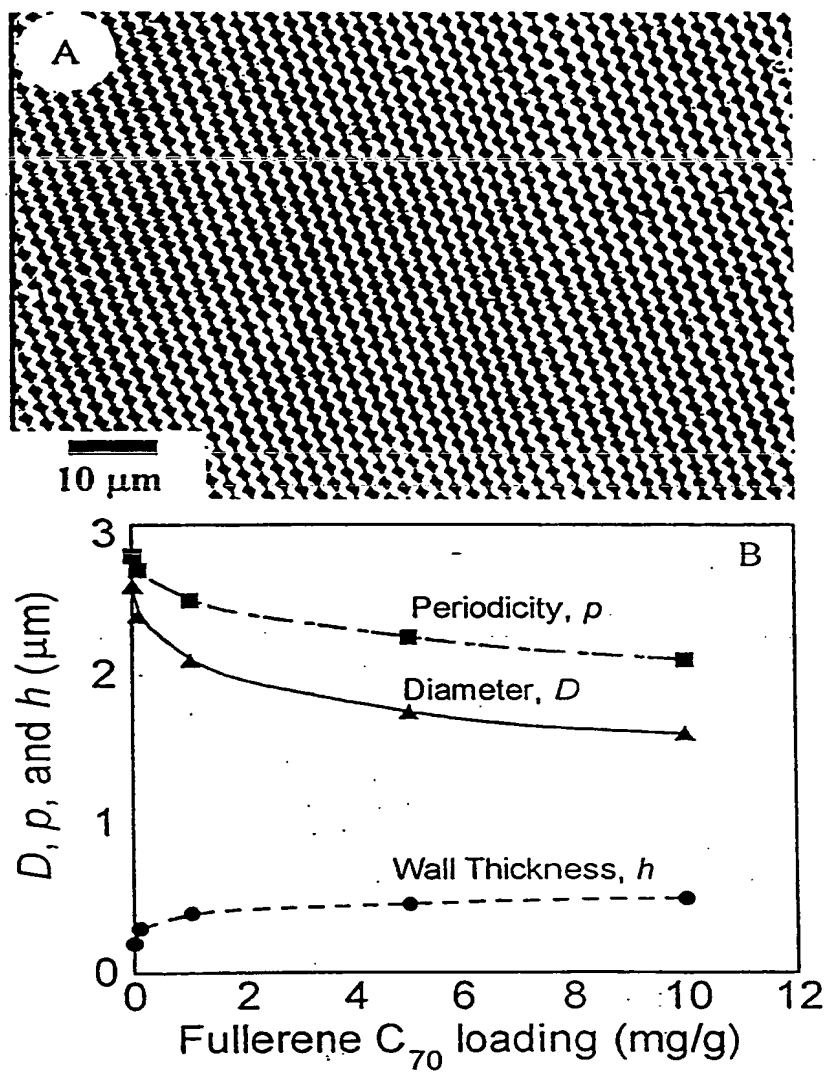
FIGURE 49
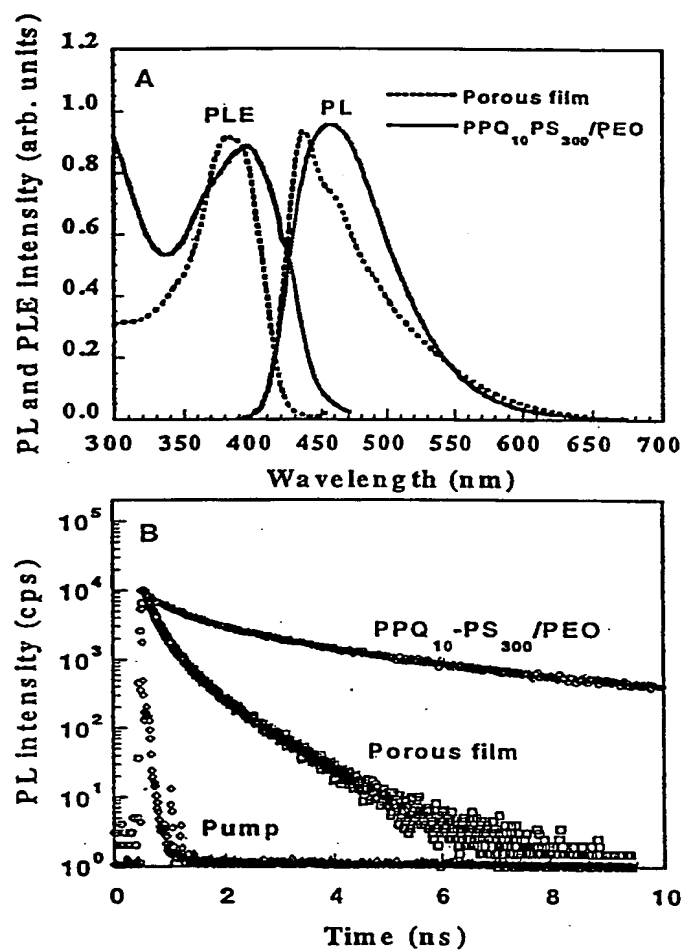
FIGURE 50

INTERNATIONAL SEARCH REPORT

A. CLASSIFICATION OF SUBJECT MATTER

IPC(6) :C08F 6/26
US CL :528/491, 493, 494, 495, 499

According to International Patent Classification (IPC) or to both national classification and IPC

B. FIELDS SEARCHED

Minimum documentation searched (classification system followed by classification symbols)

U.S. : 528/491, 493, 494, 495, 499

Documentation searched other than minimum documentation to the extent that such documents are included in the fields searched

Electronic data base consulted during the international search (name of data base and, where practicable, search terms used)

C. DOCUMENTS CONSIDERED TO BE RELEVANT

Category*	Citation of document, with indication, where appropriate, of the relevant passages	Relevant to claim No.
A	US 5,686,031 A (CORONADO et al) 11 November 1997.	1-86
A	US 5,145,583 A (ANGLERAUD et al) 08 September 1992.	1-86

☐ Further documents are listed in the continuation of Box C.   ☐ See patent family annex.

* Special categories of cited documents:	"T" later document published after the international filing date or priority date and not in conflict with the application but cited to understand the principle or theory underlying the invention
"A" document defining the general state of the art which is not considered to be of particular relevance	
"E" earlier document published on or after the international filing date	"X" document of particular relevance; the claimed invention cannot be considered novel or cannot be considered to involve an inventive step when the document is taken alone
"L" document which may throw doubts on priority claim(s) or which is cited to establish the publication date of another citation or other special reason (as specified)	
	"Y" document of particular relevance; the claimed invention cannot be considered to involve an inventive step when the document is combined with one or more other such documents, such combination being obvious to a person skilled in the art
"O" document referring to an oral disclosure, use, exhibition or other means	
"P" document published prior to the international filing date but later than the priority date claimed	"&" document member of the same patent family

Date of the actual completion of the international search	Date of mailing of the international search report
21 JUNE 1999	02 JUL 1999

Name and mailing address of the ISA/US	Authorized officer
Commissioner of Patents and Trademarks Box PCT Washington, D.C. 20231	BERNARD LIPMAN
Facsimile No. (703) 305-3230	Telephone No. (703) 308-0661

Form PCT/ISA/210 (second sheet)(July 1992)★